DOE/ET/10692-T1

MECHANISM OF CORROSION OF STRUCTURAL MATERIALS IN CONTACT WITH COAL CHARS IN COAL GASIFIER ATMOSPHERES

Final Report

By
D. L. Douglass
V. S. Bhide
E. J. Vineberg

May 1980

Work Performed Under Contract No. AT03-76ET10692

School of Engineering and Applied Science
University of California
Los Angeles, California

U. S. DEPARTMENT OF ENERGY

DISCLAIMER

DISCLAIMER

Available from the National Technical Information Service, U. S. Department of Commerce, Springfield, Virginia 22161.

Price: Printed Copy A05
Microfiche A01

DOE/ET/10692-T1
Distribution Category UC-90c

MECHANISM OF CORROSION OF STRUCTURAL MATERIALS IN CONTACT WITH COAL CHARS IN COAL GASIFIER ATMOSPHERES

Final Report
May, 1980

D.L. Douglass, V.S. Bhide, and E. Vineberg

Materials Department
School of Engineering and Applied Science
University of California
Los Angeles California 90024

Prepared for:

S. Dapkunas
Division of Fossil Energy Research
United States Department of Energy
Washington D.C., 20545

Contract No. EY-76-S-03-0034

TABLE OF CONTENTS

ABSTRACT

Six alloys, 310 stainless steel, Hastelloy X, Inconel 671, Incoloy 800, Haynes 188, and FeCrAlY (GE1541 and MA956), were corroded in two chars at 1600 and 1800°F. The chars, FMC and Husky, contained 2.7 and 0.9% sulfur, respectively. Various parameters were investigated, including char size, cover gas, char quantity, char replenishment period, gas composition, and the use of coatings.

The corrosion process was strictly sulfidation when the char was replenished every 24 hours or less. The kinetics of reaction were nearly linear with time. The reaction resulted in thick external sulfide scales with extensive internal sulfidation in the substrate. The kinetics and reaction-product morphologies suggested that diffusion through the sulfide scale played a minor role and that an interfacial reaction was the rate-controlling step. A mathematical model was developed which supported this hypothesis.

The reaction rates showed a relatively minor role on alloy composition, depending upon whether the alloys were tested singularly or in combination with others. Inconel 671, the best alloy in CGA environments, consistently corroded the most rapidly of the chromia-former types regardless of char sulfur content or of the temperature. Type 310 stainless was marginally better than Inconel 671. Incoloy 800 was intermediate, whereas, Haynes 188 and Hastelloy X exhibited the best corrosion resistance. The FeCrAlY alloys reacted very rapidly in the absence of preoxidation treatments. All alloys corroded in char at least 1000 times more rapidly than in the CGA (MPC-ITTRI) environment. None of the alloys will be acceptable for use in contact with char unless coatings are applied.

INTRODUCTION

The corrosive nature of coal-gasification atmospheres is well-known and is the object of numerous research efforts. Most studies performed to date or in progress, involve the reaction between various metals and atmospheres deemed typical of various gasification processes. Few of the studies have involved interactions between metals and char, which is a prime ingredient of gasifiers.

Chars vary widely in composition, depending upon the composition of the coal from which the chars are made. All chars have very high carbon contents but may also contain appreciable sulfur as well as inorganic ash (various oxides). The corrosiveness of the char will depend to a large extent on its sulfur content, although other elements may be involved. In general, one may expect that the char-metal reactions will involve simultaneous sulfidation and carburization, which combination is quite different from the usual one of sulfidation and oxidation involved in reactions between metals and coal-gasification atmospheres. However in actuality the attack is primarily due to sulfidation.

This study was designed to ascertain the general features of attack, to determine the reaction mechanisms, and to investigate a number of experimental parameters. The results obtained will enable the anticipated lifetimes of various components to be predicted in coal gasifiers.

Alloy selection was made to cover several possibilities. First, a stainless steel, type 310, the expected "workhouse" of gasifiers, was chosen because of its relative low cost, availability and reasonable corrosion

resistance. Second, two Fe-Ni-Cr alloys were chosen, Hastelloy-X and Incoloy-800. These alloys are generally regarded as having good high-temperature corrosion resistance but are more expensive than 310 stainless. Incoloy-800 has a fairly high iron content (47%) and is somewhere between a stainless steel and a nickel-base superalloy. Hastelloy-X has a lower iron content (18%) and a higher nickel content than Incoloy-800 and is closer to a superalloy than a stainless steel. Inconel-671 has the highest chromium content of any commercial alloy (48%) and is regarded as having outstanding sulfidation resistance. A cobalt-base alloy, Haynes Alloy 188, was chosen so that the general behavior of cobalt versus nickel alloys could be compared. Lastly, an alloy which is an alumina former during oxidation, Fe-Cr-Al-Y, was chosen. This report summarizes work performed during the period February 1977 - February 1980.

EXPERIMENTAL PROCEDURES

Alloys

Five commercial alloys were purchased in sheet form. Four of the materials were 0.125" thick (310 stainless steel, Hastelloy-X, Incoloy 800 and Haynes 188). The fifth alloy, Inconel 671 was 0.25" thick. Two FeCrAlY alloys were used. The first was GE1541, and the second was Incoloy MA956. The compositions are listed in Table I.

Corrosion samples approximately 10 x 20 mm were sheared from the sheets. The sharp edges were rounded slightly to reduce their effect on scale spallation during corrosion. All surfaces were abraded through 4/0 silicon carbide paper, washed in acetone, and air-dried.

Char

Two chars, FMC and Husky, were received from IITRI. The char analyses, as supplied by IITRI, are listed in Table II. The chars represent a high-sulfur one (FMC-2.7%) and a low-sulfur one (Husky - 0.9%). The chars were crushed and screened into various size fractions. Initial tests were performed with -170 mesh particles. However, experiments performed with these chars by Lockheed Space and Missile Corp. Research Laboratories (Mr. Roger Perkins) resulted in expulsion of the fine particles by the moving gas stream, and subsequent work was performed with coarser particles, -32 + 42 mesh. A particle-size effect of the char was discovered and will be discussed subsequently.

Gaseous Environment

The question arose as to what the actual atmosphere would be to which a metal sample embedded in char would be exposed. For example, an "ambient" atmosphere such as the IITRI/MPC GAS (which will be referred to as the Coal-Gasification-Atmosphere, CGA) might not reach the metal surface if the char were either very fine or slightly sintered on the metal surface. The CGA atmosphere, composition listed in Table III, has an oxygen pressure of about 10^{-15} atm. at 1800°F and 1000 psi, which oxygen pressure is sufficiently high to permit the formation of stable oxides such as Al_2O_3 or Cr_2O_3. If this gas reached the surface, and depending upon the sulfur activity as well as the activities of the various metals in the alloy, stable oxide films might form which would offer considerable protection of the metal form the char. On the other hand, if this gas does not penetrate to the metal surfaces, the conditions would be much more reducing, and oxides would probably not form. Thus, the initial experiments were performed using slowly flowing argon which was thought to be a more corrosive environment. Samples were imbedded in char

in ceramic boats, while other samples were placed downstream from the char and exposed to the species removed from the char by the argon stream. As will be shown subsequently, the argon did pick up the corroding species from the char as evidenced by extensive corrosion of the downstream samples.

A relative evaluation of the two atmospheres was made by comparing these results with those obtained by Mr. Roger Perkins of Lockheed using our samples and char.

Corrosion Apparatus

Two units were built which consist of horizontal tube furnaces with mullite tubes. Aluminum end-fittings were attached with rubber gaskets to maintain a gas-tight seal. Water cooling was used to keep the temperature of the end fittings and gaskets low enough to ensure their proper functioning.

In order to eliminate the long heating and cooling times involved because of the large mass of the furnaces, etc., a mechanical device was constructed to rapdily insert and remove the samples from the hot zone.

Gas Analyses

Furnace gases were taken from the system in evacuated gas sample bottles at various times and for a variety of conditions. The gas sample was then bubbled through 50 cc of 0.0213 N NaOCl (sodium hypochloride) using argon to flush the samples completely. Hydrogen sulfide is absorbed by the reaction

$$H_2S + NaOCl = H_2O + S + NaCl \qquad (1)$$

The remaining NaOCl was neutralized by the addition of 0.01 N $Na_2S_2O_3$ (sodium thiosulphate) solution. The amount of $Na_2S_2O_3$ required for neutralization and the sample pressure and volume were then used to calculate the amount of H_2S in the gas.

A Perkin Elmer Model 881 gas chromatograph was available for analysis. This instrument has a hot wire thermal conductivity detector and uses helium

as a carrier gas. Since mixtures of hydrogen and helium have anomalous values of thermal conductivity, it could not be used for hydrogen analysis. This technique was also used as a check for wet chemical analysis.

Evaluation

Samples were weighed prior to corrosion. After corrosion the samples were brushed lightly to remove loosely adherent char and reweighed.

The corroded specimens were examined using standard methods of X-ray diffraction (generally with a chromium tube to eliminate fluorescence), metallography, and dispersive energy analysis in a scanning electron microscope. Some of the metallographic samples were copper-plated in order to preserve the edges during grinding and polishing.

RESULTS

General Behavior

The extent of corrosion was found to depend on numerous parameters which will be discussed individually. One important observation was that the manner in which the test performed was extremely important. In general, the attack was essentially due to sulfidation, although some oxidation was observed when the runs were continued for long times without replenishing the char. This effect, termed the char-replenishment effect, was attributed to the depletion of sulfur in the char during the course of reaction and a subsequent increase in the oxygen partial pressure to a value at which oxides became stable. Once this effect became apparent, tests were always performed with replenishment of the char every 12 hours. It was thought that this was more realistic than exposing samples to a given batch of char after the sulfur had been depleted. Replenishment of the char frequently corresponds to steady-state conditions which might exist in a gasifier, e.g., a nearly continuous flow of char past

any given point.

It was further found that the reaction kinetics depended upon whether a sample was run by itself or with others. If a given alloy was run with others which sulfidized more rapidly, less sulfur was available for reaction than if the alloy had been run by itself.

It was of interest early in the program to ascertain if the corrosion resulted from sulfidation by a solid-state process when the char was in contact with the samples or if a gaseous species formed from the sulfur in the char and then reacted with the samples. An experiment was performed in which samples were embedded in char in a ceramic boat and other samples were placed downstream in a slowly flowing stream of argon so that the downstream samples were not in contact with the char. Figure 1 shows samples corroded in char for 50 hours at 1800°F, whereas, Fig. 2 shows the same samples in the same experiment which were downstream from the char. The extensive corrosion depicted in Fig. 2 clearly shows that the argon picked up a gaseous species which was the prime corrodant.

Corrosion in high-sulfur char was much greater than in low-sulfur char. This effect, to be discussed in detail, arose from the higher partial pressure of sulfur existing in the high-sulfur char.

As mentioned already, the attack was sulfidation with virtually no evidence of oxidation unless the char became severely depleted in sulfur. No evidence of carburization was observed for any of the alloys, even though the carbon activity was sufficiently high to enable carbides to form.

Corrosion Kinetics

The kinetics depend markedly on how the results are measured and how the experiments are run. Let us consider first the method by which the corrosion is measured. Samples are placed in a ceramic boat or graphite container and

completely submerged in char. The char contacts the sample surface, and in some cases tends to act as an inert marker. In other words, the sulfide scale grows outward, and char particles become embedded in the scale. After the desired exposure time has elapsed, the samples are removed, and the surface is brushed lightly to remove loosely adhering char particles. The sample is weighed, and the extent of the corrosion is expressed as a weight gain per unit area. However, this method suffers from two sources of error. First, not all of the particles adhering to the surface can be removed without dislodging some of the scale. Second, the scale almost always contains some embedded particles which became part of the scale as "markers." Thus, the weight gains are too high, and corrosion rates obtained from weight gains represent the most pessimistic values.

A more realistic measure of corrosion can be obtained by determining how much metal is degraded in a given exposure period. However, this method is destructive, and each datum point represents a different sample. Aside from this shortcoming, the method is laborious and requires a large number of samples.

The bulk of the data reported herein are weight-gain measurements which will give an overly pessimistic outlook. This technique was employed because of its relative simplicity. The errors involved should be about the same percentagewise for all alloys. Limited degradation data are given as backups for weight gain data, Table IV, but they are not available for all tests.

The manner in which the experiments are run is very important, because the sulfur in the char is depleted over a given period of time. The use of a solid reactant, unlike a continuously flowing gas, introduces a finite amount of sulfur which will equilibrate with the atmosphere to yield a certain sulfur fugacity. As the sulfur species is consumed, both the sulfur and oxygen

fugacities change. Thus, the conditions appear to be highly sulfidizing initially, but subsequently the atmosphere becomes oxidizing. The amount of char per sample as well as the frequency with which the char is replaced determine the rates of reaction. The kinetics of reaction between FMC char (2.7% S) and six alloys are shown in Figs. 3-7 for three test conditions. First, 3 gms. of char per sample were reacted with the alloys for a continuous period of 96 hours. Second, the char (3 gms.) was replenished at 24 hour intervals, and third, the char (3 gms.) was replenished every 12 hours. The corrosion rate increased as the replenishment period decreased. The reaction products formed during the 96-hour period were primarily sulfides with lesser amounts of oxides. On the other hand, only sulfides formed when the char was replenished every 12 hours.

The corrosion of the five chromia former alloys in FMC char at 1800 F in 3 gms. of char per sample, replenished every 12 hours is shown in Fig. 8. Four of the alloys exhibited rates in the same general vicinity, whereas Inconel 671 showed a considerably higher rate. The rates were nearly linear with time, although some alloys appeared to corrode less rapidly with increasing time. 310 Stainless Steel spalled excessively after 36 hours and was not tested further.

The corrosion kinetics of these alloys were determined in both the low-sulfur (Husky) and high-sulfur (FMC) chars at both 1600 and 1800^{o}F. The alloys were run together in 50 gms. of char which was replenished every 12 hours. Results are shown in Figs. 9-12. It is interesting to note that higher weight gains were measured for a given time for the experiments performed with 50 gms. of char (10 gms. per sample) compared to those observed when only 3 gms. of char were used, Fig. 8. As stated earlier, this is the "char-quantity" effect which will be covered subsequently.

There is an effect of temperature on the corrosion rate in FMC char for three of the alloys, 310 stainless, Inconel 671 and Haynes 188. The corrosion rates at 1800°F are higher than those at 1600°F as expected. The other two alloys, Incoloy 800 and Hastelloy X, show virtually no temperature dependence on corrosion rates. In fact, if the data are correct, the corrosion rate of Hastelloy X at 1600°F is actually slightly greater than at 1800°F.

A very marked temperature effect was observed concerning corrosion rates in Husky char. The rates at 1600°F in Husky char were considerably less than those in FMC char for all alloys. However, little difference existed in corrosion rates in the two chars for Incoloy 800, Hastelloy X, and Haynes 188 at 1800°F in spite of the difference in sulfur content of the two chars (2.7 vs. 0.9% S for FMC and Husky, respectively). Both 310 stainless and Inconel 671 corroded more rapidly at 1800°F in the higher sulfur char.

The alumina former, FeCrAlY, was received considerably later than the other alloys and was not tested with the chromia formers. The most severe condition was employed, 40 gms. of char, because this was the alloy for which preoxidation treatments appeared promising. The corrosion kinetics of both the GE alloy and of MA 956 were determined at 1800°F in both FMC and Husky chars. Results, Fig. 13, showed very little difference between the alloys and between the low-sulfur and high-sulfur chars. The FeCrAlY alloys corroded more rapidly in Husky char than any of the other alloys and at about the same rate as Inconel 671 in FMC char. In the absence of any preoxidation, this alloy exhibited very poor corrosion resistance and must be rated as the worst alloy.

Comparison between Corrosion in Char and in CGA

It was of interest to establish differences that might exist in corrosion behavior when the CGA gas was used (composition and fugacities

listed in Table III) as a cover gas with char compared to char-argon (and the atmosphere resulting from this combination). Four alloys were tested at Lockheed Space and Missiles Laboratory, Palo Alto, Calif., courtesy Mr. Roger Perkins. The same char, FMC, was used for periods of 24 and 96 hours at 1800°F. Samples were exposed to only CGA in one experiment and to both char (samples embedded in the char) plus CGA in another experiment.

A comparison of the alloys exposed in CGA with and without char is shown in Fig. 14. Hastelloy X exhibited extensive formation of liquid sulfides when CGA was used, but no liquid sulfides formed in char plus argon. Both Inconel 671 and 310 stainless appeared to have good corrosion resistance in these experiments, but when char plus argon was used these alloys exhibited the poorest corrosion resistance.

It should be noted that the char was not replenished during the 96 hour run with the CGA as a cover gas. It is likely that the sulfur pressure was higher during the early stages and continuously decreased with time. No gas analyses were made, thus it is not possible to compare actual H_2S levels with those determined in runs made with char plus argon.

The main conclusion reached from these experiments was that a major difference exists in corrosion resistance of a given alloy between CGA or CGA plus char compared to char plus argon. An alloy that appears to offer outstanding resistance in one environment, e.g., Inconel 671 in CGA, may be the worst in another environment. In fact, a difference of over 3000 times was observed for the corrosion rate of this alloy in the two environments.

Char Replenishment Effect

Figures 3-7 clearly show that the corrosion was more severe as the char was replenished more frequently. This effect is attributed to the changes in both sulfur and oxygen fugacities as the char is depleted during the longer

periods. X-ray diffraction of the reaction products formed when one batch of char was used continuously for 96 hours revealed the presence of oxides, Table V, whereas, replenishment every 12 hours for a total duration of 96 hours resulted in the formation of sulfides only.

The depletion in sulfur content of the char during the course of the reaction was determined by analyzing the char as a function of reaction time for Inconel 671 reacted at 1800°F in FMC char. Table VI lists some values which indicated that a lower limit of approximately 0.5% sulfur was reached for the longer-time experiments. The ash content was also measured from a previous analysis and was used in conjunction with the ash content to calculate the amount of pyrite (FeS) in the char. A value of approximately 0.6% sulfur as FeS was obtained which corresponds to the lower sulfur limit observed in the depleted chars. This means that the organic sulfur was the reacting species and that the pyritic sulfur was not reacting with the alloys to any large extent.

Another way in which the sulfur depletion of char during a run can be ascertained is to measure the H_2S content of the gas during reaction. As will be shown in the discussion of the char quantity effect, there is an equilibrium H_2S content achieved in the absence of samples which corresponds to the amount of char present in the closed system of a given volume. The equilibrium H_2S level is attained rapidly and does not vary with time as long as no samples are present to remove the sulfur. The H_2S in the atmosphere results from the removal of volatile constituents from the char; the pyritic sulfur does not enter into H_2S formation. Samples of two alloys, Haynes 188 and Incoloy 800, were reacted in 5 gms. of FMC of char at 1800°F, and gas samples were taken as a function of reaction time. Table VII shows that the H_2S level decreases during reaction. The calculated ratio of the H_2S to H_2

pressures decreased with reaction time as noted in Fig. 15 for these two alloys. The values of the ratio were lower at any given time for Inconel 671 than for Hastelloy X. Similar curves are given in Fig. 16 for Haynes 188 and Incoloy 800, the latter having lower ratios for all times.

The volatile sulfur was rapidly removed from the char to form an atmosphere containing H_2S. Reaction between the alloys and the gas consumed the H_2S which reduced the sulfur partial pressure, resulting in a decrease in reaction rate during the 12-hour period during which the char was not replenished. Replenishment of the char restores the H_2S level to the equilibrium value.

Char Quantity Effect

The marked effect of char quantity is illustrated in Figs. 17 and 18 for Inconel 671 in FMC char at 1800°F. Fig. 17 shows the kinetics curves for three different char quantities, and Fig. 18 shows the weight gain in 12 hours as a function of char quantity.

The dependence of corrosion rate, as measured by the weight gain in 12 hours at 1800°F, is shown in Fig. 19 for three other alloys, FeCrAlY, Hastelloy X, and Haynes 188, in FMC char. The curves should extrapolate through the origin. The fact that two of the alloys have curves for which the extrapolation gives a positive weight gain is believed to be due to embedded char particles in the scales.

Numerous gas analyses revealed that both the H_2S and CH_4 contents increased with increasing char content as noted in Fig. 20.

Gas Analyses

Gas compositions were determined for various amounts of char; the complete compositions are listed in Table VIII. All of the values were measured except those for hydrogen which could not be determined by gas

chromatography when helium was present. The hydrogen content was calculated from the equilibrium between methane, hydrogen, and carbon, according to the reaction

$$CH_4 = 2H_2 + C \qquad (2)$$

A unit activity of carbon was assumed, and a value of the equilibrium constant of 93.5 at 1800°F[1] gave the following relationship

$$\text{v/o } H_2 = \sqrt{93.5 \times \text{v/o } CH_4}. \qquad (3)$$

The sulfur partial pressure was calculated from the reaction

$$H_2S = H_2 + \tfrac{1}{2}S_2 \qquad (4)$$

which has an equilibrium constant of 7.4×10^3 at 1800°F[1].

Both the CO and CO_2 contents were low as expected from the lack of oxygen in the char. The random variations noted can be rationalized on the basis of the amount of carbonates present. The primary source, if not the only source, of oxygen in the char is the carbonates, but the carbonate quantity can vary from sample to sample with a given batch of char.

The important parameter obtained from the gas analyses, Table VIII and Fig. 21, is the partial pressure of sulfur which is observed to increase with char quantity. Thus, the more rapid corrosion with increasing char quantity is clearly related to the higher sulfur pressure. The linear corrosion kinetics observed experimentally should increase linearly with the sulfur pressure. It may be noted also in Fig. 21 that the sulfur pressure is higher at 1800 than at 1600°F.

Char Particle-Size Effect

The earlier experiments were performed with char of two different sizes, -32 + 42 mesh and -170 mesh. The corrosion rates were greater in the finer char as noted in Table IX. In order to explain this effect, sulfur analyses were made on FMC char which had been sieved to a number of size fractions,

each fraction being analyzed separately. The results, Table X, show that the sulfur content varied from about slightly over 2% for the coarse char to nearly 3% for the finest char. The ash content varied slightly with the particle size, but no definite trends were apparent.

It was also observed in metallographic sections that the coarse char was more readily embedded in the scale than the finer char. The larger particles offer more resistance to movement as the scale grows by outward cation movement, and thus the particles behave as fixed markers as opposed to the finer particles which most likely are pushed outward by the scale.

The absolute reaction rates in finer char are probably much higher than those actually measured for the coarse char, because the weight gains in coarse char contain a larger contribution from embedded particles. Once the particle-size effect had been established and explained, all tests thereafter were performed on char which had been sieved to -32 +42 mesh.

Test Mode--Single versus Multiple Samples

As was noted earlier, the extent of corrosion depended upon whether a sample was run by itself or with other alloys. When several alloys were tested simultaneously the alloy having the poorest corrosion resistance reacted most extensively and thus depleted the atmosphere of sulfur available for reaction with the more corrosion-resistant alloys. This effect is dramatically illustrated for Haynes 188, which was generaly the most corrosion resistant alloy when run with other alloys. The corrosion kinetics are shown in Fig. 22 for individual samples run singularly. The linear corrosion rate was about 25 times greater at 1600 and about 5 times greater at 1800^{o}F compared to rates measured when the alloy was run with the other four chromia formers. A thick, nonprotective sulfide layer formed. The tailing off of the curves at longer times was due to nearly complete consumption of the samples.

The significance of these observations is that the corrosion rates are determined to a large extent by the available sulfur. In other words, if nonresistant alloys are present and preferentially remove the sulfur from the system, a more corrosion-resistant alloy will appear to have good resistance. However, the absolute corrosion rates of all alloys were excessively high when they are run by themselves.

The slightly higher rate at 1600°F compared to 1800°F was due to a higher H_2S/H_2 ratio at the lower temperature. The respective values of the gas ratio were 0.5 and 0.4.

A relative ranking of the alloys can be made from tests performed when all alloys were run simultaneously. Inconel 671 and 310 stainless have the poorest corrosion resistance, and Haynes 188 has the best corrosion resistance. Hastelloy X and Incoloy 800 exhibited intermediate behavior.

The reaction rates for alloys run singularly do not vary nearly as much as when they run simultaneously. Figs. 23 and 24 show the kinetics on plots of log relative weight gain versus reaction time (after the sample had reached the reaction temperature). Haynes 188 was marginally better than Incoloy 800 which was better than Hastelloy X. Inconel 671 was the worst alloy, although it did not appear as poor in these tests as when tested with other alloys.

Effect of Char Presence

The gas analyses revealed that H_2S existed in the atmosphere when char was present and that the H_2S content increased with char quantity. Other experiments showed that samples placed away from the char corroded, supporting the contention that H_2S was the corroding species. It was therefore of interest to see if corrosion in a gas containing just H_2S with no char present resulted in comparable corrosion rates observed in our experiments with char.

Two alloys, Inconel 671 and Hastelloy X, were corroded in H_2-10% H_2S at McMaster University, Hamilton, Ontario, Canada. The gas composition used, 10% H_2S, was slightly higher than the value of 7% measured experimentally in FMC char at 1800°F (980°C). This was the lowest value of H_2s that could be obtained experimentally at McMaster University. However, a lower temperature was used for these experiments, 950°C, and thus the combination of H_2S content and temperature gives a sulfur partial pressure nearly identical to that existing in the FMC char experiments.

Weight gain versus time plots for the two alloys are given in Fig. 25. The calculated values of k_p from these plots are 3.36×10^{-5} and 90.58×10^{-7} $gm^2/cm^4/sec$ for Hastelloy X and Inconel 671, respectively. The corresponding values of k_p in char are 1.09×10^{-8} and 1.58×10^{-7} $gm^2/cm^4/sec$. The ratios of the k_p values in H_2-10% H_2S to those in char are 3.08×10^3 and 6.0 for Hastelloy x and Inconel 671, respectively. Thus, Hastelloy X corrodes much faster in the H_2S environment, and Inconel 671 corrodes slightly faster.

Thus, as corrosive as FMC char is, H_2S giving about the same sulfur pressure was even worse. It appears that the char physically blocks complete access of the gas to the sample surfaces.

Corrosion of Coated Incoloy 800

Some coated samples of Incoloy 800 were received from R. Perkins, Lockheed Laboratories, Palo Alto, CA. and tested in FMC char at 1800°F. The coating consisted of 63%Al-33%Crf-4%Hf and proved to be very effective in reducing the corrosion rate as shown in Fig. 26. However, one of the two samples exhibited spalling after 72 hours reaction.

Characterization of Reaction Products

Sulfidation was the only reaction occurring as long as the char did not become depleted in sulfur sufficiently to allow the oxygen fugacity to rise

and shift the gas composition into the oxide stability field of the stability diagram. It was originally thought that carburization would occur simultaneously with sulfidation due to the high carbon activity existing in the char. However, X-ray diffraction studies and electron microprobe analyses have unequivocally established that carbides did not form.

The reaction generally produced thick external sulfide scales and internal sulfides in the substrate, both within grains and as intergranular particles and/or networks. The general nature of the corrosion products as well as the effect of char replenishment is shown in Fig. 27. The thickness of the external sulfide scale and of the internal sulfidation zone increased with increasing frequency of char replenishment.

The effect of increasing the amount of char per sample on the scale morphology is particularly noteworthy in the case of Incoloy 800. The greater amount of sulfur available resulted in more extensive sulfidation. The samples exposed to 10 gms. of char during each period formed a grain boundary network of sulfides which was "continuous" with the external sulfide scale. The network appeared to anchor the scale mechanically and minimized the subsequent parting of scale from the substrate during either cooling and/or metallographic preparation. Some microstructures of samples exposed to 10 gms. of char are shown in Fig. 28.

Alloys exposed continuously for periods of 50 and 96 hours were observed to form some oxides as noted previously. The scale structure and X-ray images of numerous elements in two of the alloys, Incoloy 800 and Hastelloy X, are shown in Figs. 29 and 30 for a continuous run of 50 hours. Generally, the external scales appear to be mixtures or iron and chromium sulfides with the residual manganese concentrated in the external scale. Some nickel sulfide exists also but to a lesser extent than the other sulfides. Aluminum,

titanium and silicon are present as oxides beneath the sulfide layer and as internal oxides.

A more detailed examination with the microprobe was performed with Incoloy 800 run for a 96 hour continuous period, as shown in Figs. 31-33. The matrix of the alloys, Fig. 31, contained a semi-continous intergranular network of a chromium-rich phase as noted from the EDAX (lower right corner). Aluminum and titanium existed as very fine precipitates within the grains. The internal products formed in these alloys are shown in Fig. 32 which depict the region at the advancing front of the internal attack. The intergranular phases in the internal reaction zone are aluminum and titanium oxides. The sulfides formed inside the grains and were either chromium or manganese sulfides. No carbides were detected. A portion of the region shown in Fig. 32 was examined at a higher magnification as seen in Fig. 33. The sulfur-rich regions are associated only with the chromium-rich regions, whereas, the oxygen-rich regions are associated only with titanium and aluminum. The grain-boundary phase(s) in the internal reaction zone have a different morphology than the grain boundary phase in the unreacted matrix, both of which are apparent in Fig. 33. The chromium-rich phase in the unreacted alloy is a thick, blocky structure, whereas, the grain-boundary phase in the reaction zone is much thinner and more elongated. The implication of this observation is that the chromium-rich phase is not converted to a sulfide in situ. This behavior will be discussed subsequently.

The effect of sulfur content of the char is illustrated in Figs. 28 and 34 at 1800^{o}F for FMC and Husky chars, respectively. A similar sequence at 1600^{o}F is portrayed in Figs. 35 and 36. All micros in Figs. 28 and 34 are at the same magnification and same time, thus the enhanced corrosion in the higher sulfur char (FMC-2.7%S) is readily apparent. This effect existed at

both temperatures, the micros in Fig. 36 being at a much higher magnification than in Fig. 35. The effect of temperature is also readily apparent in these two set of micrographs.

The microstructures of scales formed on all five alloys with the exception of the samples corroded in Husky char at 1600°F, consisted of massive external scales and extensive internal reaction (sulfidation). The details of the structure varied somewhat, depending upon the temperature and the char. Both the external scales and the internal produces are primarily Cr_3S_4 for all alloys. Minor amounts of spinel sulfides, $FeCr_2S_4$, exist in the alloys containing iron, and small amounts of NiS or metallic nickel were found in the scales of the nickel-base alloys. Incoloy 800 always formed a grain-boundary network of internal sulfides, whereas, other alloys such as Inconel 671 and 310 stainless formed random internal sulfides in FMC char at 1800°F but discrete bands of internal sulfides in FMC char at 1600°F and in Husky char at 1800°F. The most notable difference in scale structure was observed on Hastelloy X which showed a much thicker external scale after corrosion in FMC char at 1600°C compared to that formed in the same char at 1800°F. There was little internal sulfidation at the lower temperature. The observed scale structure supports the higher weight gains measured at the lower temperature. There appears to have been a marked change in the reaction mechanism with temperature in FMC char for this alloy.

The scales formed in H_2-10% H_2S were markedly different than those formed during corrosion in char. Inconel 671 formed a thick external scale which was duplex in nature, Fig. 37a. The thinner outer portion consisted of a NiS matrix containing dendrites of Cr_3S_4, the dendrites having some nickel in solution. A very thin rim of NiS, Fig. 37b, was at the outermost extremity of the layer containing the dendrites. The inner layer was compact, although

porosity can be noted in the photomicrograph. The porosity was the result of pullout during polishing and was not caused by sulfidation. The compact layer was Cr_3S_4 which contained some very fine stringers perpendicular to the layer, Fig. 37c. Nickel, chromium, and sulfur were detected in the stringers; the relative peak heights suggests that the stringers are the spinel sulfide, $NiCr_2S_4$. A thin zone of internal sulfidation existed which also appeared to be the spinel sulfide. EDX spectra for all the regions are shown in Fig. 38.

Hastelloy X sulfidized in H_2S formed a thin outer layer seen in Fig. 39. The matrix is a mixed sulfide. An inner zone exists which is about ten times thicker than the outer zone. The matrix is the alloy which is nearly completely depleted in chromium. The dark particles (which appear to touch and to constitute more than half the volume) are chromium sulfide containing some iron. EDX spectra are given in Fig. 40.

It was noted previously that weight gains were measured after brushing the sample to remove loosely adherent char particles. It was also mentioned that char particles became embedded in the sulfide scales because they acted as a Kirkendall marker. An example of an embedded char particle is given in Fig. 41. Large particles became embedded more readily than small particles because the small particles were easily pushed outward and became incorporated into the scale. This behavior clearly shows that the weight gains represent an overly pessimistic measure of the corrosion behavior, because some char is included in the total weight gain.

The marked differences in corrosion behavior between samples tested in char plus argon compared to those test in just CGA may be seen in a comparison of microstructures of the corrosion products. Fig. 42 shows Inconel 671 which formed a thick external scale of chromium sulfide plus a significant zone of internal sulfidation in char. The scale and internal sulfidation layer were

each about 100 microns thick (corroded for 50 hrs.), whereas, the sample test in just CGA formed an adherent, protective film of Cr_3O_3 about 8 microns thick in 96 hours.

A similar behavior was observed for 310 stainless steel, Fig. 43, which formed a thick sulfide scale plus internal sulfides in argon plus char and only Cr_2O_3 in CGA.

The differences are even more striking if the thin Cr_2O_3 films formed in CGA are compared against the corrosion products formed in FMC are compared against the corrosion products formed in FMC char when the char was replenished every 12 hours for the same total time of 96 hours (Fig. 28). The external scales formed in char are more than 100 times thicker than the oxide scales formed in CGA.

The coated samples of Incoloy 800 formed an external scale of Cr_3S_4 and an internal zone of Al_2S_3 precipitates in a matrix of $CrAl_2S_4$. The coating cross section as well as the reaction products are shown in Fig. 44. The complex nature of the coating at the coating-alloy interface, Fig. 44b, is readily apparent. EDX spectra for various regions are shown in Fig. 44c.

DISCUSSION

Corrosion of the six alloys tested in this program in char is a sulfidation reaction. No evidence of carburization was found. However, if the char is not replenished frequently, the volatile sulfur species in the char giving rise to H_2S in the atmosphere will be depleted, and the oxygen fugacity may rise to a value sufficiently high to enable oxides to form. No evidence of oxide formation was observed if the char was replenished every 24 hours or more frequently.

The corrosion products consisted of an external scale and a rather extensive zone of internal sulfidation. The external scales were primarily Cr_3S_4 with sulfides of the base metal and/or spinel (ternary) sulfides of the base metal and chromium. The nickel base alloys also had external scales which contained metallic nickel. It is hypothesized that the metallic nickel formed by a displacement reaction involving the reduction by chromium of a nickel sulfide which formed initially.

$$4NiS + 3Cr = Cr_3S_4 + 4Ni \qquad (5)$$

The internal sulfides were mostly Cr_3S_4 and in some cases MnS. In general the most stable sulfides formed internally.

The scales were quite porous and generally cracked. They offered little protection to the H_2S gas which formed from the char. The gas was able to permeate through the interstices of the char to the metal surface which resulted in the initial formation of a sulfide of the base metal with some chromium sulfidation. The non-protective scale was readily permeated by the gas through the fissures and pores, resulting in further scale formation. Simultaneously, sulfur dissolved into the substrate and reacted with chromium to form internal chromium sulfides.

The reaction kinetics were not quite linear with time, nor were they parabolic. Obviously, some solid-state diffusion occurred in the sulfide, but gaseous permeation of the scale was probably predominant. The near-linear aspect of the kinetics strongly suggested that an interfacial reaction was the rate-controlling step. It was thought earlier that gas-phase diffusion of the gas through the char might be rate-controlling, however, samples partially immersed in char showed equivalent corrosion behavior on both the submerged and exposed portions. Solid-state diffusion through the scale can be relegated to a minor role due to non-parabolic behavior. Thus, let us

consider the interfacial reaction model.

A mass balance for the sulfur is given by:

$$dP_{H_2S} = - \frac{A\ dw}{M_S} \cdot \frac{V_{id}}{V} \tag{6}$$

where A = area of the sample

V = furnace volume

M_S = atomic weight of sulfur

V_{id} = molar volume of ideal gas at STP

dw = incremental change in weight gain per unit area

dP_{H_2S} = incremental change in H_2S partial pressure

$$d\left(\frac{P_{H_2S}}{P_{H_2}}\right) = - \frac{22.4A}{32V} \cdot \frac{dw}{P_{H_2}} \tag{7}$$

or

$$\frac{d\ P_{H_2S}/P_{H_2}}{dt} = - \frac{22.4A}{32V} \cdot \frac{1}{P_{H_2}} \cdot \frac{dw}{dt} \tag{8}$$

It has been shown [2,3] that

$$\frac{1}{P_{H_2}} \cdot \frac{dw}{dt} \propto \frac{P_{H_2S}}{P_{H_2}} \tag{9}$$

thus

$$\frac{d\left(P_{H_2S}/P_{H_2}\right)}{dt} = - \frac{22.4A}{32V} \cdot K_1 \left(\frac{P_{H_2S}}{P_{H_2}}\right) \tag{10}$$

Integration gives:

$$\ln(R) - \ln(R_o) = - K_2(t - t_o) \tag{11}$$

where

$$R = \frac{P_{H_2S}}{P_{H_2}} \quad \text{at time} = t \tag{12}$$

$$R_o = \frac{P_{H_2S}}{P_{H_2}} \quad \text{at time} = t_o \tag{13}$$

t_o = furnace heat up time

$$K_2 = \frac{22.4A}{32V} K_1 = K_3 A K_1 \tag{14}$$

or

$$\ell n\left(\frac{P_{H_2S}}{P_{H_2}}\right)_t = \ell n \left(\frac{P_{H_2S}}{P_{H_2}}\right)_{t_o} - K_2(t_2 - t_o) \tag{15}$$

But

$$\frac{R}{R_o} = \exp[-K_2(t - t_o)] \tag{16}$$

$$\frac{R_o - R}{R_o} = 1-\exp[-K_2(t - t_o)] \tag{17}$$

Integration of the mass-balance equation gives

$$R_o - R = \frac{K_3 A}{P_{H_2}} (w - w_o) \tag{18}$$

$$R_o \left(\frac{P_{H_2}}{K_3 A}\right)^{\frac{w - w_o}{}} = 1-\exp[-K_2(t - t_o)] \tag{19}$$

However, $R_o \left(\frac{P_{H_2}}{K_3 A}\right)$ is the weight gain per unit area if all the available H_2S (at $t = t_o$) is consumed. Hence

$$\frac{w_o - w + w'}{w'} = e^{-K_2(t - t_o)} \tag{20}$$

where

$$w' = R_o \left(\frac{P_{H_2}}{K_1 A}\right) \tag{21}$$

Thus, at $t = t_o$, $w = w_o$, and at $t = \infty$, $w = w' + w_o$

$$\ell n \left(\frac{w_o + w' - w}{w'} \right) = -K_2(t - t_o) \qquad (22)$$

The relative weight gain $\left(\frac{w_o + w' - w}{w'} \right)$ is unity at $t = t_\delta$ (23)

Equations (15) and (22) predict a linear dependence of the log of the pressure ratio and of the log of the weight change with time. The experimental data plotted in Figs. 15, 16, 23, and 24 verify this relationship Thus, it may be concluded that the rate-controlling step is the interfacial reaction between the H_2S in the gas phase and the scale formed on the alloys.

The rate data reported are erroneously high due to the presence of embedded char particles in the scales. Although the data are pessimistic regarding the long-term lifetime of components in coal gasifiers, they should be regarded as the worst possible case. The char-metal reactions have many aspects of gas-solid reactions, but the gaseous reactant is derived from the solid char which completely surrounds the metal. Sulfides are typically cation diffusers, which means that the scale will grow by outward cation migration. Char particles contacting the specimen surface are prevented from moving outward by the restraining effect of other char particles packed in the crucible and particles become embedded in the scale. In other words, the char particles are acting as Kirkendall markers.

The kinetics data plotted in Figs. 9-12 represent weight gains when the five alloys indicated were run simultaneously in 50 grams of char which was replenished every 12 hours. These data vary somewhat from earlier results which were obtained prior to the discovery that the rates were "alloy

dependent." Fig. 23 clearly shows that Incoloy 800 reacts more rapidly than Haynes 188, and Fig. 24 shows that Inconel 671 reacted more rapidly than Hastelloy X. If a rapidly reacting alloy coexists in the char-gas environment with other less rapidly reacting alloys, the results are influenced by the fact that the sulfur is preferentially removed by the most rapidly reacting sample. Thus, the data shown are relative reaction rates for the stated conditions. It is possible to obtain absolute reaction rates by running each alloy separately, but due to the time involved for such tests, it was deemed more expedient to obtain relative rates. It should be noted, however, that Figs. 23 and 24 represent data obtained on individual samples.

Notwithstanding the lack of absolute reaction rate measurements, it is possible to generalize some obvious trends. Inconel 671 and 310 stainless steel exhibited the poorest corrosion resistance under all conditions. Generally Inconel 671 was the worst, although in one case (FMC char at 1600°F) their relative positions were reversed. Haynes 188 and Hastelloy X were the most corrosion resistant in all cases and were nearly identical except for one condition (FMC char at 1600°F) for which Haynes 188 was considerably better. Incoloy 800 was always an intermediate alloy between the worst and the best.

It is interesting to compare these results to those obtained during long-time tests at IITRI[4,5] in the MPC CGA atmosphere*. Inconel 671 survived 10,000 hours at 1800°F with a net weight loss of 2.2 mg/cm^2 and was perhaps the best alloy tested under the conditions of that run (IITRI run No. 29 and continued in No. 42). The reaction rate of Inconel 671 in the MPC CGA environment was about 3000 times less than that measured in FMC char. The

*24% H_2, 18% CO, 12% CO_2, 5% CH_4, 1% NH_3, 0.5% H_2S, 39.5% H_2O

results obtained in the IITRI and UCLA tests are diametrically opposite and clearly point out the danger of assuming that a corrosion resistant alloy in one environment will be corrosion resistant in a different environment. The IITRI tests also revealed that 310 stainless steel exhibited very poor corrosion resistance, but their results on Haynes 188 were variable. There is a high degree of specificity for each alloy and each environment, and thus if an alloy is a candidate in a given system, it must be tested under the anticipated operating environment. There is no extrapolation for the behavior from one system to another. A further verification of this is the behavior of 310 stainless. IITRI tests at 1600°F with 1% H_2S showed that 310 survived 6000 hours exposure with a small weight gain, but at 1800°F with 0.5% H_2S, 310 formed liquid sulfides and had to be removed from the test after only 2000 hours.(4)

The unusual temperature effect on the corrosion rate of Hastelloy X in FMC char, i.e., higher rate at 1600°F than at 1800°F, involves the formation of different reaction products at each temperature as noted in Figs. 28 and 35. The dark phase (Fig. 35) in the sample corroded at 1600°F is mounting compound which infiltrated an extremely porous reaction-product zone which was chromium sulfide and alloy substrate depleted in chromium. The 1600°F sample spalled, whereas, the 1800°F sample did not. It is thought that the spalling led to the porous morphology of the scale at 1600°F, although the mechanism of the process is not understood.

Sulfidation of Inconel 671 and Hastelloy X in H_2S/H_2 at 950° at approximately the same sulfur activity as that existing in the char experiments at 1800°F results in much more rapid attack and a reversal in the relative corrosion resistances of the alloys. The scale structures formed in the two environments are considerably different as noted in Figs. 28, 35 and

37. The reasons for the wide differences in rates in the two systems is not known with certainty, but it is thought that the slow heat-up period in char (about 1 hour) compared to the immediate insertion of the samples into the H_2S atmosphere may cause different reaction products to form at the lower temperatures during heat-up.

The measurement of weight gain is an expedient method by which an approximate measure of the reaction kinetics can be made in spite of the limitations already mentioned. However, the final verdict on how well a given alloy resists the hostile environment is really a question of how much useful metal remains at any time. A significant portion of the reaction results in conversion of metal into an external sulfide scale, but on the other hand, a significant amount of the substance is being converted into something different than the starting metal. The reaction causes internal sulfides to form both within the grains and in grain boundaries. If the char is not replenished often enough, oxide formation also takes place in the grain boundaries. Obviously the sulfide-containing portion of the substrate will possess properties quite different, and most likely inferior to, the original alloy. Selective removal of various alloying constituents from either solid solution or in the form of second-phase particles by the formation of internal sulfides will produce sulfide particles in an alloy-depleted matrix. The strength of the affected zone will decrease, and thus the load-bearing capability of the structural member will decrease.

The depth of penetration of the internal products can be rather appreciable. In fact, some specimens which were originally 1/8" thick have shown complete penetration, meaning that the two fronts coming from opposite sides have met in the center.

The formation of oxides during experiments in which char is not replenished was studied in Incoloy 800. The long-time exposure, 96 hours, caused a change in the alloy microstructure. A grain-boundary phase rich in chromium formed which subsequently dissolved in the substrate near the advancing internal reaction front, chromium diffused toward the exterior, reacted with sulfur diffusing inward to form discrete particles of chromium sulfide inside the grains. Chromium did not appear to oxidize during the long runs. On the other hand, aluminum and titanium existed in the matrix as fine particles within the grains. These particles dissolved also, but the aluminum and titanium appeared to diffuse down the grain boundaries towards the surface where the aluminum and titanium reacted to form grain-boundary oxides. In other words, the intergranular alloy phase supplied chromium to form intragranular sulfides, whereas, the intragranular particles in the alloy supplied aluminum and titanium to form intergranular oxides.

The marked reduction in reaction rate on Incoloy 800 obtained with the coating is attributed to the formation of a compact Cr_3S_4 scale and the presence of both Al_2S_3 and $CrAl_2S_4$. The beneficial effect of chromium[5] has been known for over twenty years. The corrosion rate decreases abruptly at a critical chromium concentration, depending upon temperature and sulfur activity, in a manner analogous to the onset of "stainless" behavior in stainless steels for both oxidation and corrosion in aqueous solutions. A similar behavior exists with aluminum additions.[6] Vineberg[7] has studied the mechanism of the reactions and finds that if sufficient chromium and/or aluminum are in the alloy, the reaction rates are decreased by the formation of continuous layers of Cr_2S_3 and Al_2S_3 which phases form a lamellar reaction product. Reactive-metal additions such as yttrium or hafnium promote the formation of the continuous layers.

CONCLUSIONS

1. Corrosion in char is strictly a sulfidation reaction if the char does not become depleted in sulfur. The reaction produces a massive external sulfide scale consisting of chromium and iron sulfides on iron-base alloys and primarily chromium sulfide on nickel-base alloys. Extensive internal sulfidation occurred in both the substrate grain boundaries and grains to form primarily chromium sulfide.
2. Char particles acted as Kirkendall markers and became embedded in the scales. Large particles were embedded more readily than small particles. This phenomenon showed that outward cation diffusion occurred in the sulfides. Weight gains were always higher than actual weight gains due to the embedded char particles.
3. The char contained volatile sulfur which formed H_2S in the gas as well as pyritic sulfur (about 0.6%) which did not enter into the reactions. The use of a closed system allowed the volatile sulfur to become depleted as it was consumed by the alloys. If the char was not replenished at least every 24 hours or sooner, the sulfides formed initially became slightly oxidized as the gas composition shifted into the oxide field of the respective stability diagrams.
4. A char particle-size effect existed due to a slightly higher sulfur content of the fine char. This effect existed for some of the char, but not all batches behaved similarly.
5. Reaction kinetics depended upon the mode of testing, i.e., whether samples were run singularly or with other alloys. When several alloys were run simultaneously, the less corrosion-resistant ones preferentially

removed sulfur from the system and made the more corrosion-resistant alloys appear better than they actually were. Individual tests revealed much smaller corrosion rates between the various alloys.

6. The reaction kinetics were nearly linear with time. Solid-state diffusion played a relatively minor role. A mathematical model was developed which supported the hypothesis that an interfacial reaction was the rate-controlling step.

7. The reaction rates showed a relatively minor dependence on composition. However, certain trends were obvious. Inconel 671, the best alloy in CGA, corroded the most rapidly in char regardless of char or of temperature. Type 310 stainless was marginally better than Inconel 671. Incoloy 800 was intermediate, whereas, Haynes 188 and Hastelloy X were consistently the most corrosion resistant. The FeCrAlY type alloys corroded extremely rapidly in the absence of preoxidation treatments.

8. Gas analyses of the atmosphere resulting from the char showed increasing H_2S contents with increasing char quantity. The H_2S/H_2 ratio increased with char quantity, giving higher sulfur partial pressures. Corrosion rates increased with char quantity. The log of the pressure ratio decreased linearly with time during reaction, consistent with the proposed model.

9. The high-sulfur char (FMC) was more corrosive than the low-temperature char (Husky) due to a higher H_2S content resulting from the high-sulfur char.

10. Corrosion at 1800°F was generally much greater than at 1600°F with one exception; Hastelloy X appeared to corrode more rapidly at 1600°F in FMC char. This effect has been attributed to the formation of different corrosion products at each temperature.

11. Char plus argon was more corrosive than char plus CGA (MPC-ITTRI gas). Physical contact of the char with the alloy was not necessary as evidenced by extensive corrosion of samples placed downstream from the char.
12. Reaction rates were at least 1000 times more rapid in char than in the CGA-ITTRI tests.
13. Alloys corroded in H_2S-H_2 at a slightly lower temperature (but giving the same sulfur fugacity as in the char experiments) reacted much more rapidly than in char. The presence of char may influence the accessibility of the H_2S to the metal surface.
14. A coating of 63Al-33Cr-4Hf on Incoloy 800 was very effective in reducing corrosion. The beneficial effect was attributed to the formation of chromium and aluminum sulfides and/or spinel sulfides.
15. The reaction fronts on each side met at the center of samples 1/8" thick in 96 hours in some instances.

REFERENCES

1. Darken, L.S. and Gurry, R.W., Physical Chemistry of Metals, McGraw-Hill, N.Y. (1953).

2. Kobayoshi, H.K. and Wagner, C., J. Chem. Phys., 26 (1957) 1609.

3. Turkdogan, E.T., McKewan, W.N., and Zwell, L., J. Phys. Chem., 69 (1965) 327.

4. Schaefer, A.O., "A Program to Discover Materials Suitable for Service under Hostile Conditions Obtaining in Equipment for the Gasification of Coal and Other Solid Fuels", FE-1784-33, Quarterly Progress Report, Metal Properties Council, December, 1977.

5. Backensto, E.B., Drew, R.D., and Stapleford, C.C., "High Temperature Hydrogen Sulfide Corrosion", Corrosion, 12 (1956) 22.

6. Setterlund, R.B. and Prescott, G.R., "Corrosion Characteristics of Iron-Aluminum and Iron-Chromium-Aluminum Alloys in High Temperature Petroleum Applications", Corrosion, 17 (1961) 103.

7. Vineberg, E.J., "The Sulfidation Behavior of Ni-Cr, Ni-Aℓ, and Ni-Cr-Aℓ Alloys with and without Ytrrium", Ph.D. Thesis, School of Engineering and Applied Science, UCLA (1979).

TABLE I

CHEMICAL ANALYSES OF ALLOYS STUDIED

	Fe	Ni	Cr	Co	Mo	W	Aℓ	Ti	Mn	Si	C	B	Cu	P	Y
310 Stainless	53.55	19	24	-	-	-	-	-	2.0	1.5	0.25	-	-	0.045	-
Hastelloy-X	18.4	Bal.	21.9	2.0	9.0	0.64	-	-	0.64	0.49	0.08	0.002	-	-	-
Incoloy-800	46.8	30.7	19.7	-	-	-	0.46	0.49	0.88	0.78	0.04	-	0.67	-	-
Inconel-671	0.30	Bal.	48	-	-	-	-	0.35	0.03	0.03	0.05	-	-	-	-
Haynes 188	1.1	22.9	22.3	Bal.	-	13.6	-	-	0.8	0.4	0.11	0.003	-	0.01	-
GE1541	Bal.	-	14.4	-	-	-	3.8	-	-	-	-	-	-	-	1.0
MA956	Bal.	-	20.0	-	-	-	4.5	0.5	-	-	-	-	-	-	$0.5Y_2O_3$

TABLE II

CHAR ANALYSES*

	FMC (W. Kentucky Colonial Mine, High-Volatile B Bituminous)	Husky (N. Dakota Lignite)
Proximate Analysis, w/o dry		
Volatile Matter	3.5	3.7
Fixed Carbon	81.5	69.2
Ash	15.0	23.1
Ultimate Analysis, w/o dry		
Carbon	75.0	72.3
Hydrogen	1.7	1.6
Nitrogen	1.5	0.9
Sulfur	2.7	0.9
Oxygen	4.1	1.2
Ash	15.0	23.1
Ash Analysis, w/o dry		
SiO_2	47.8	40.7
Al_2O_3	14.0	9.1
Fe_2O_3	24.1	11.5
CaO	3.7	12.7
MgO	0.2	8.7
K_2O	1.3	1.8
Na_2O	4.0	4.0
SO_3	3.9	10.9
TiO_2	0.9	0.6

*The chars and their analyses were supplied by Mr. V. Hill, IITRI, Chicago, Illinois.

TABLE III

GAS COMPOSITIONS

	CGA		Argon
	Raw Gas 70°F	Equilibrated 1 atm., 1800°F	(Liquid Carbonics) 99.998%
H_2	24 V/O	36.6 V/O	
H_2O	39	30.5	5 ppm H_2O
CO	18	20.6	5 ppm O_2
CO_2	12	10.9	
CH_4	5	5.2×10^{-4}	
NH_3	1	0.89	
H_2S	1	2.2×10^{-4}	
P_{O_2}		9.9×10^{-16} atm.	
P_{S_2}		2.4×10^{-6} atm.	
a_c		3.1×10^{-3}	

TABLE IV

COMPARISON OF WEIGHT GAINS, INTERNAL PENETRATION & TOTAL METAL DEGRADATION

Alloy	Test Conditions at 1800° F	ΔW mg/cm^2	Internal Penetration, mils	Metal Degradation,* mils
310 S.S.	96 hrs. - 170, 3gms/specimen	22.0	9.6	9.8
Hast. X	" "	9.1	5.6	4.0
Inc. 671	" "	21.9	7.9	19.0
Inc. 800	" "	14.9	9.0	10.8
Haynes 188	" "	4.1	2.3	10.1
310 S.S.	54.5 hrs. - 170, 3gms/sp.	13.8	6.1	10.3
Hast. X	" "	7.1	4.3	4.8
Inc. 671	" "	15.2	10.3	14.6
Inc. 800	" "	11.9	6.6	9.7
Haynes 188	" "	3.1	0.8	2.7
Hast. X	96 hrs. unsieved, 3gms/sp.	11.6	4.0	7.6
Inc. 671	" "	20.1	4.2	10.2
Inc. 800	" "	17.7	16.0	26.8
Haynes 188	" "	4.3	4.0	5.6
310 S.S.	4 x 24 hrs., unsieved, 3gms/sp.	44.1	12.5	13.9
Hast. X	" "	29.4	6.8	8.1
Inc. 671	" "	27.5	15.2	31.5
Inc. 800	" "	34.4	12.2	12.3
Haynes 188	" "	9.7	3.6	25.1
Hast. X	8 x 12 hrs., unsieved, 3gms/sp.	36.7	15.7	17.1
Inc. 671	" "	98.7	21.1	22.7
Haynes 188	8 x 12 hrs., unsieved, 3gms/sp.	41.0	7.9	25.0
Hast. X	12 hrs., unsieved, 10gms/sp.	15.5	5.9	24.5
Haynes 188	" "	19.2	5.9	29.0

*Original thickness - distance between internal "fronts") ÷ 2

TABLE IV (continued)

Alloy	Test Conditions at 1800° F	ΔW mg/cm^2	Internal Penetration, mils	Metal Degradation,* mils
GE 1541		45.8	7.9	27.0
310 S.S.	2 x 12 hrs. unsieved, 10gms/sp.	101.0	15.8	16.3
Hast. X	" "	33.0	11.8	19.1
Inc. 671	" "	110.0	15.2	12.7
Inc. 800	" "	39.2	18.3	14.8
Inc. 671	1 x 12 hrs. unsieved, 10gms/sp.	44.2	7.9	14.0
Inc. 671	" " 20gms/sp.	70.2	6.9	9.7
Inc. 671	" " 40gms/sp.	88.7	17.7	29.6
Inc. 671	1 x 12 hrs., unsieved, 40gms/sp.	84.6	14.4	28.3
Inc. 671	2 x 12 hrs., " 20gms/sp.	105.9	21.6	29.7
Inc. 671	1 x 24 hrs., " "	90.0	20.4	39.5
Inc. 671	2 x 12 hrs., " 10gms/sp.	67.1	13.6	30.4

TABLE V

X-RAY DIFFRACTION ANALYSES - EFFECT OF CHAR REPLENISHMENT ON THE REACTION PRODUCTS FORMED*

Alloy	No Char Replenishment (96 hrs. continuous run)	With Char Replenishment (8-12 hours intervals)
310 Stainless	$NiFe_2O_4$, Cr_2O_3, Cr_7S_8(?)	Cr_3S_4, $FeCr_2S_4$
Hastelloy X	Cr_2O_3, $NiFe_2O_4$	Cr_3S_4
Inconel 671	Cr_2O_3, Cr_3S_4	Cr_3S_4
Inconel 800	Cr_2O_3, $NiFe_2O_4$	Cr_3S_4, $FeCr_2S_4$
Haynes 188	Cr_2O_3, $NiFe_2O_4$(?)	Cr_3S_4
	Cr_5S_6(?)	

*Analyses performed on the sample surface and probably represent only the external scale due to non-penetration of the beam beneath the scale. The phases are listed in order of their abundance.

TABLE VI

SULFUR CONTENT OF CHAR AFTER REACTION

Time (hours)	%S	
0	2.59,	2.78
12	0.71,	0.61
24	0.50,	0.33
50	0.77	
96	0.55	

TABLE VII

H_2S DEPLETION DURING REACTION IN FMC CHAR AT 1800° F

Alloy	Time (hours)	Weight Gain, mg/cm^2	v/o H_2S
Haynes 188	t_o	0.77	2.7
"	$t_o + 2$	4.18	2.5
"	$t_o + 4$	5.53	1.9
"	$t_o + 8$	6.99	1.8
"	$t_o + 10$	7.70	1.5
Incoloy 800	t_o	1.35	2.4
"	$t_o + 2$	5.37	2.0
"	$t_o + 4$	8.84	1.7
"	$t_o + 10$	10.11	1.5

*t_o = furnace heat-up time. Some reaction occurs during heating.

TABLE VIII

COMPOSITION OF QUENCHED FURNACE GASES

Cover Gas	Char Weight (gm)	Volume Percent*					P_{H_2S}/P_{H_2}	$P^{\cdot}_{S_2}$ at 1800° F
		H_2S	CO	CO_2	CH_4	H_2		
He	6	2.60	0.066	0.51	1.2	10.6	0.25	3.4×10^{-6}
He	10	3.15	0.058	0.12	1.6	12.2	0.26	3.7×10^{-6}
He	20	3.77	0.061	0.12	2.1	14.0	0.27	4.0×10^{-6}
He	20	3.77	0.085	0.80	1.3	11.0	0.34	6.3×10^{-6}
He	30	5.21	0.054	0.26	3.1	17.0	0.31	5.3×10^{-6}
He	40	6.15	0.073	1.50	2.8	16.2	0.38	7.9×10^{-6}
He	50	6.99	0.082	1.70	3.5	18.1	0.39	8.3×10^{-6}
Ar	60	8.00	0.048	0.11	4.3	20.1	0.40	8.8×10^{-6}

*Balance - Cover Gas

TABLE IX

EFFECT OF CHAR PARTICLE SIZE ON

CORROSION WEIGHT GAINS AT 1800°F

Alloy	Time (hours)	Char Quantity, gms	Char Size	Weight Gain, mg/cm^2
Hastelloy X	96	3	Coarse	0.58
"	96	3	Fine	4.05, 6.11, 9.09
Inconel 671	96	3	Coarse	-1.56
"	96	3	Fine	6.78, 21.9
Incoloy 800	96	3	Coarse	3.24
"	96	3	Fine	4.95, 14.9
310 Stainless	96	3	Coarse	1.92, 1.75
"	96	3	Fine	22.0
Hastelloy X	12	10	Coarse	12.0, 23.2, 11.8
"	12	10	Fine	32.4, 37.0
Inconel 671	12	10	Coarse	8.54
"	12	10	Fine	61.3

TABLE X

SULFUR AND ASH CONTENT OF SIEVED FMC CHAR

Mesh	w/o of Total	% S	% Ash
+ 24	16.3	2.02, 2.26	10.9
- 24 + 32	4.3	2.03	13.4
- 32 + 42	6.7	2.00, 2.18	11.7, 14.6
- 42 + 60	11.9	1.96	11.7
- 60 + 80	11.2	2.50	14.2
- 80 + 115	10.8	2.86	12.6
- 115 + 170	10.2	2.87	11.3
- 170	28.6	2.98, 2.94	11.4, 11.2

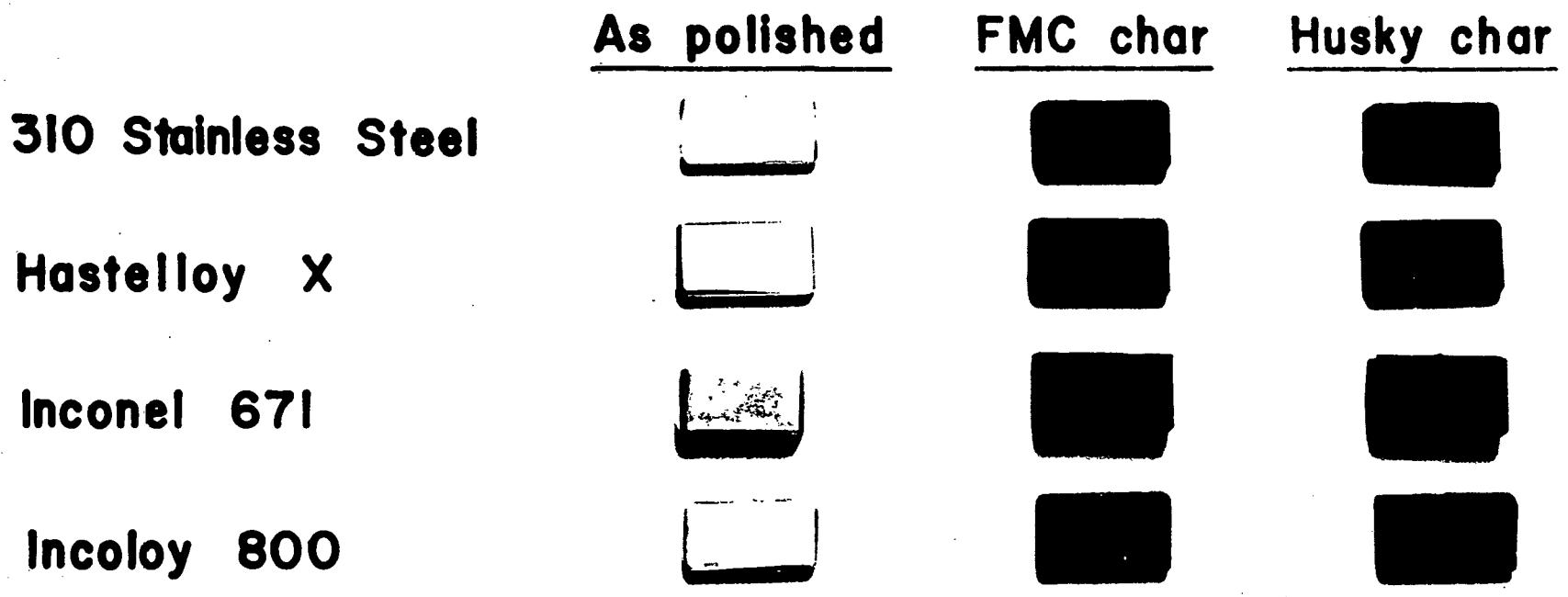

FIG. 1. ALLOYS EXPOSED 50 HRS. TO CHAR PLUS ARGON AT 1800°F

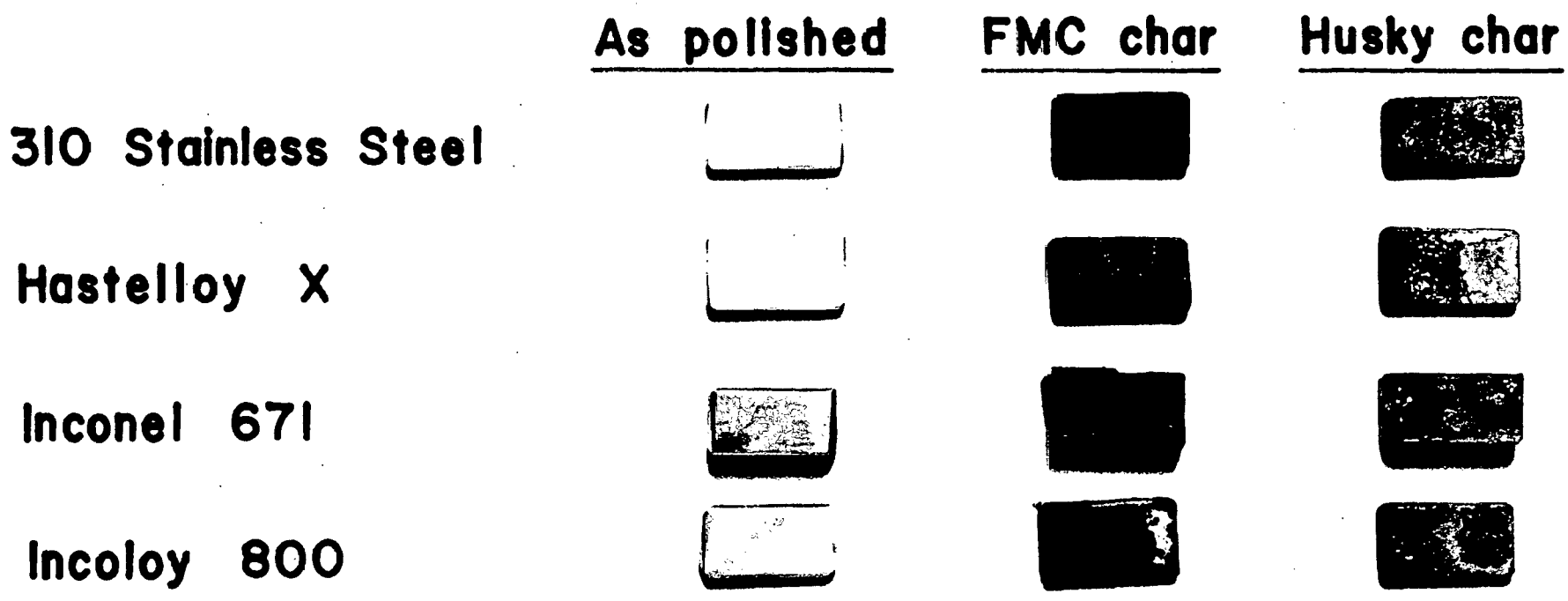

FIG. 2. ALLOYS EXPOSED 50 HRS. TO CHAR PLUS FLOWING ARGON DOWNSTREAM FROM CHAR AT 1800°F.

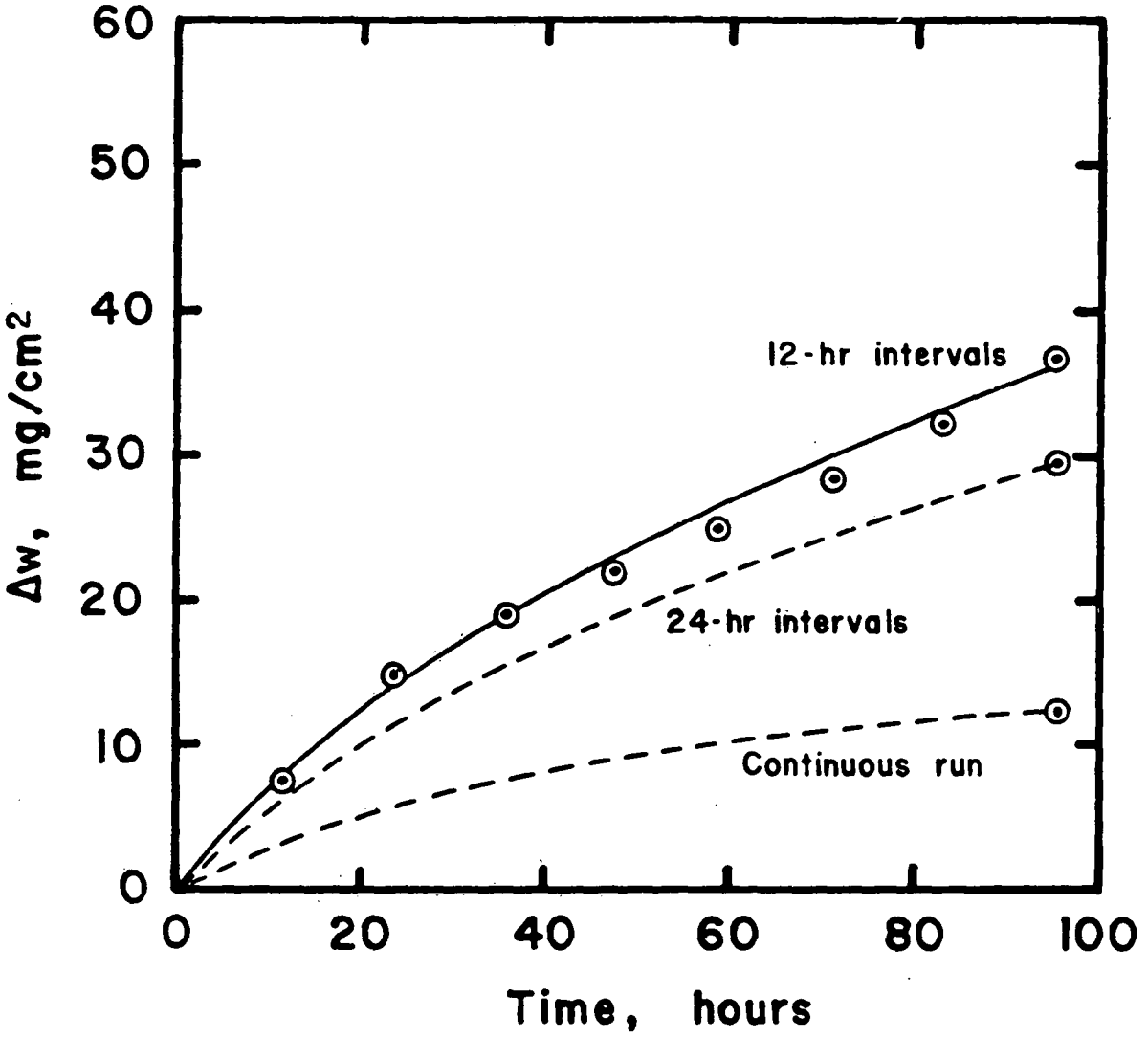

FIG. 3. EFFECT OF CHAR REPLENISHMENT ON THE CORROSION KINETICS OF HASTELLOY X AT 1800°F.

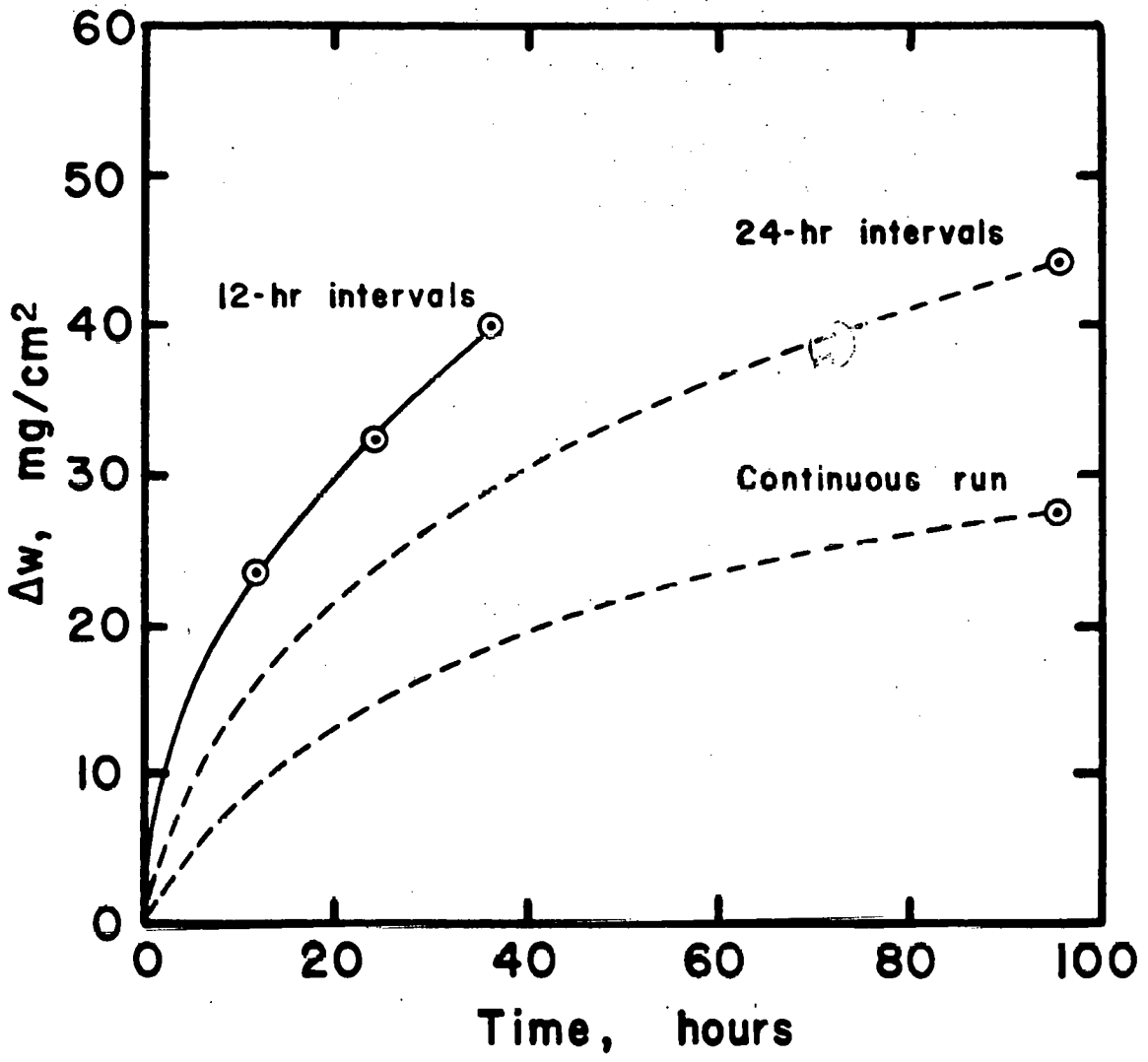

FIG. 4. EFFECT OF CHAR REPLENISHMENT ON THE CORROSION KINETICS OF 310 STAINLESS STEEL AT 1800°F.

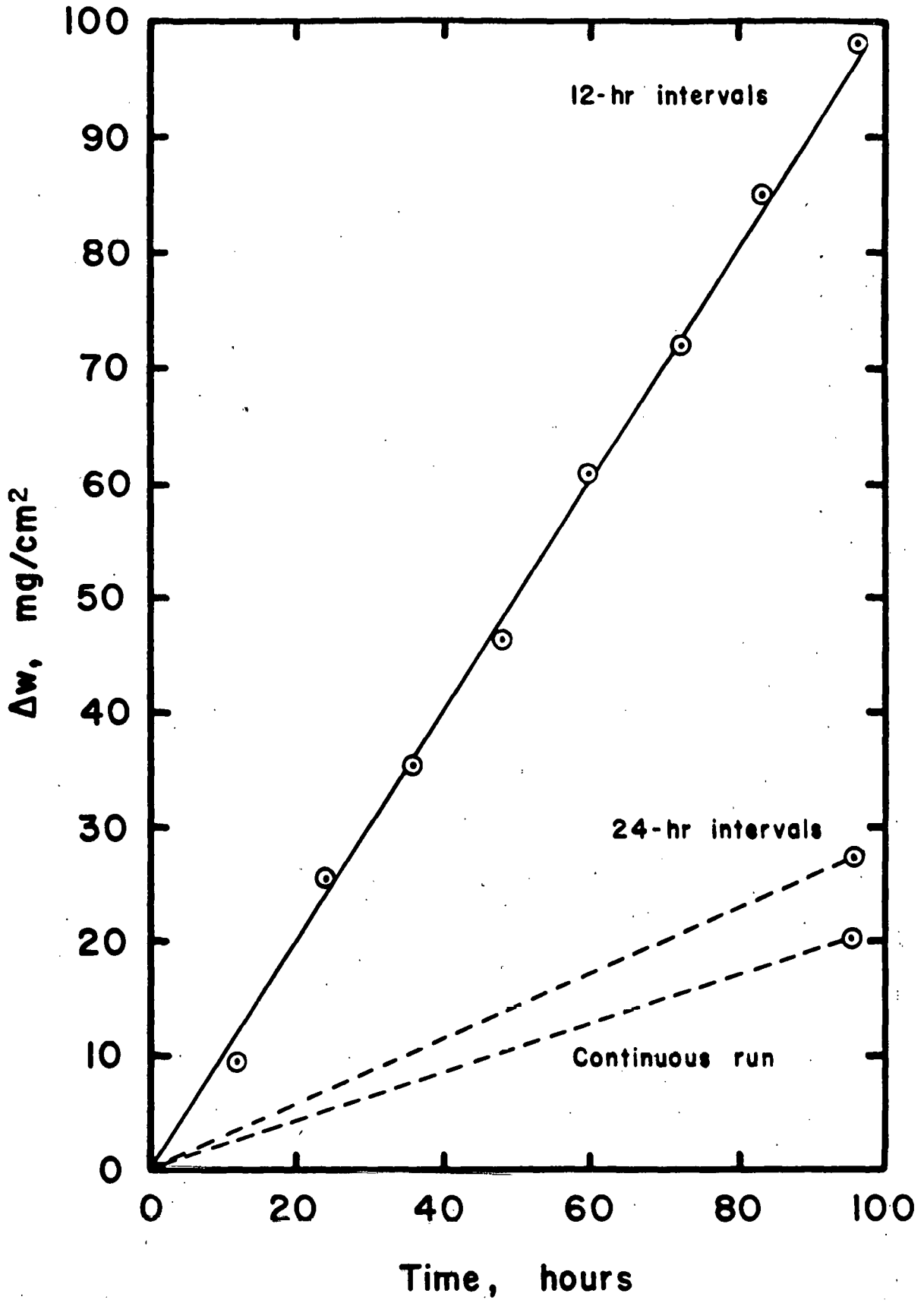

FIG. 5. EFFECT OF CHAR REPLENISHMENT ON THE CORROSION KINETICS OF INCONEL 671 AT 1800°F.

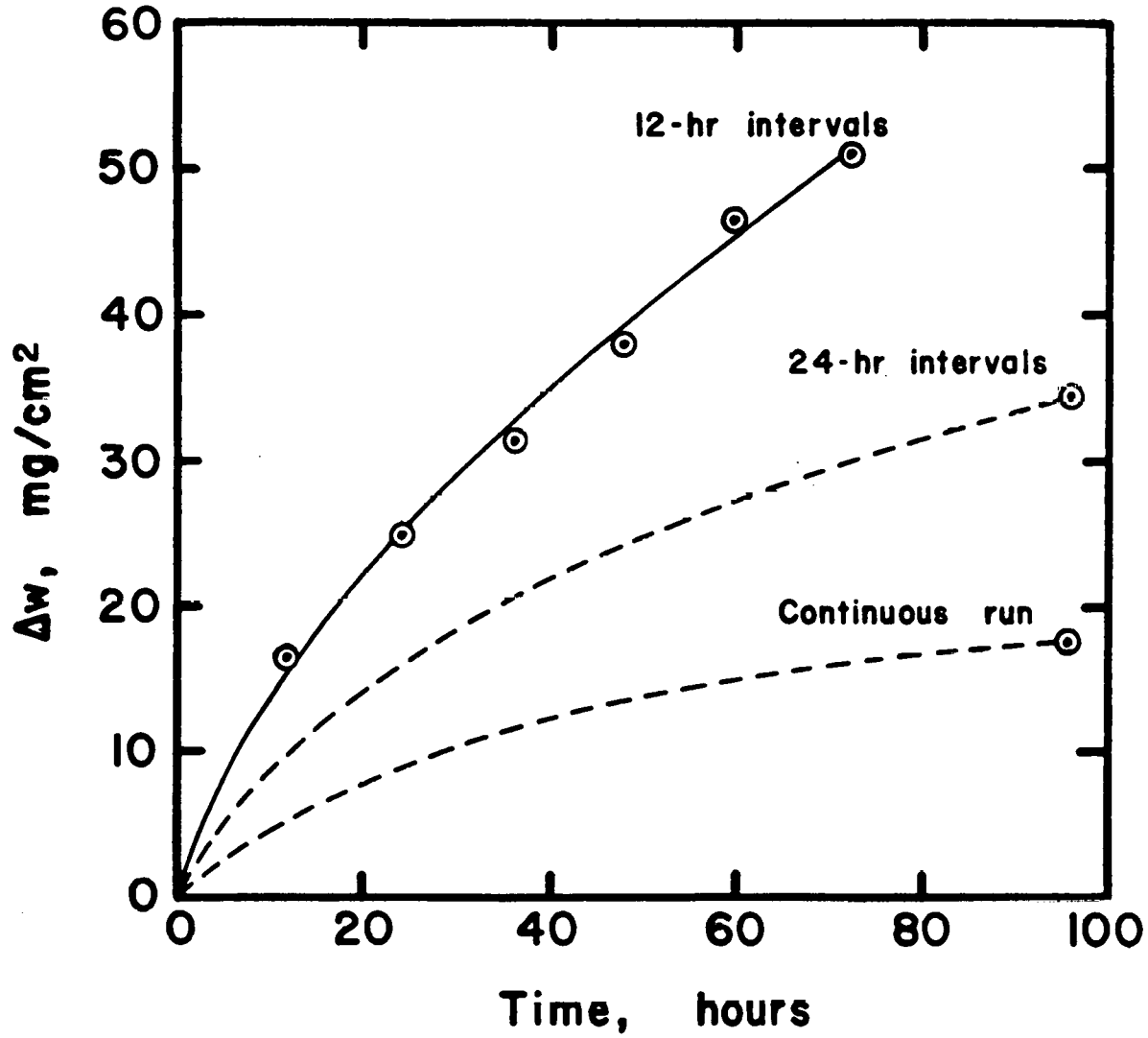

FIG. 6. EFFECT OF CHAR REPLENISHMENT ON THE CORROSION KINETICS OF INCOLOY 800 AT 1800°F.

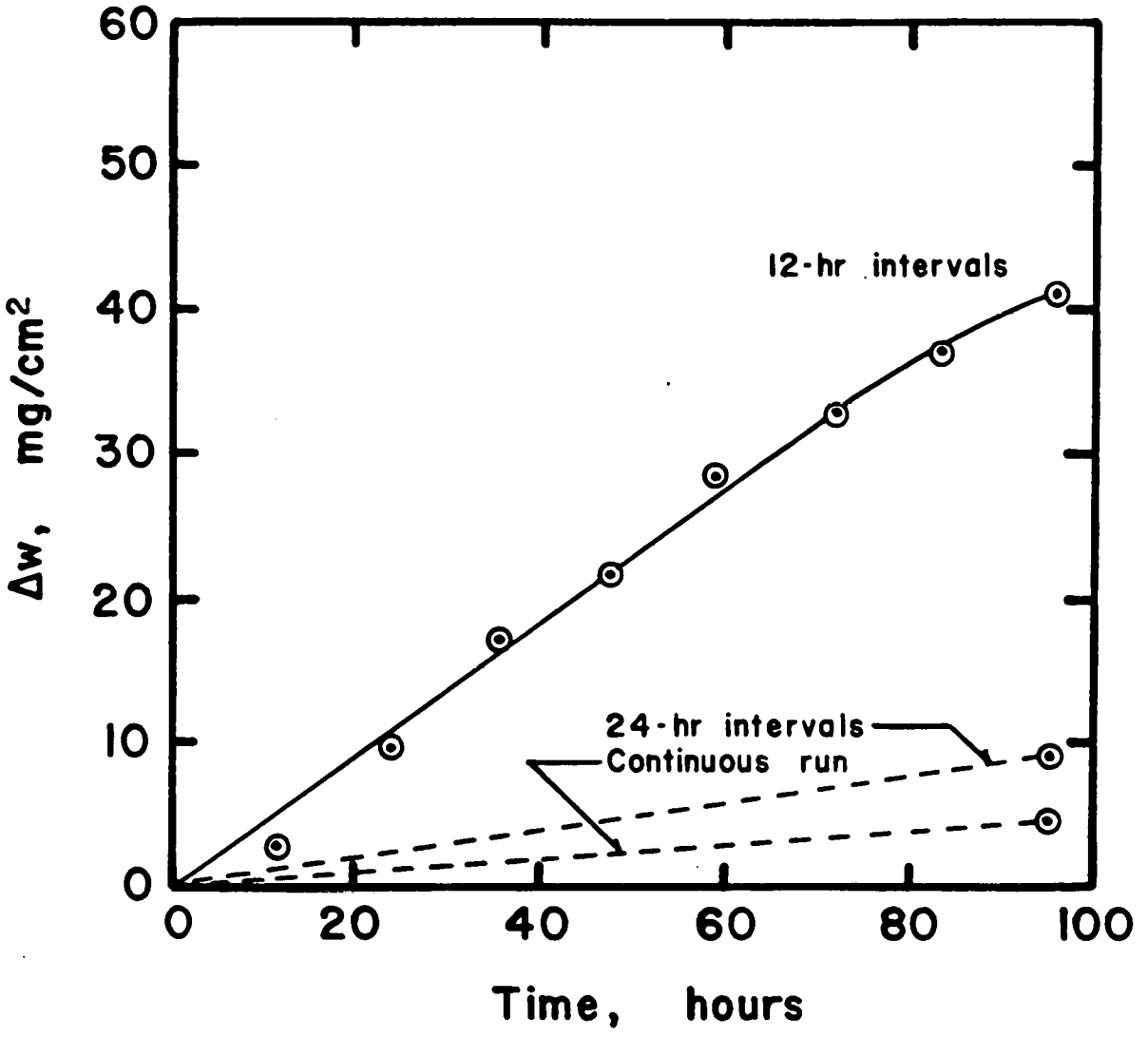

FIG. 7. EFFECT OF CHAR REPLENISHMENT ON THE CORROSION KINETICS OF HAYNES 188 AT 1800°F.

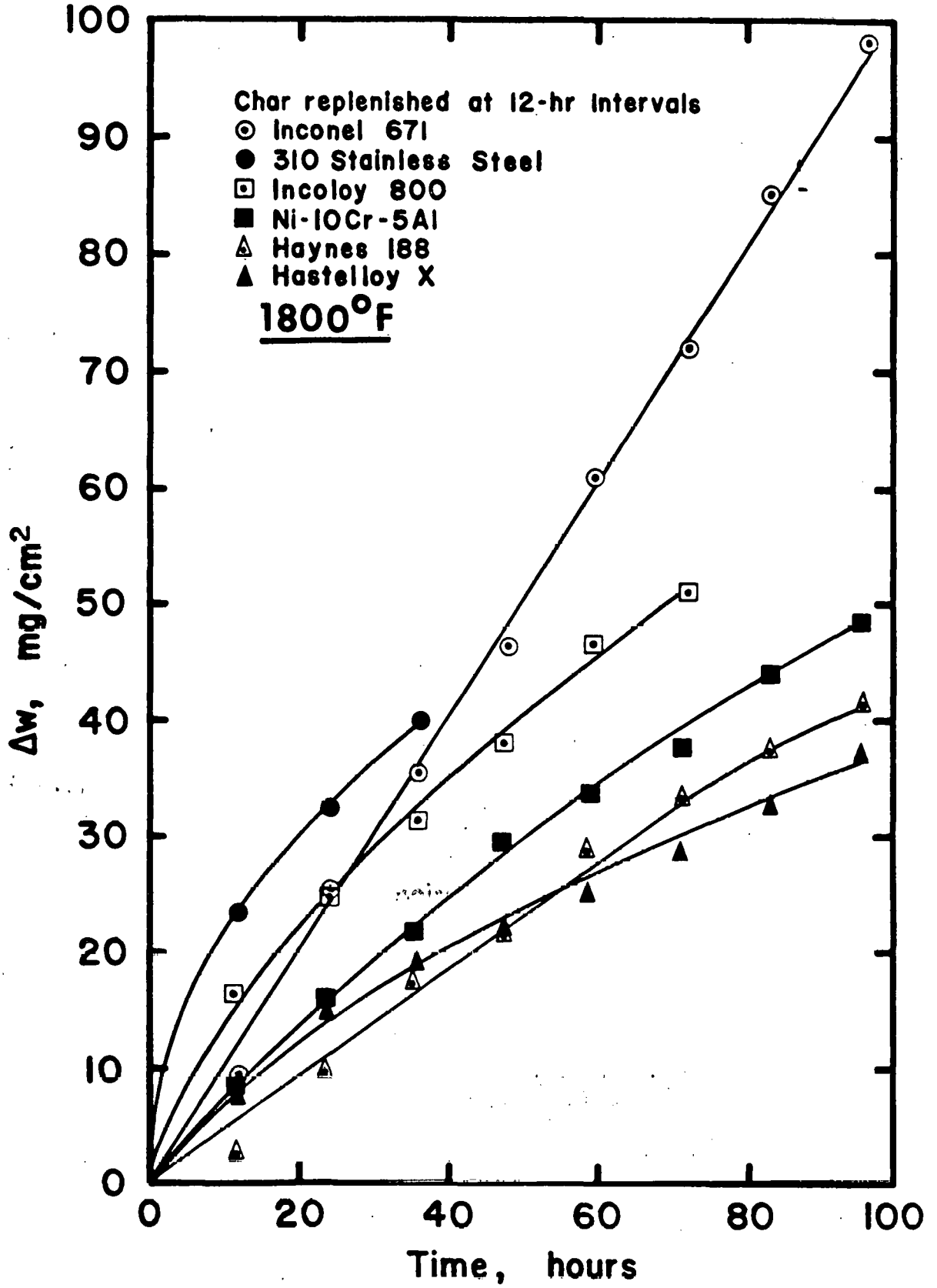

FIG. 8. COMPARATIVE CORROSION KINETICS AT 1800°F IN FMC CHAR REPLENISHED EVERY 12 HRS.

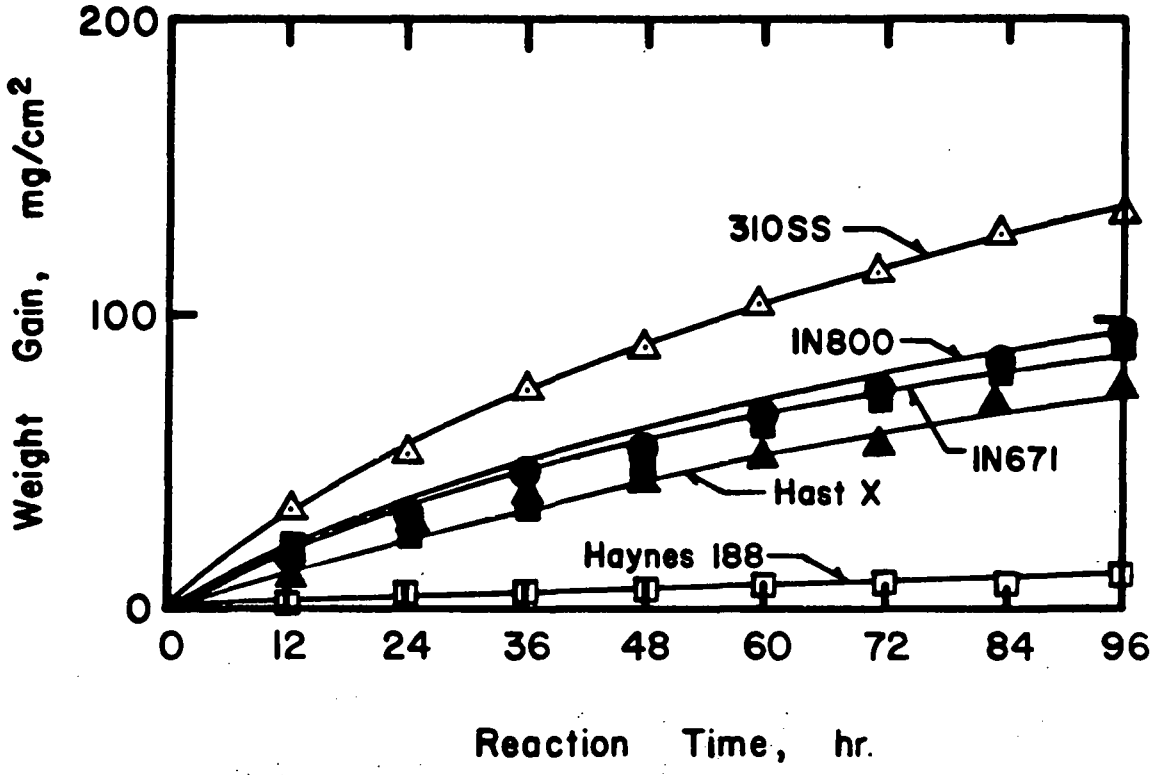

FIG. 9. CORROSION KINETICS IN FMC CHAR AT 1600°F.

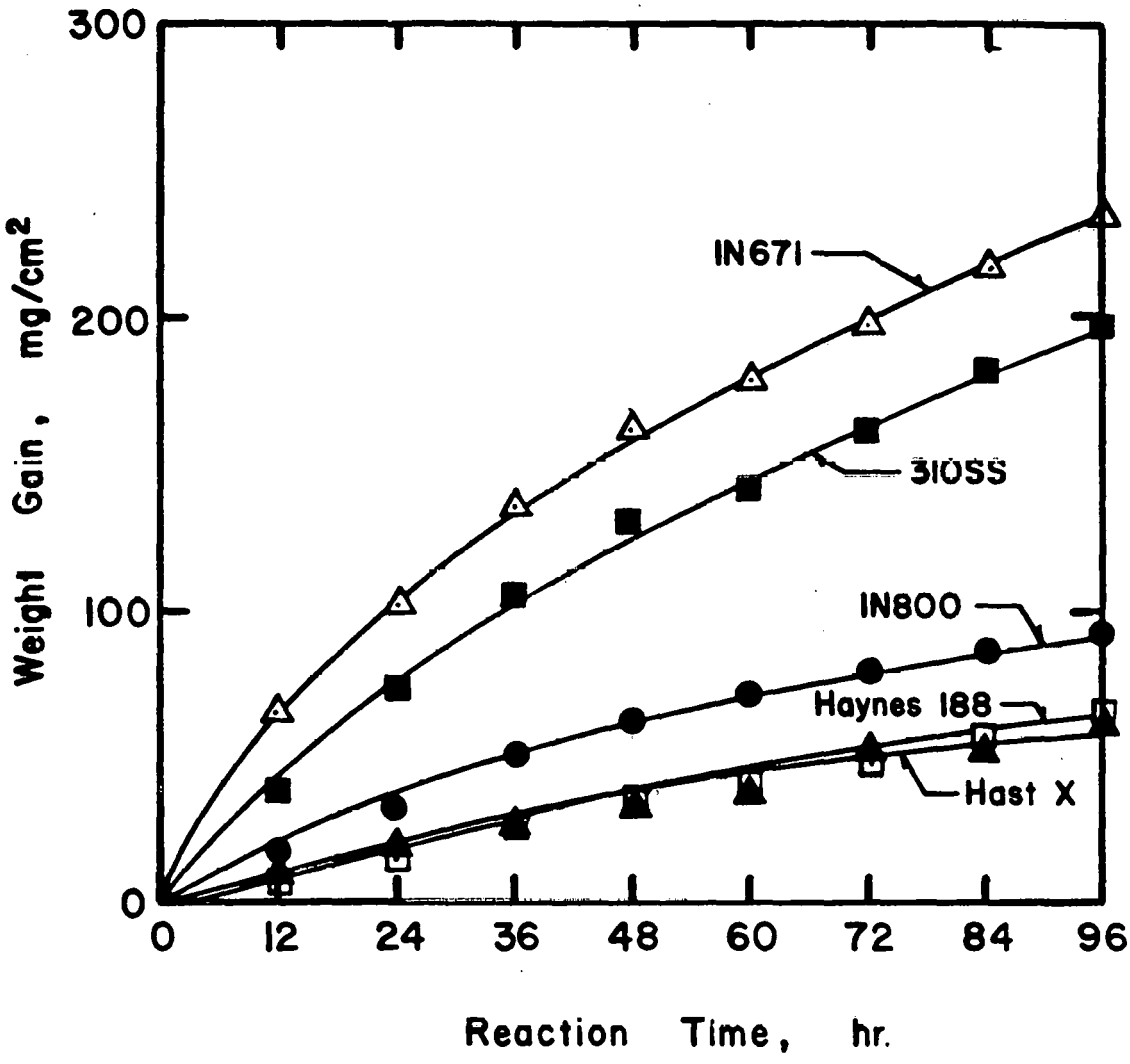

FIG. 10. CORROSION KINETICS IN FMC CHAR AT 1800°F.

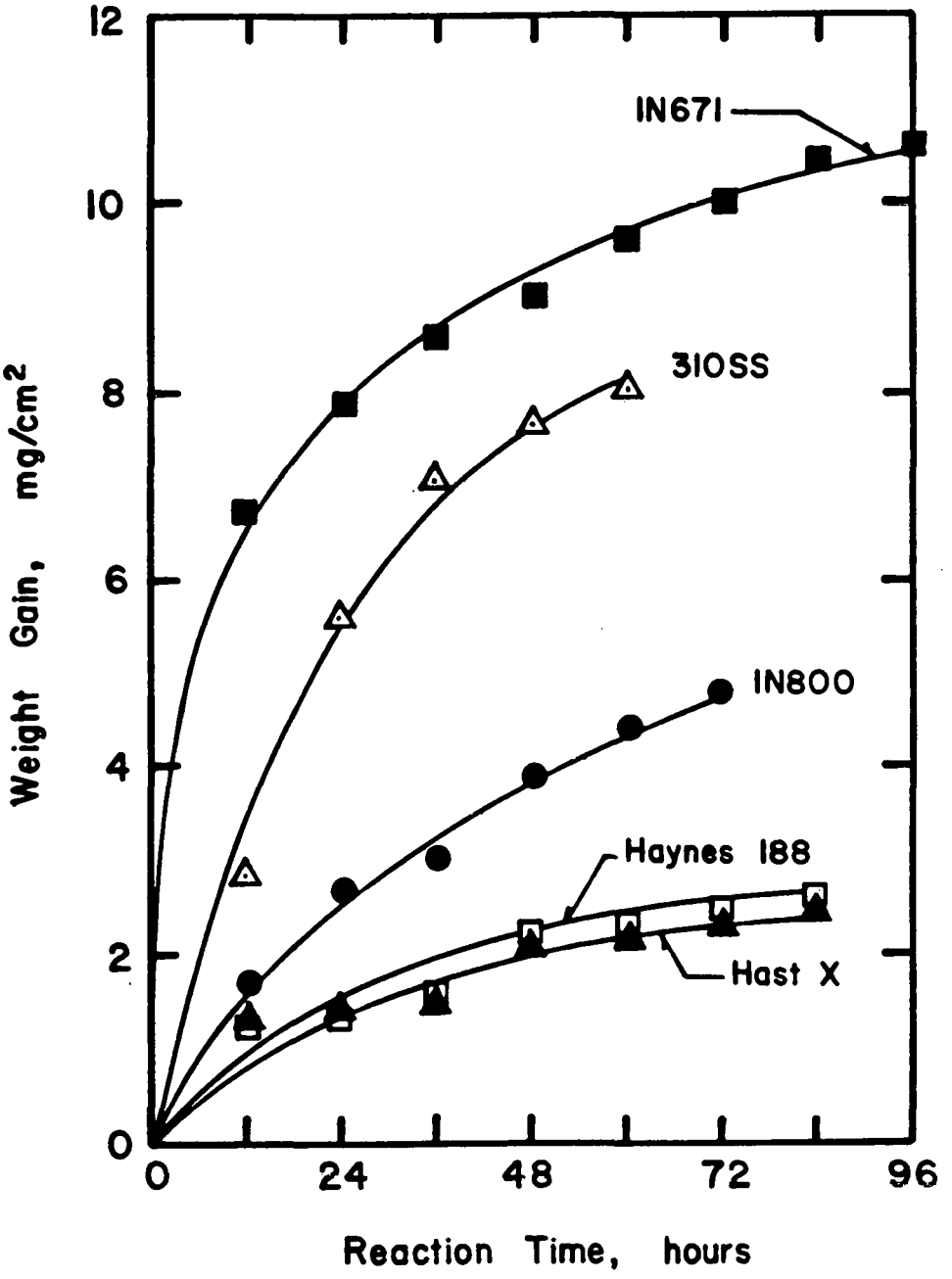

FIG. 11. CORROSION KINETICS IN HUSKY CHAR AT 1600°F.

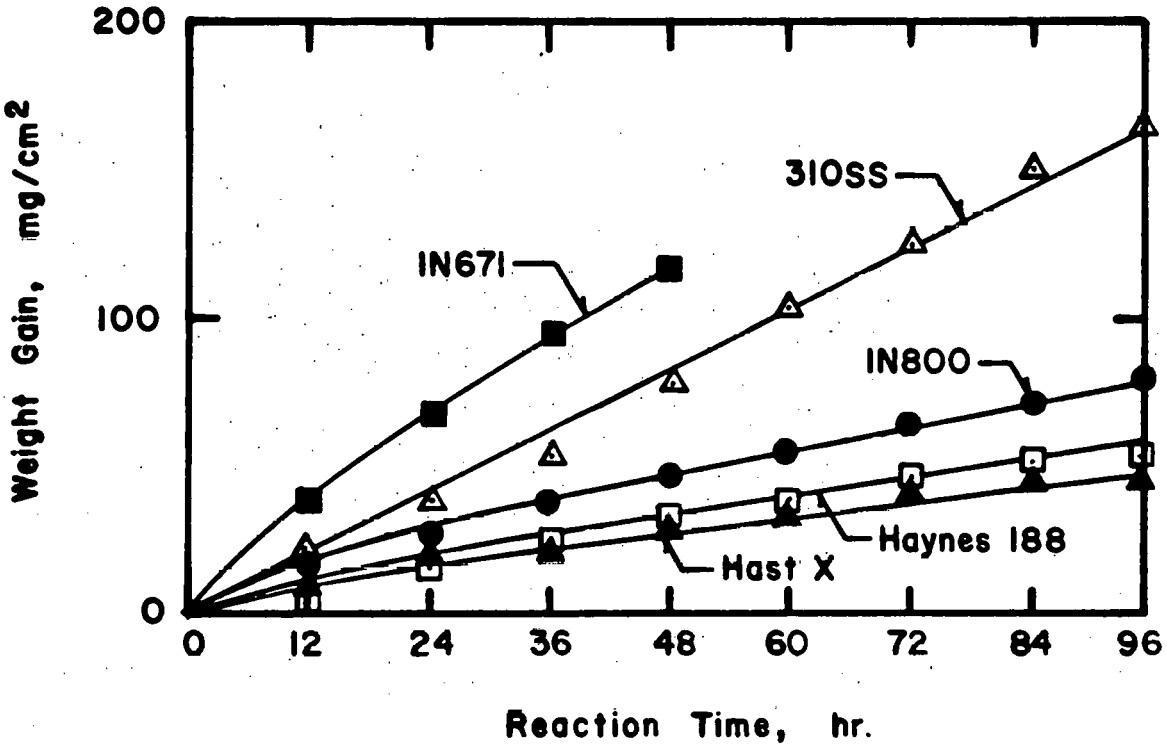

FIG. 12. CORROSION KINETICS IN HUSKY CHAR AT 1800°F.

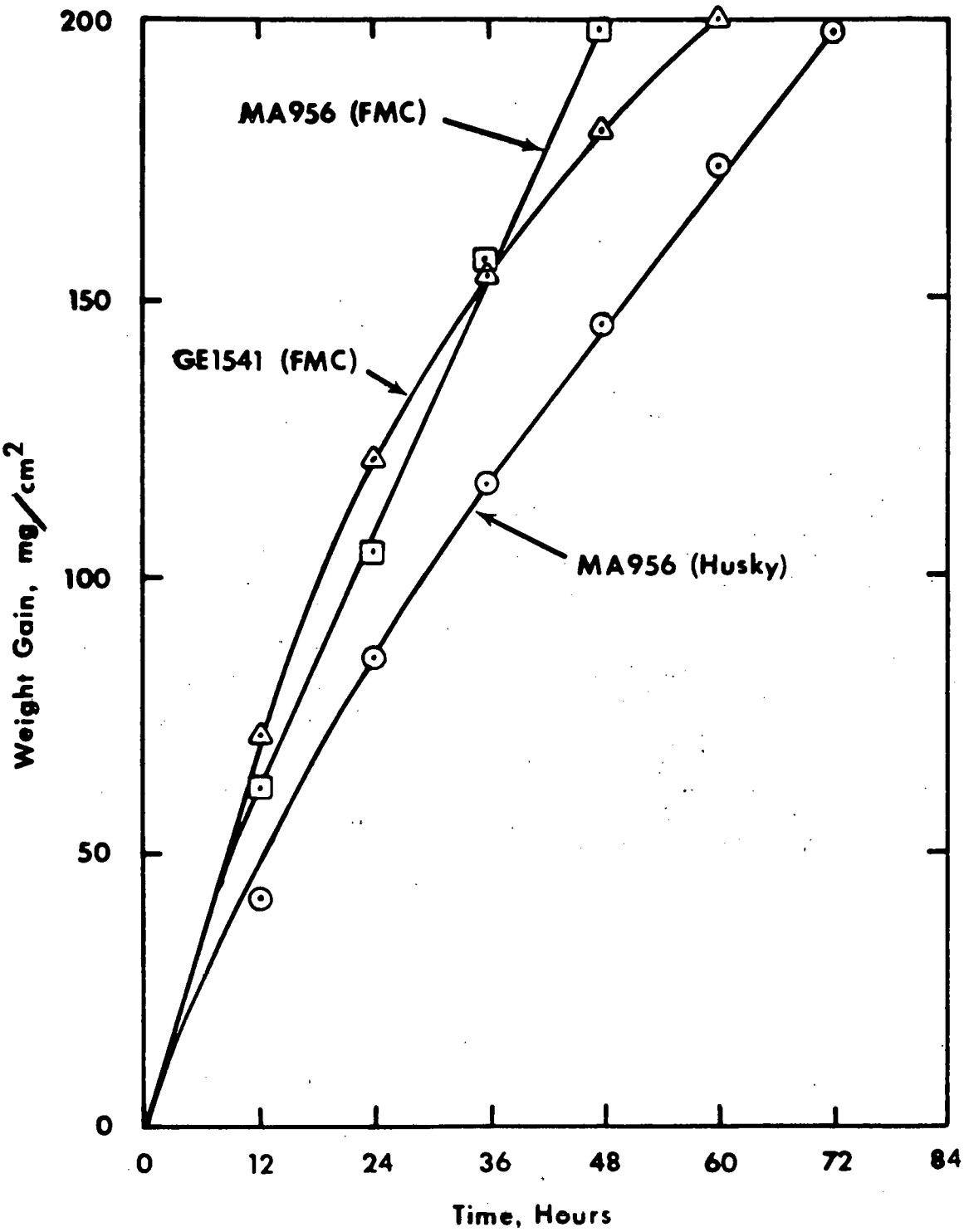

FIG. 13. CORROSION KINETICS OF FeCrAlY ALLOYS AT 1800°F.
TEN GMS. CHAR PER SAMPLE; CHAR REPLENISHED EVERY 12 HRS.

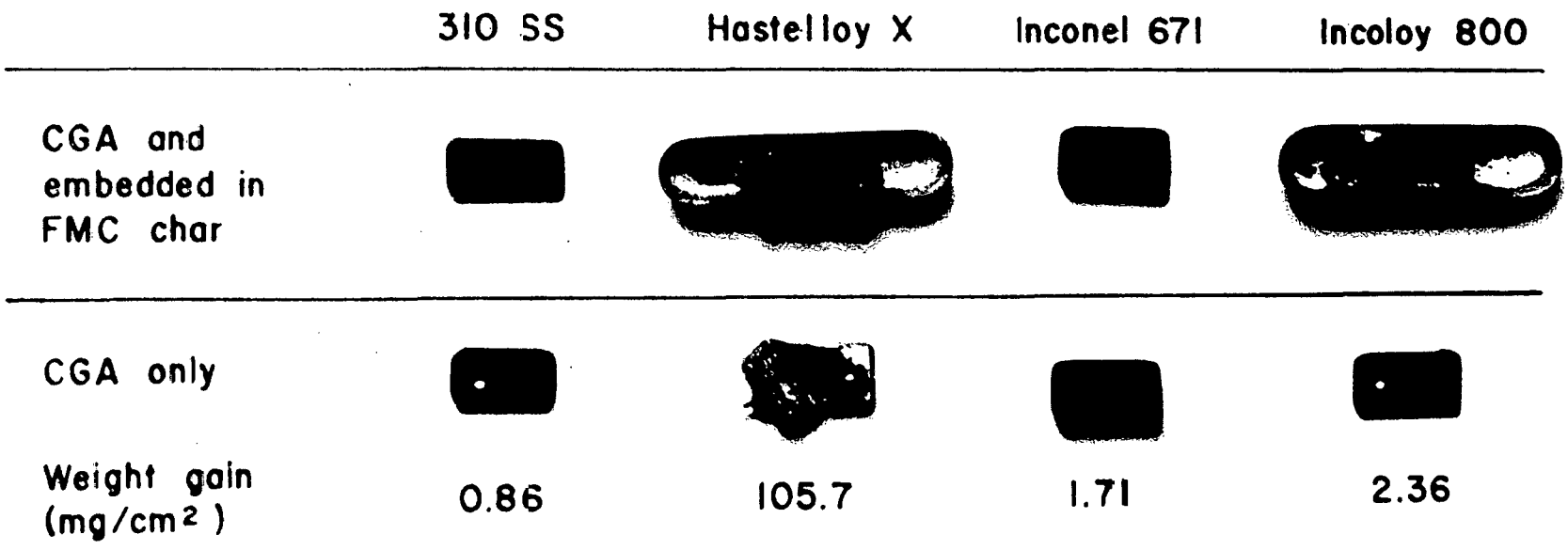

FIG. 14. COMPARISON OF ALLOYS EXPOSED 96 HRS. AT 1800°F IN CGA WITH AND WITHOUT CHAR (FMC).

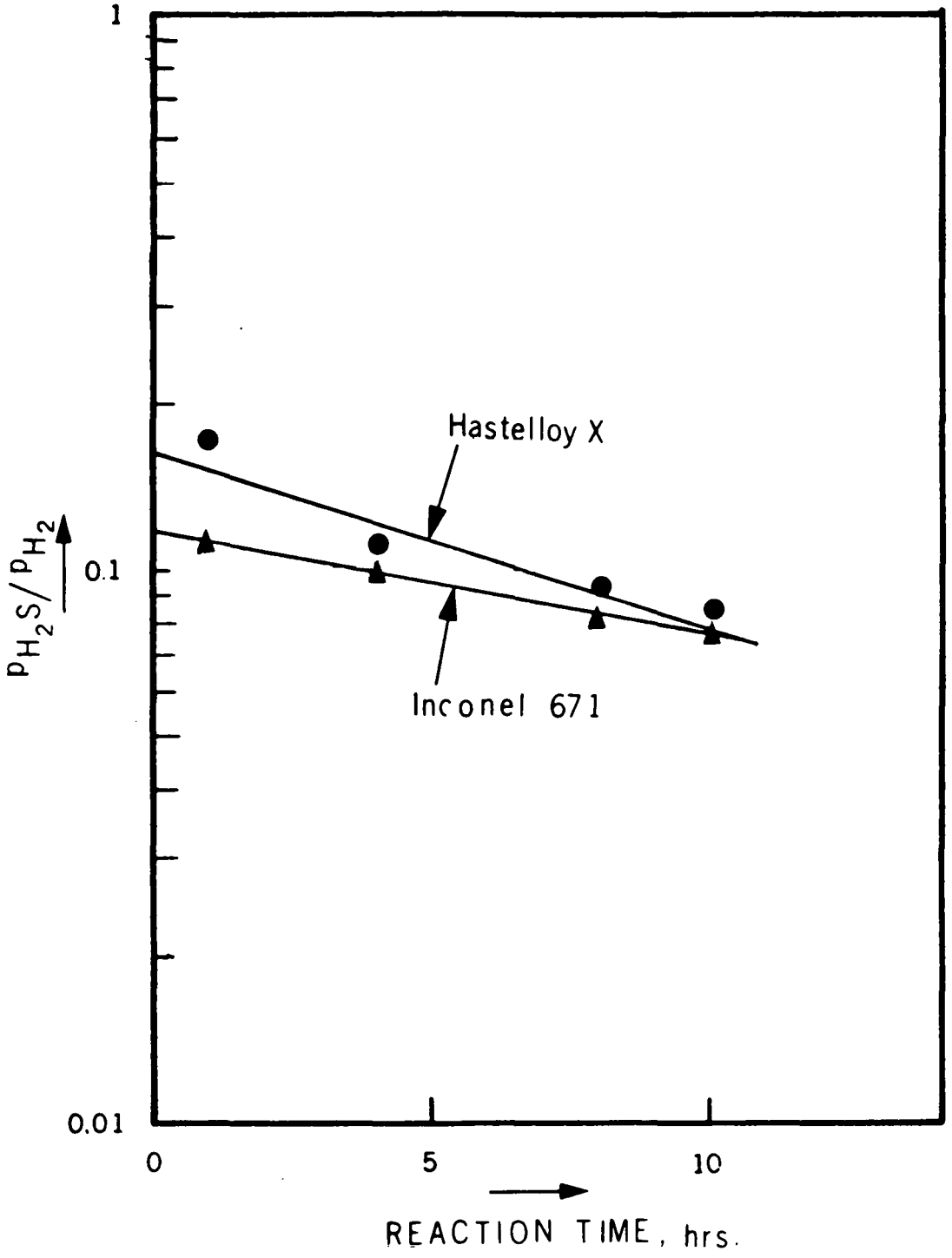

FIG. 15. VARIATION OF GAS COMPOSITION DURING CORROSION OF HASTELLOY X AND INCONEL 671 IN FMC CHAR AT 1800°F.

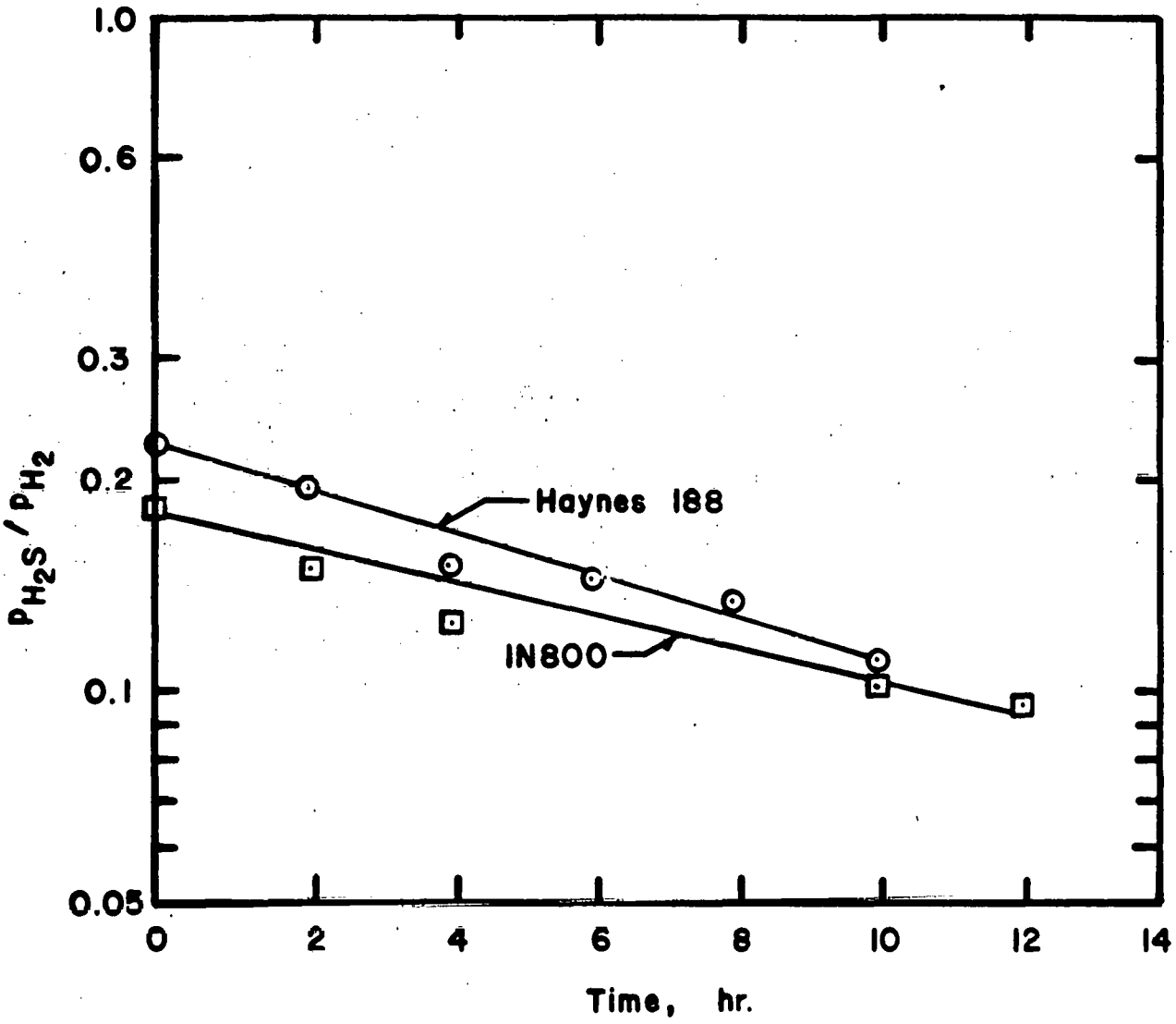

FIG. 16. VARIATION OF GAS COMPOSITION DURING CORROSION OF HAYNES 188 AND INCOLOY 800 IN FMC CHAR AT 1800°F.

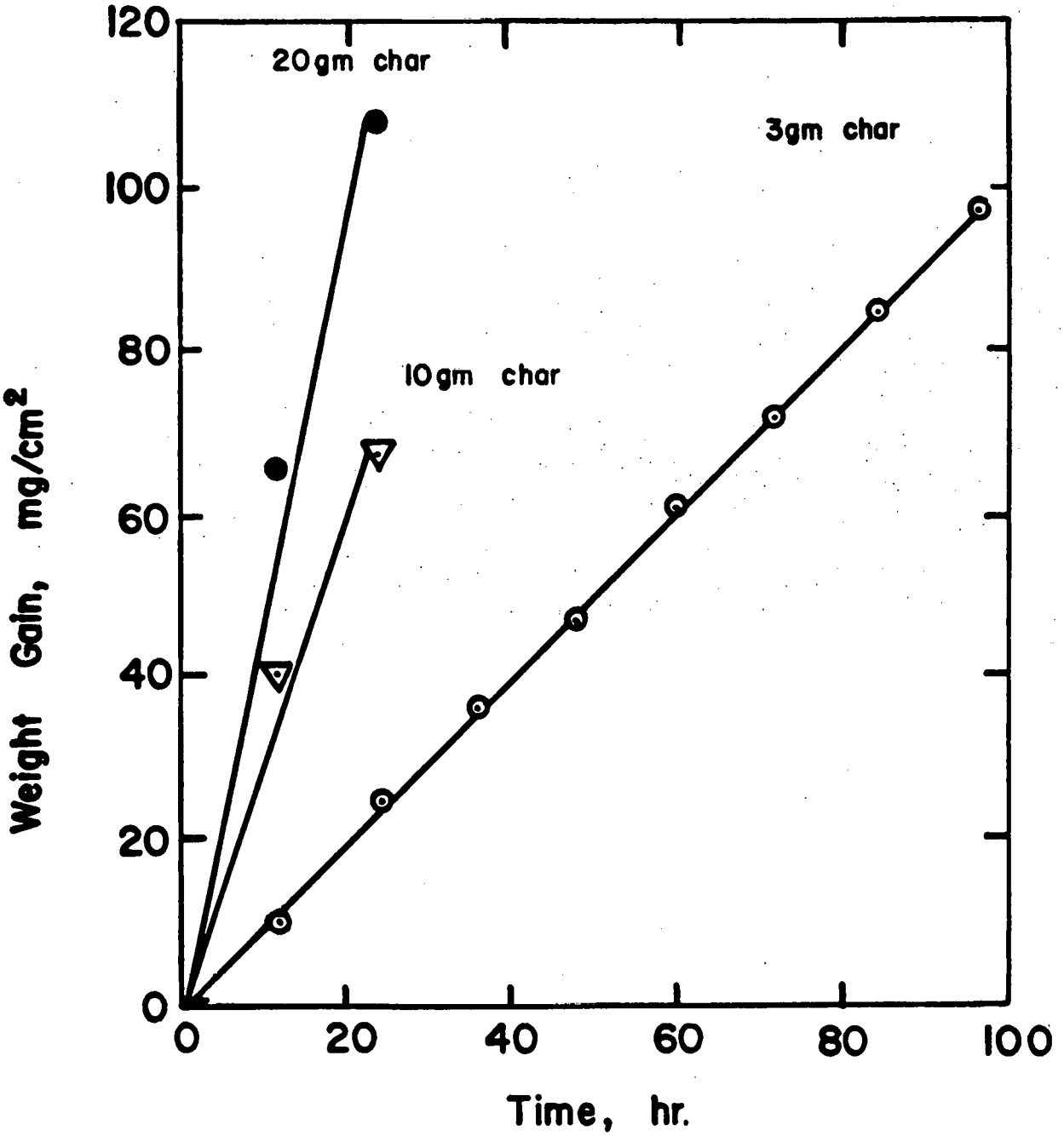

FIG. 17. EFFECT OF FMC CHAR QUANTITY ON THE CORROSION KINETICS OF INCONEL 671 AT 1800°F.

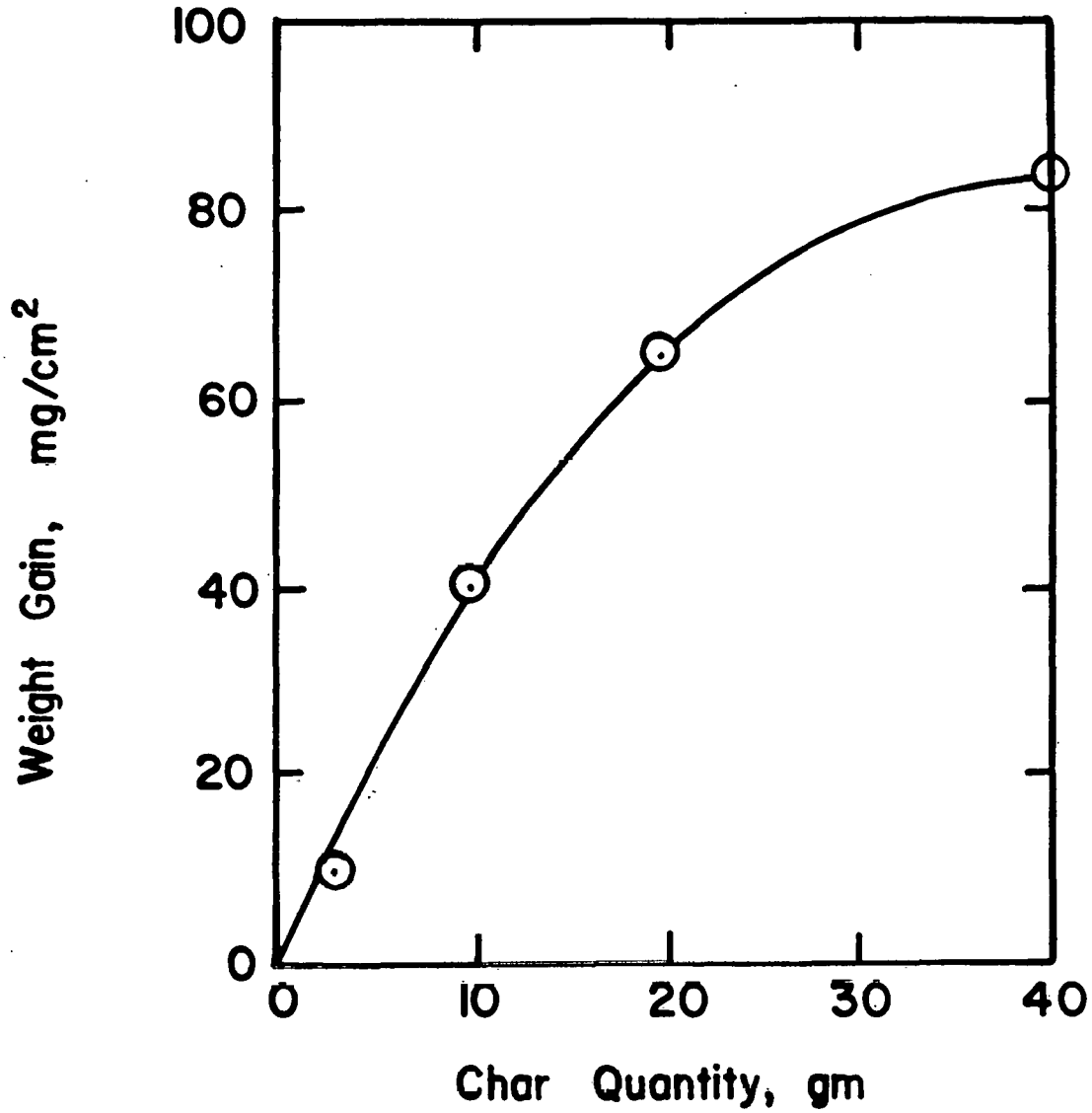

FIG. 18. EFFECT OF FMC CHAR QUANTITY ON THE CORROSION WEIGHT GAIN OF INCONEL 671 IN 12 HRS. AT 1800°F.

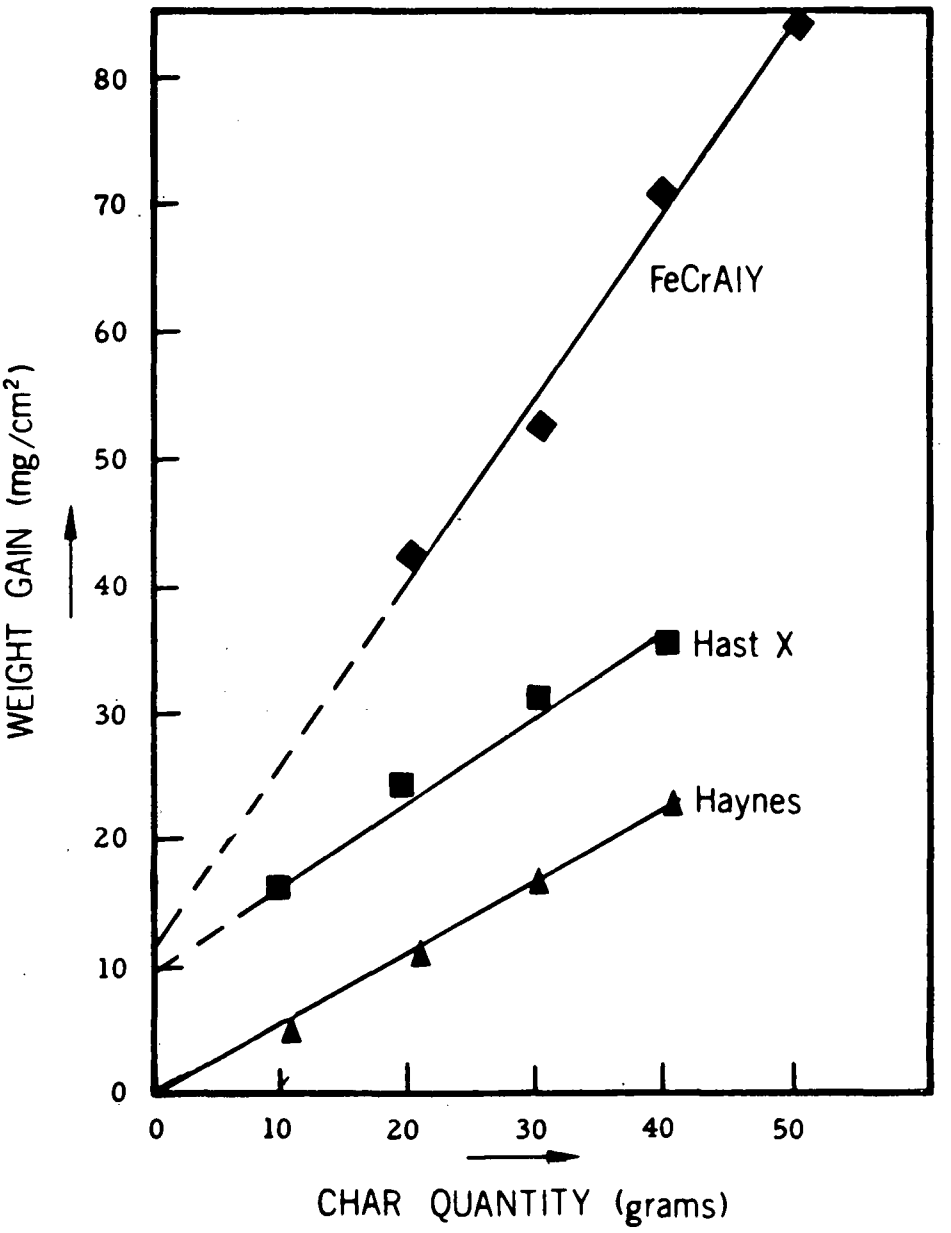

FIG. 19. COMPARATIVE WEIGHT GAIN DEPENDENCE ON FMC CHAR QUANTITY DURING 12 HRS. AT 1800°F.

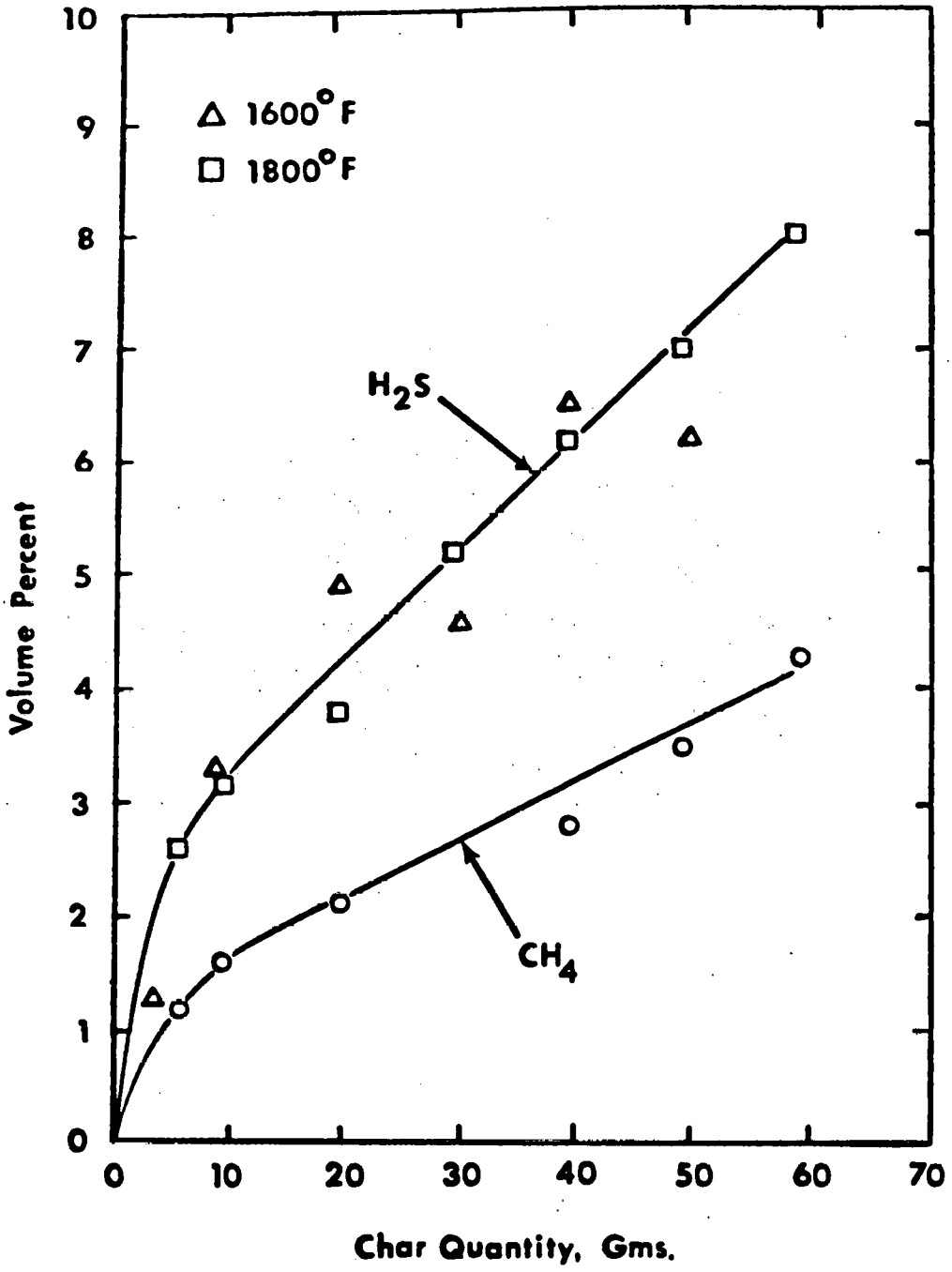

FIG. 20. EFFECT OF FMC CHAR QUANTITY ON GAS COMPOSITION IN A STATIC SYSTEM.

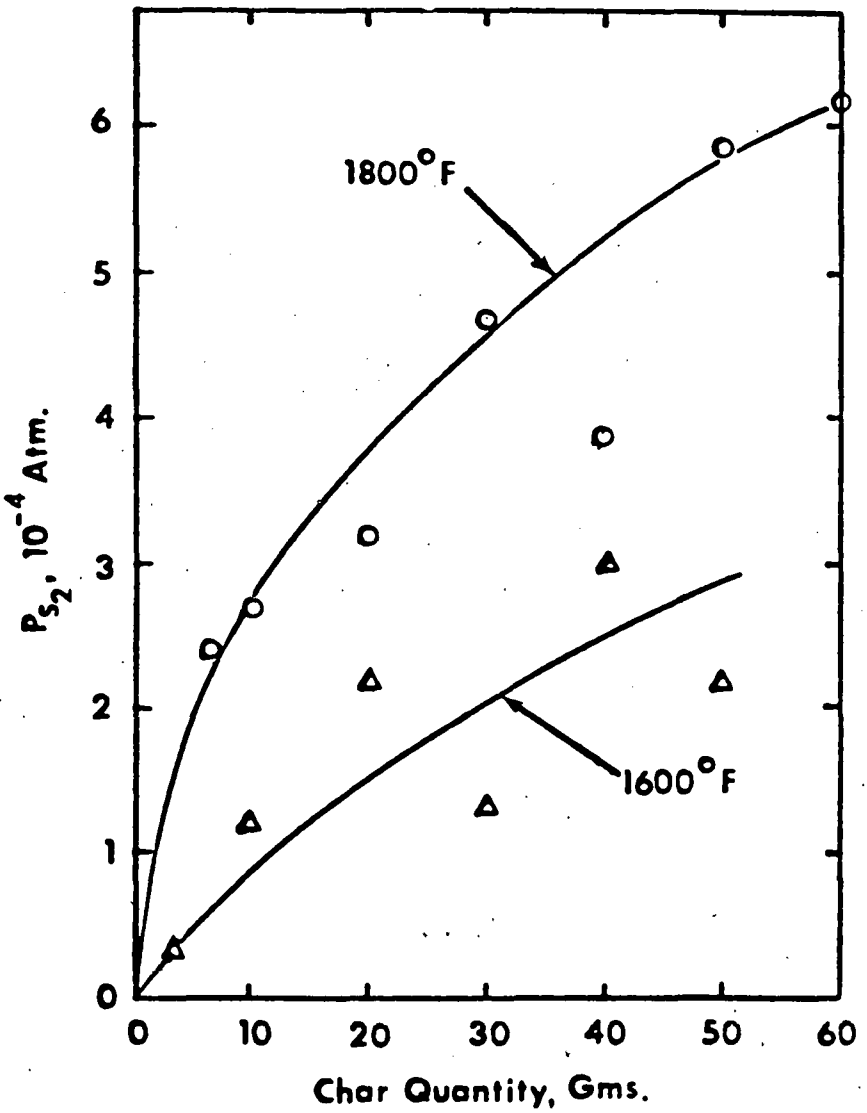

FIG. 21. EFFECT OF FMC CHAR QUANTITY ON SULFUR PARTIAL PRESSURE IN A STATIC SYSTEM.

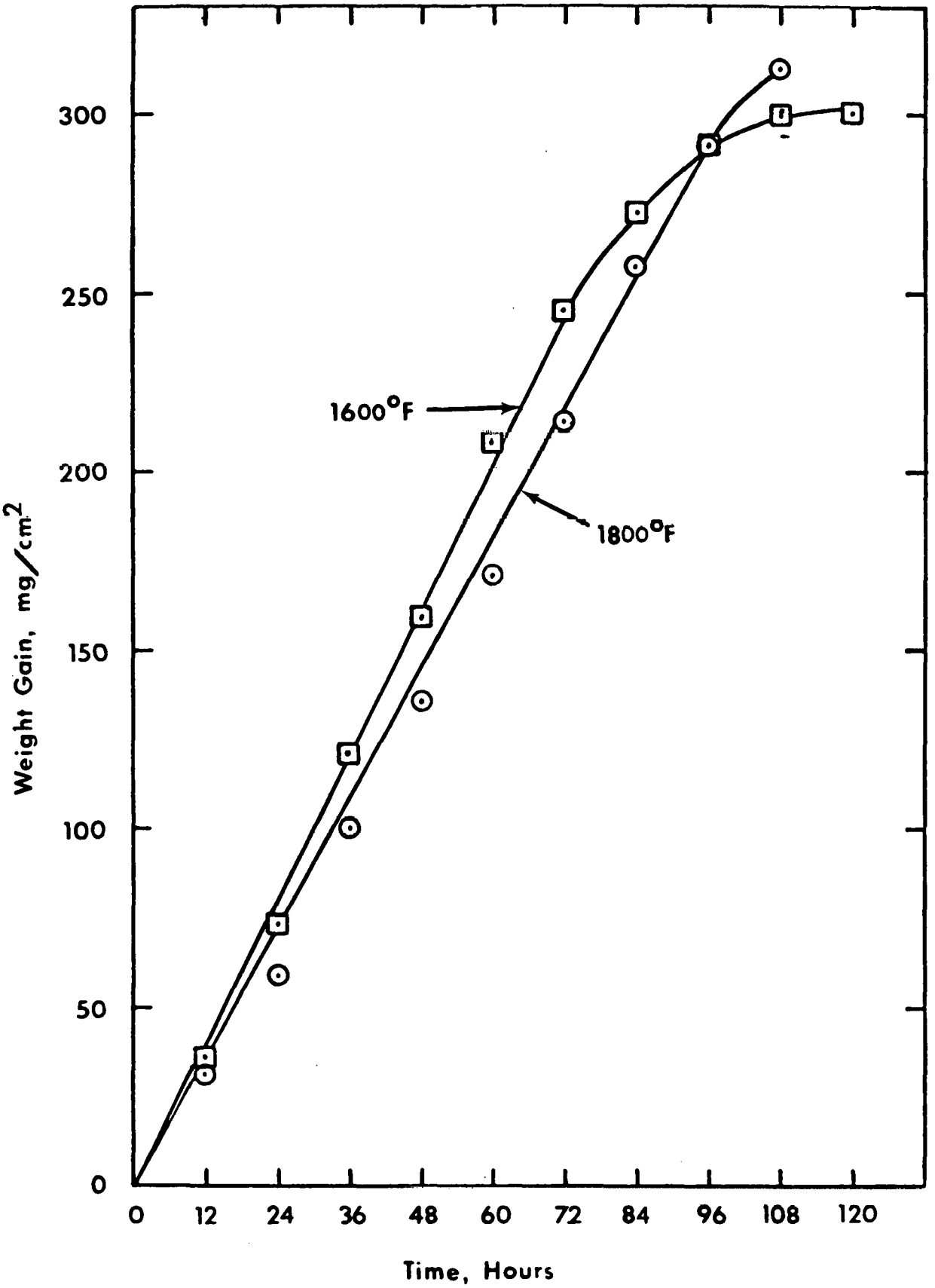

FIG. 22. CORROSION KINETICS OF HAYNES 188 IN FMC CHAR.

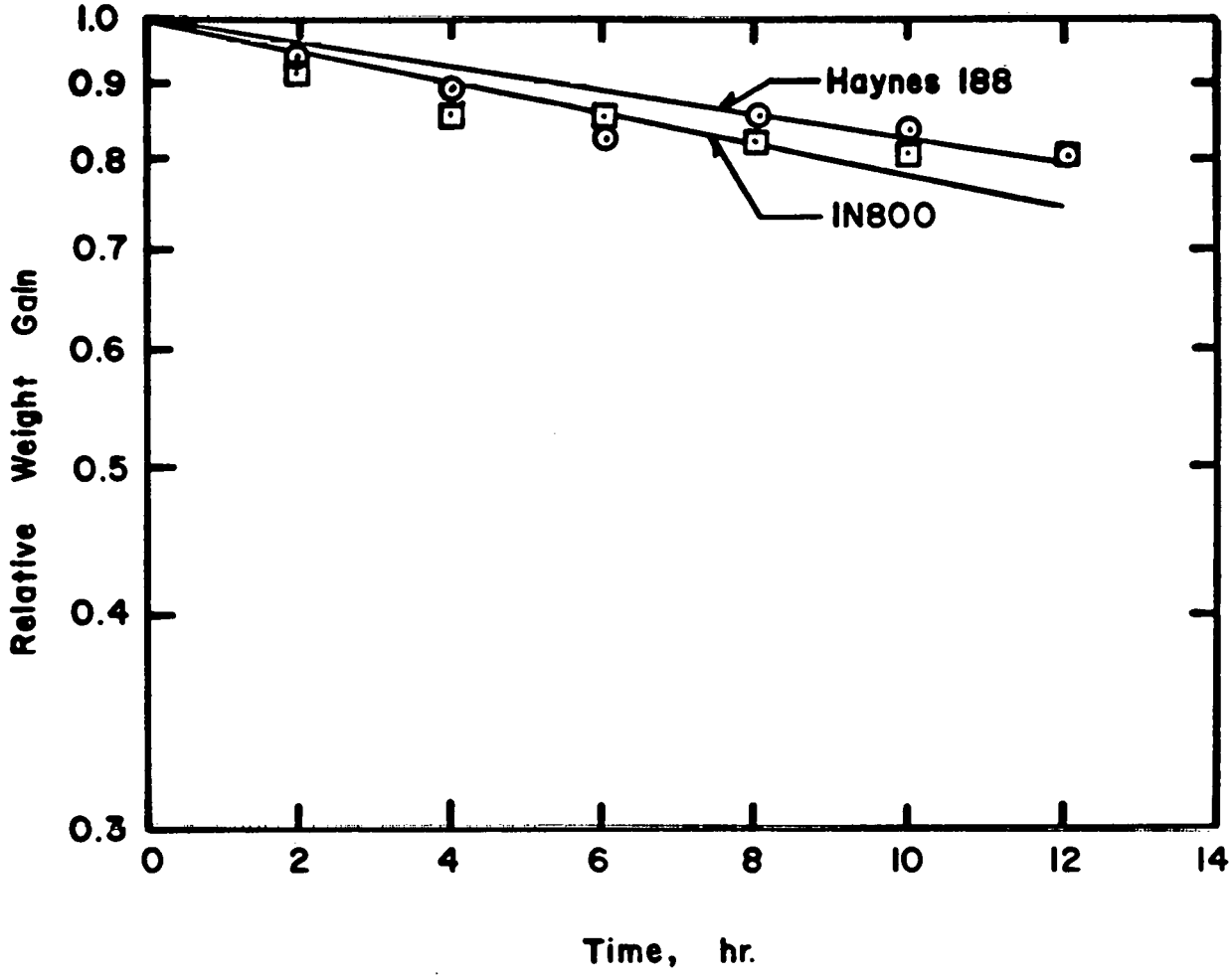

FIG. 23. VARIATION OF RELATIVE WEIGHT GAIN DURING CORROSION OF HAYNES 188 AND INCOLOY 800 IN FMC CHAR AT 1800°F.

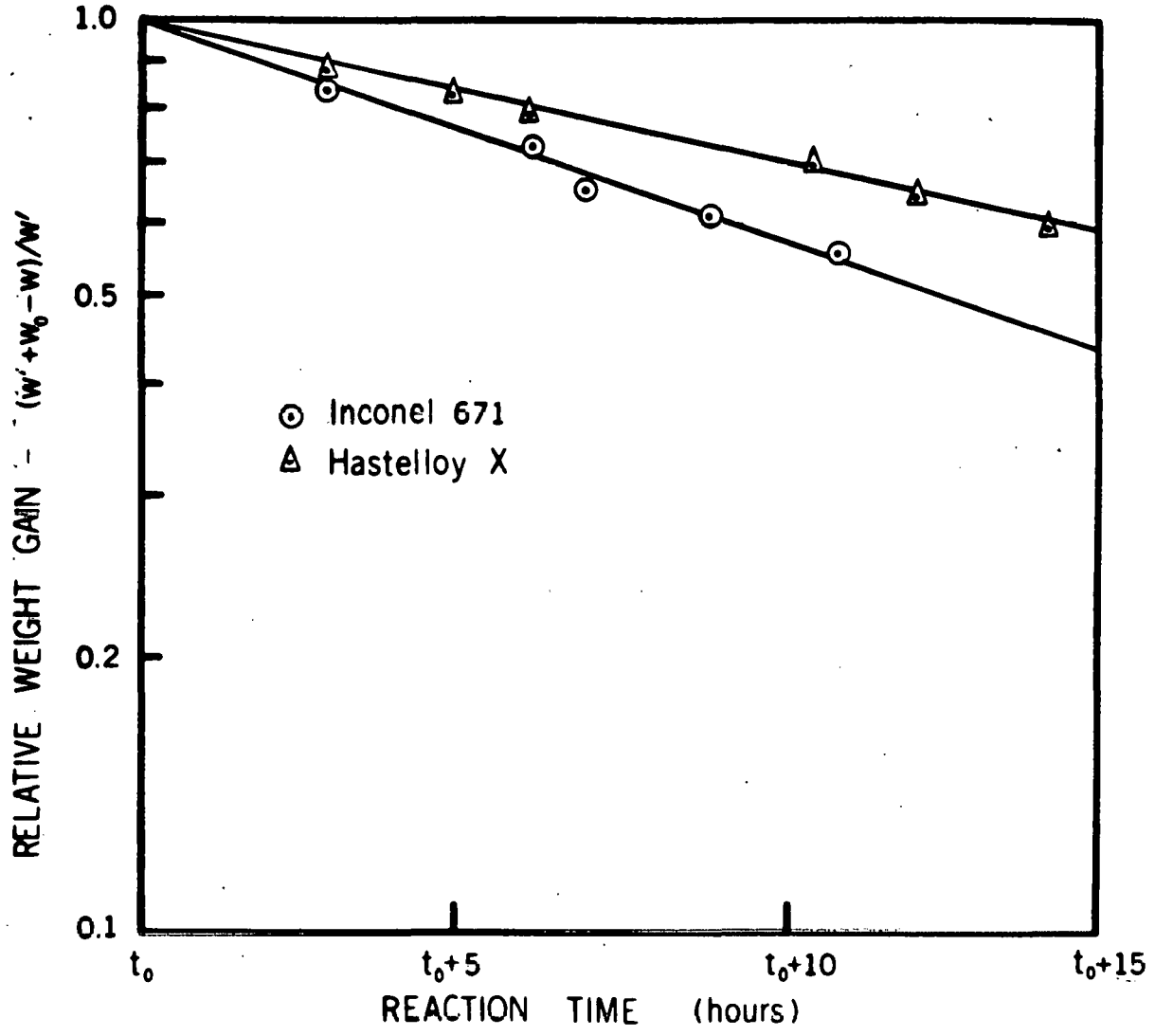

FIG. 24. VARIATION OF RELATIVE WEIGHT GAIN DURING CORROSION OF INCONEL 671 AND HASTELLOY X IN FMC CHAR AT 1800°F.

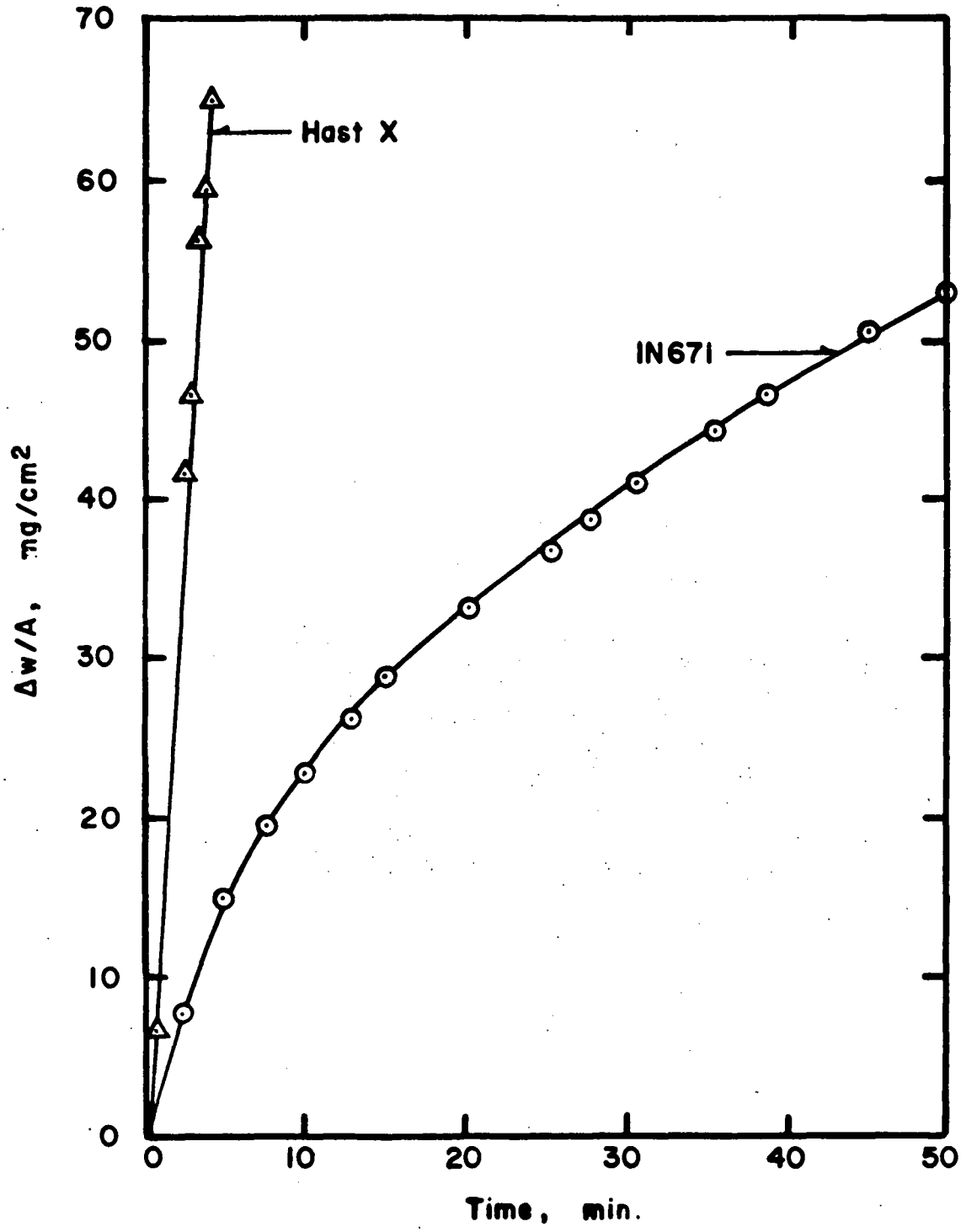

FIG. 25. CORROSION KINETICS OF INCONEL 671 AND HASTELLOY X IN H_2S AT 950°C.

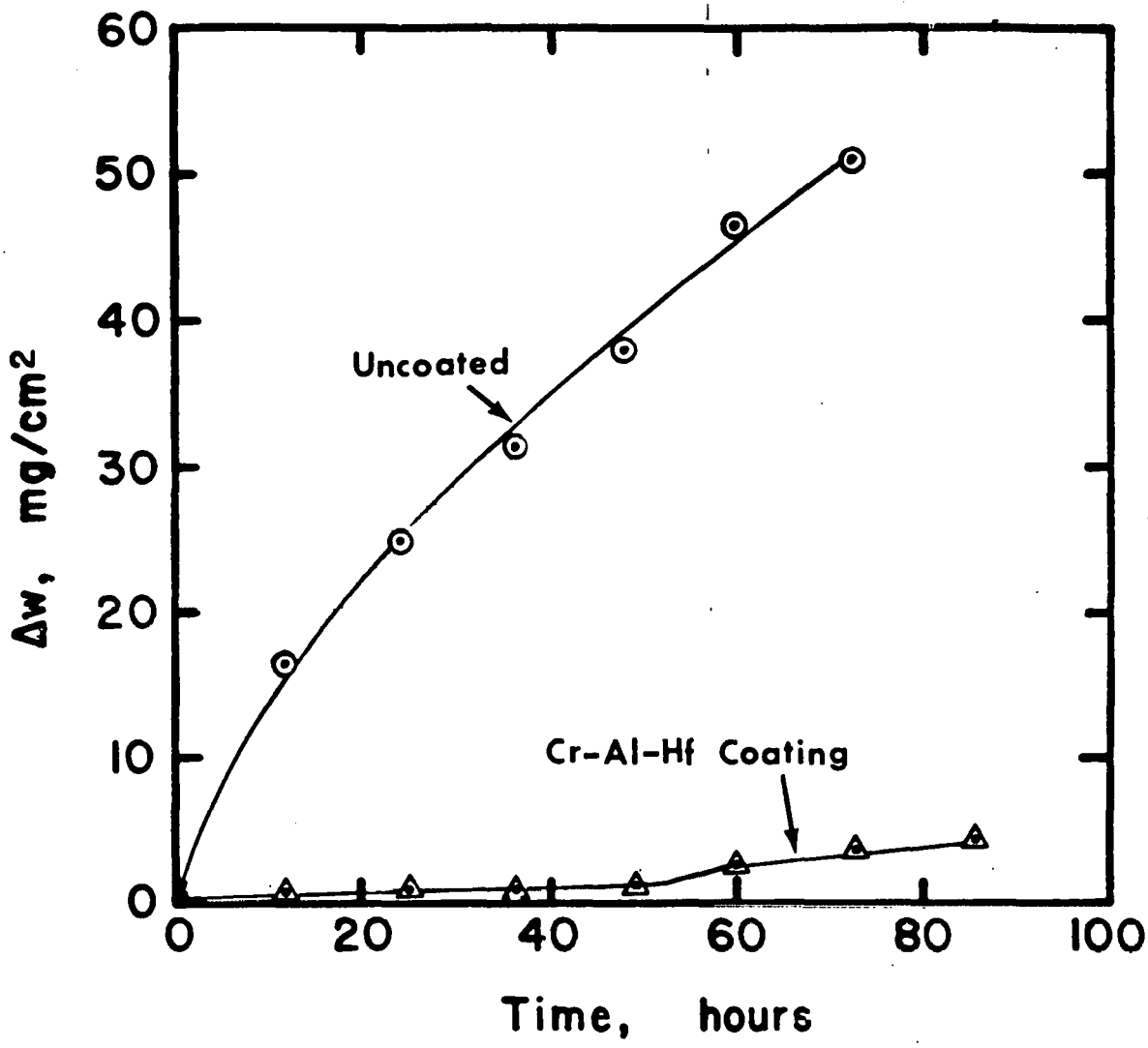

FIG. 26. THE EFFECT OF COATING ON THE CORROSION OF INCOLOY 800 IN FMC CHAR AT 1800°F.

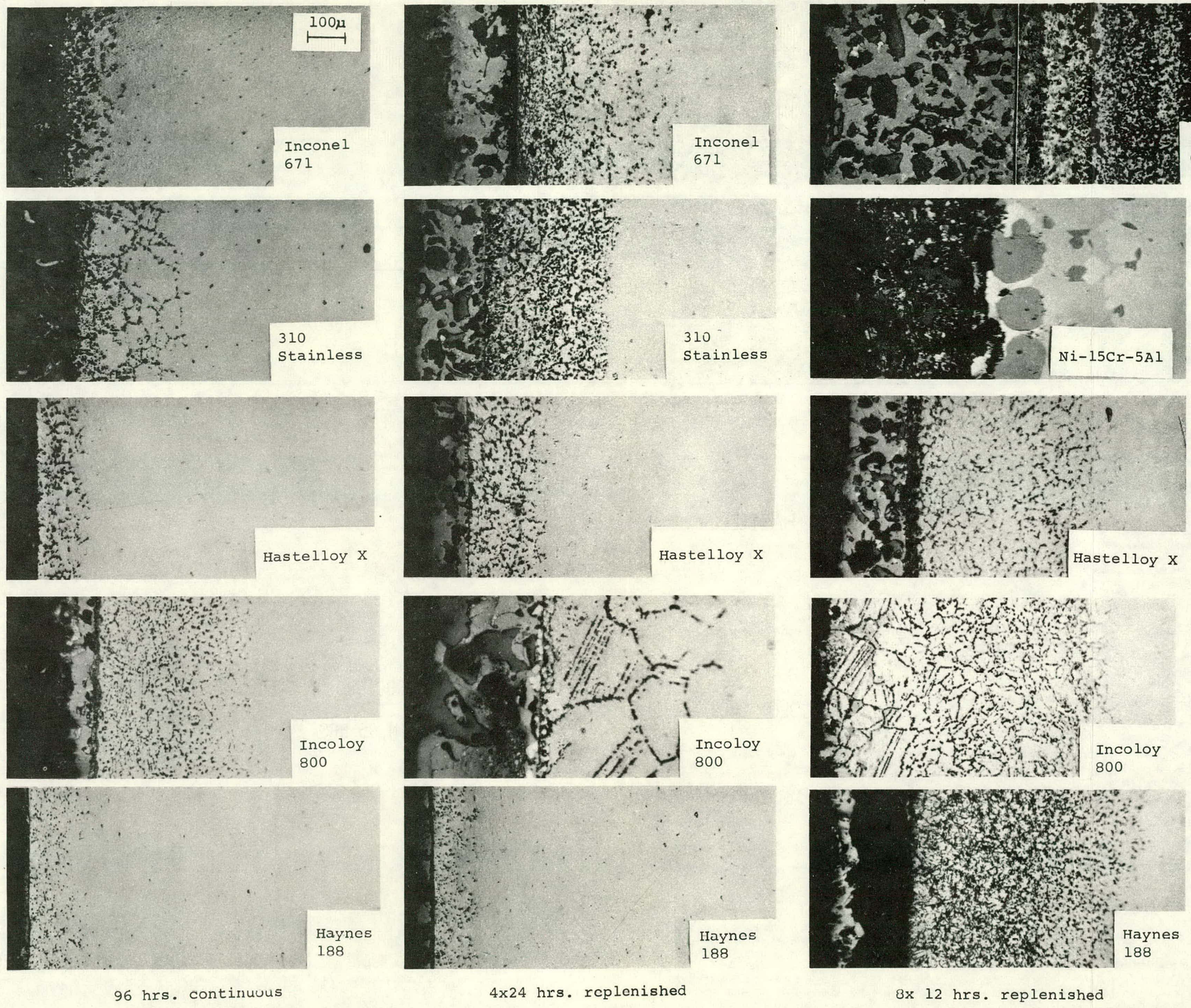

FIG. 27. EFFECT OF CHAR REPLENISHMENT ON CORROSION AT 1800°F.

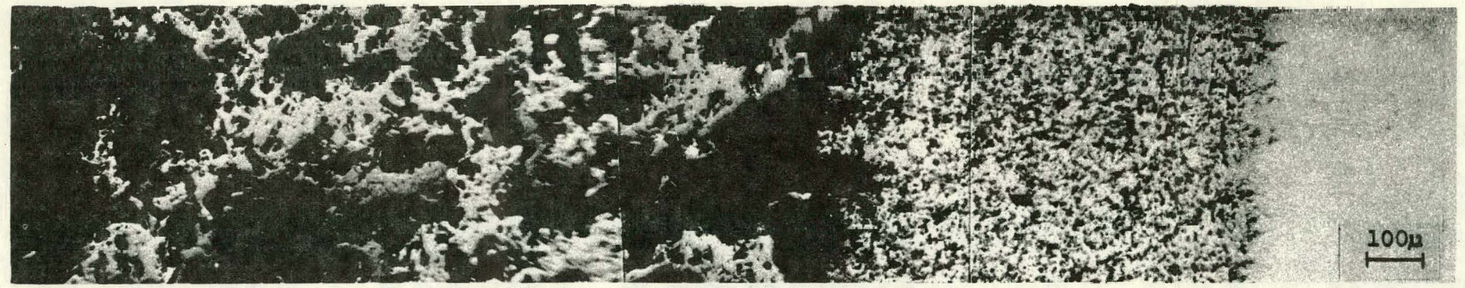

INCONEL 671

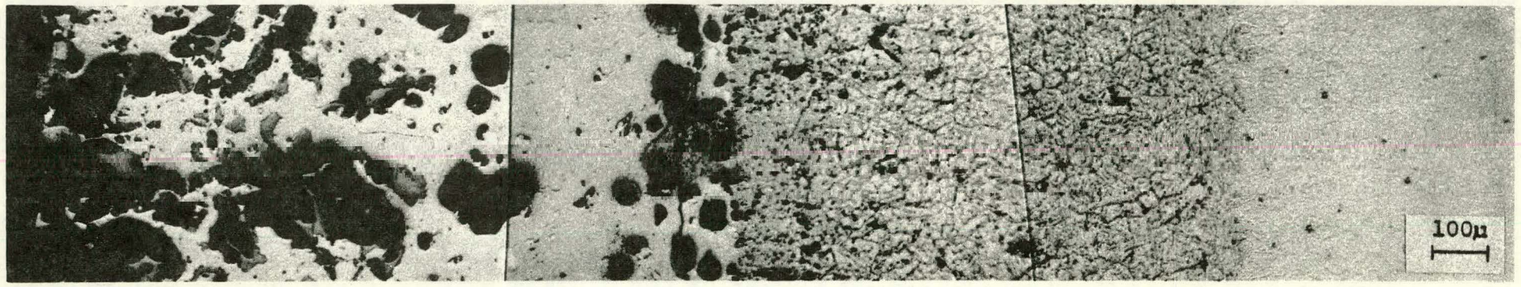

310 STAINLESS

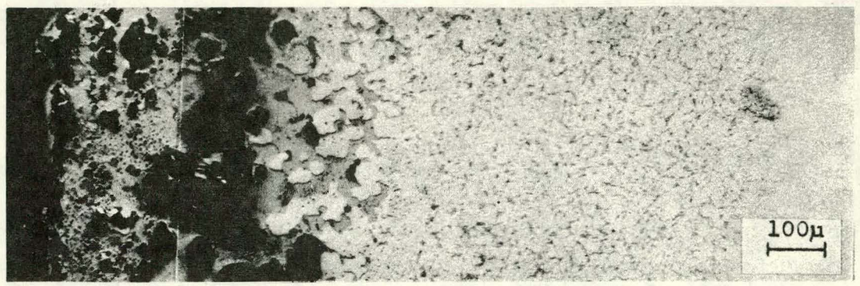

HASTELLOY X

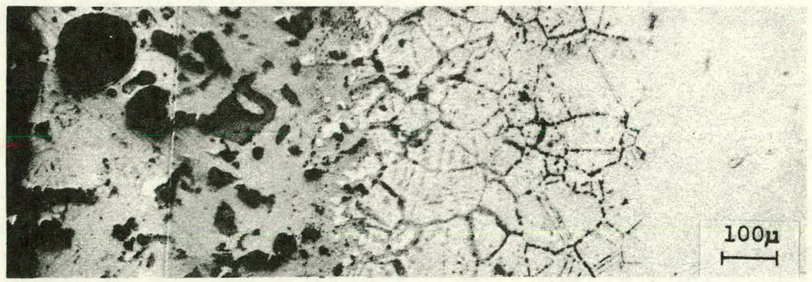

INCOLOY 800

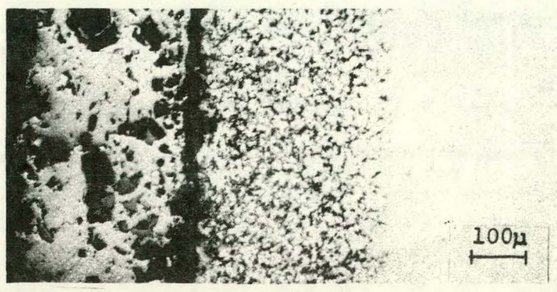

HAYNES 188

FIG. 28. MICROSTRUCTURE OF SCALES FORMED IN FMC CHAR AT 1800°F IN 96 HRS.

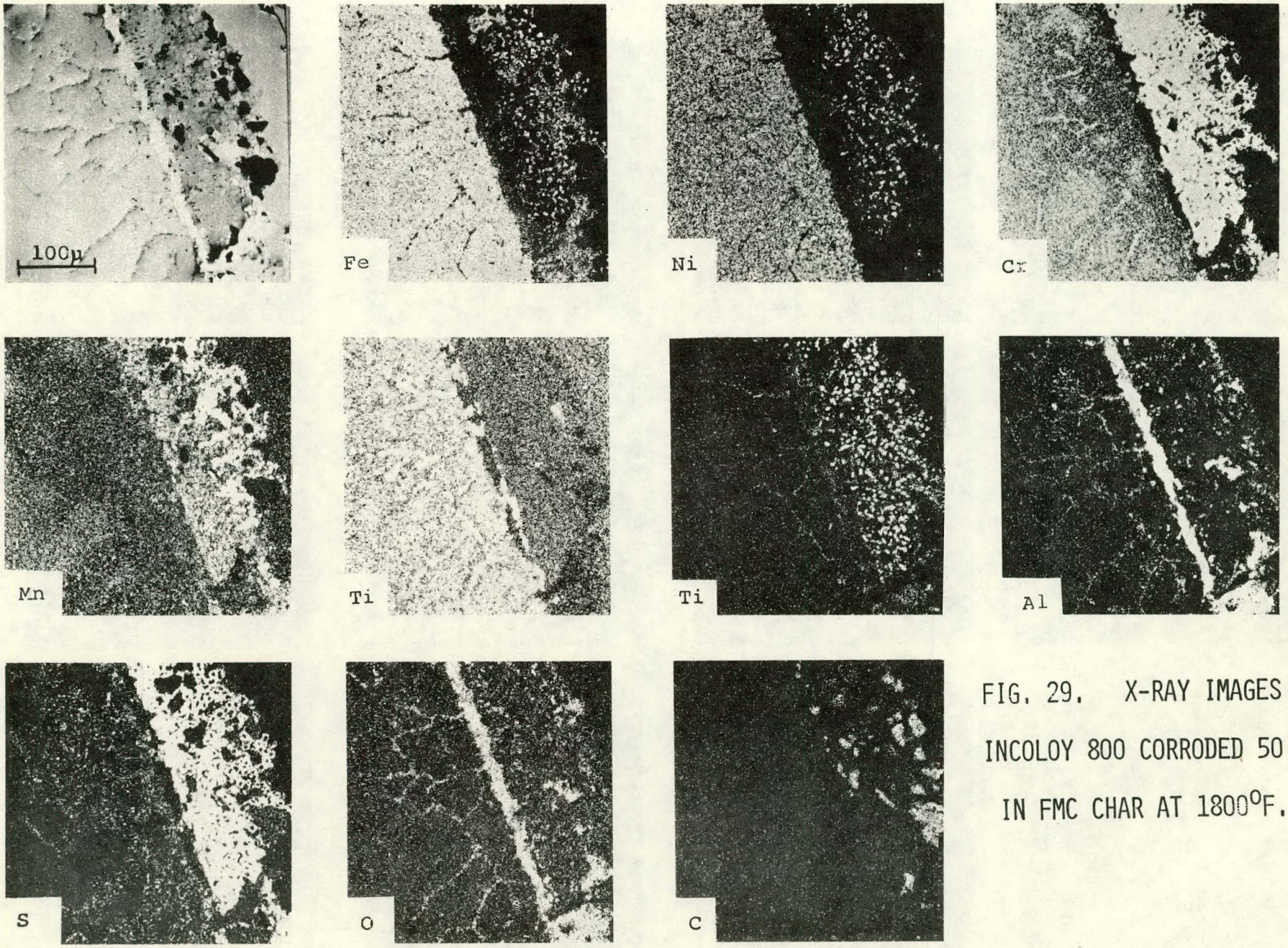

FIG. 29. X-RAY IMAGES OF INCOLOY 800 CORRODED 50 HRS. IN FMC CHAR AT 1800°F.

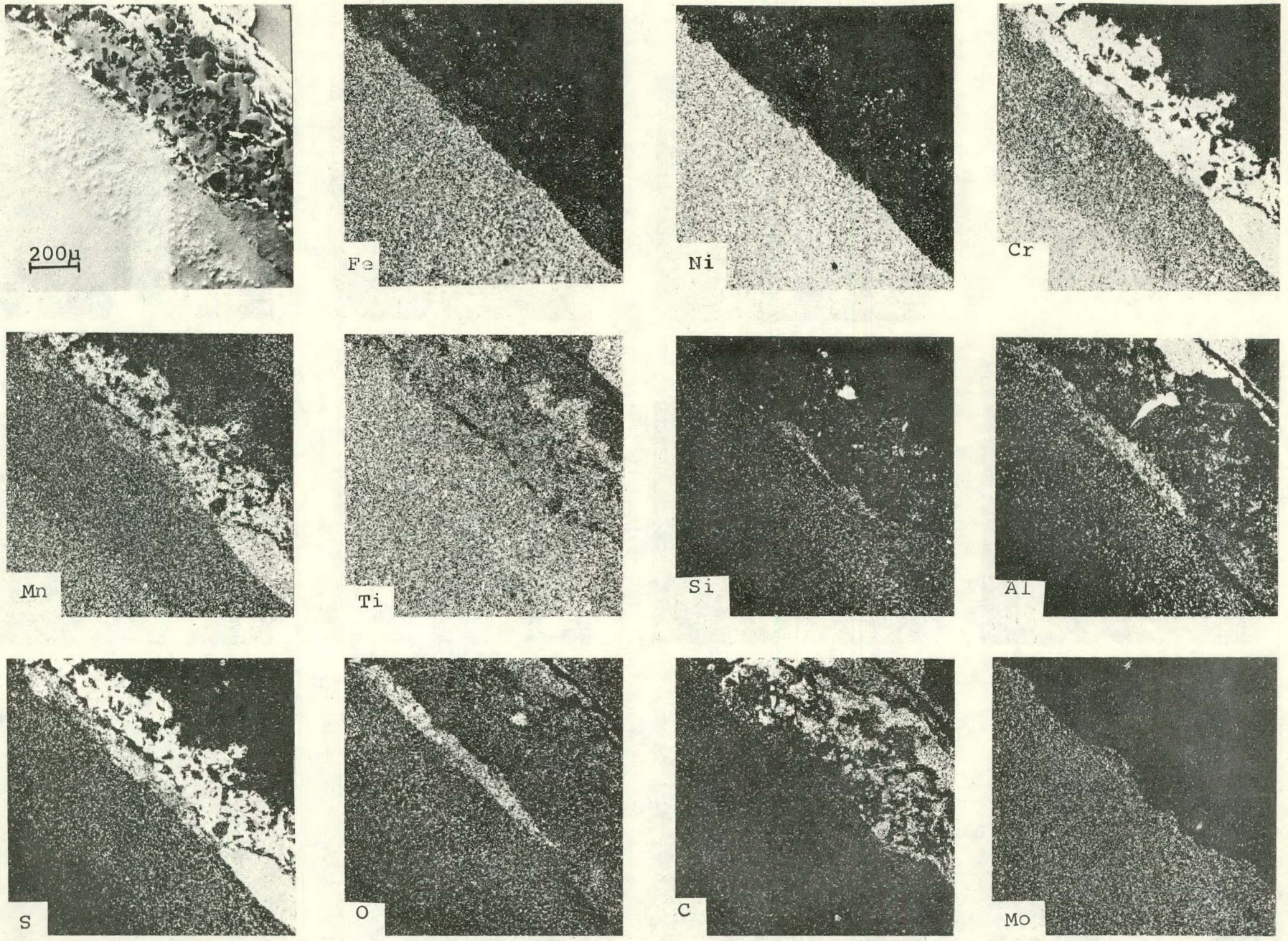

FIG. 30. X-RAY IMAGES OF HASTELLOY X CORRODED 50 HRS. IN FMC CHAR AT 1800°F.

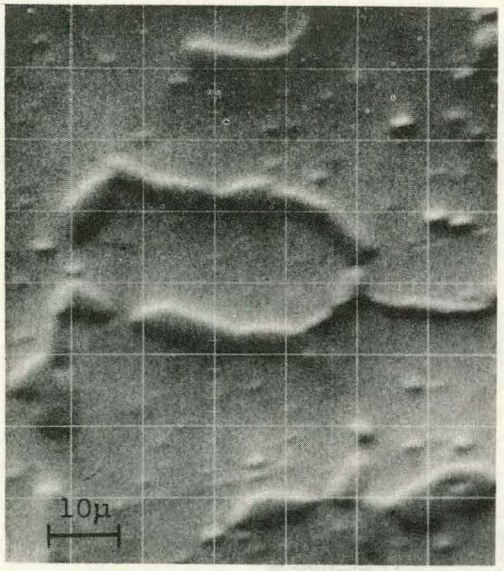

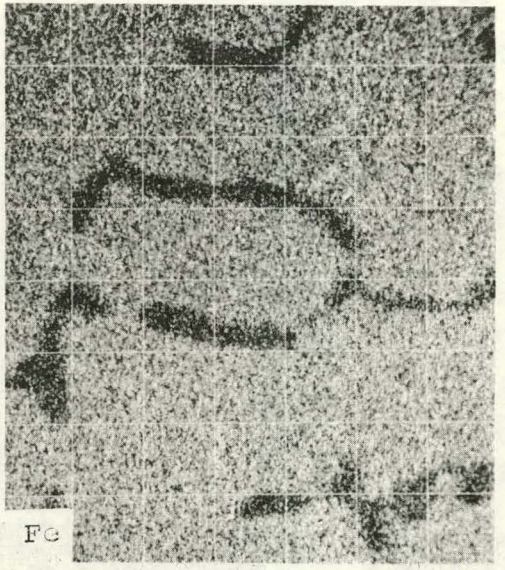

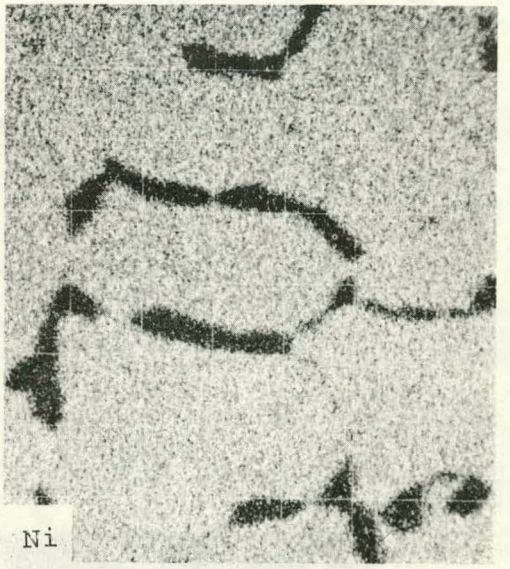

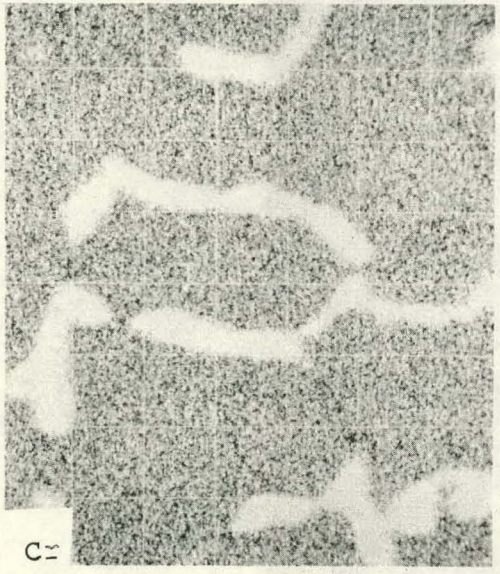

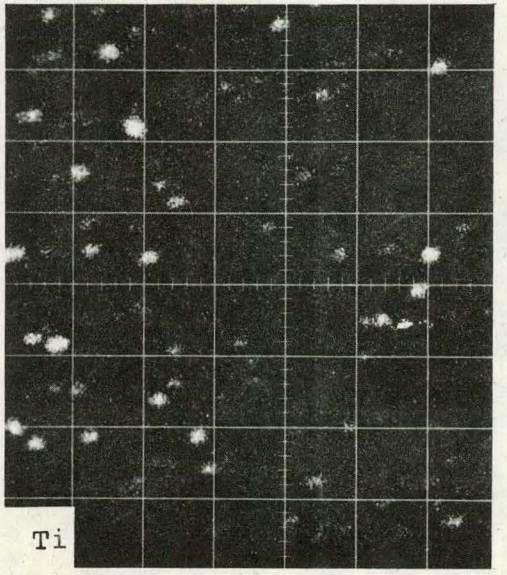

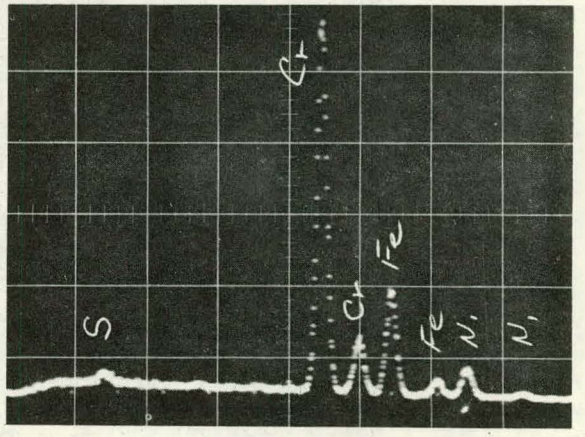

FIG. 31. X-RAY IMAGES OF INCOLOY 800 MATRIX AFTER CORROSION FOR 96 HRS. IN FMC CHAR AT 1800°F.

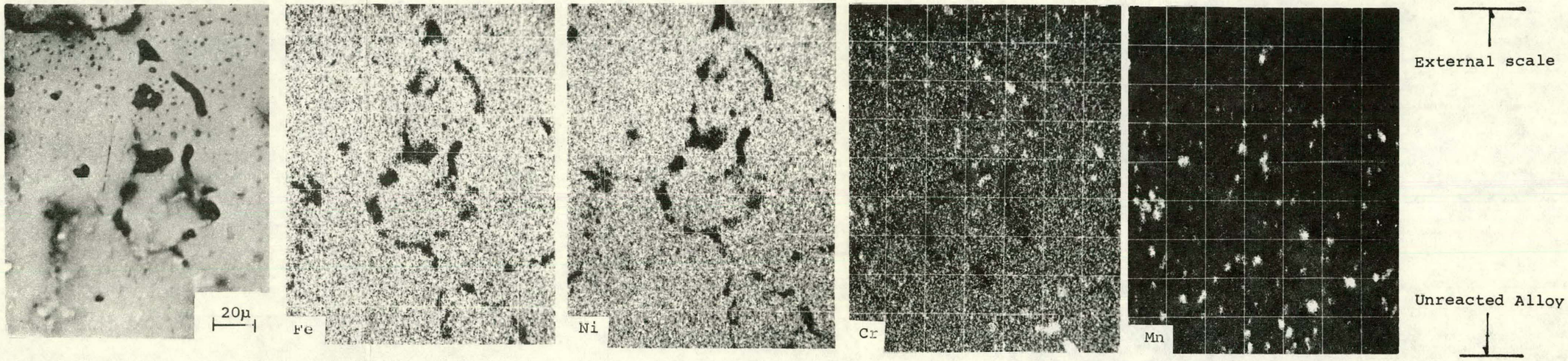

FIG. 32. X-RAY IMAGES OF INTERNAL REACTION PRODUCTS FORMED IN INCOLOY 800 DURING CORROSION IN FMC CHAR FOR 96 HRS. AT 1800°F.

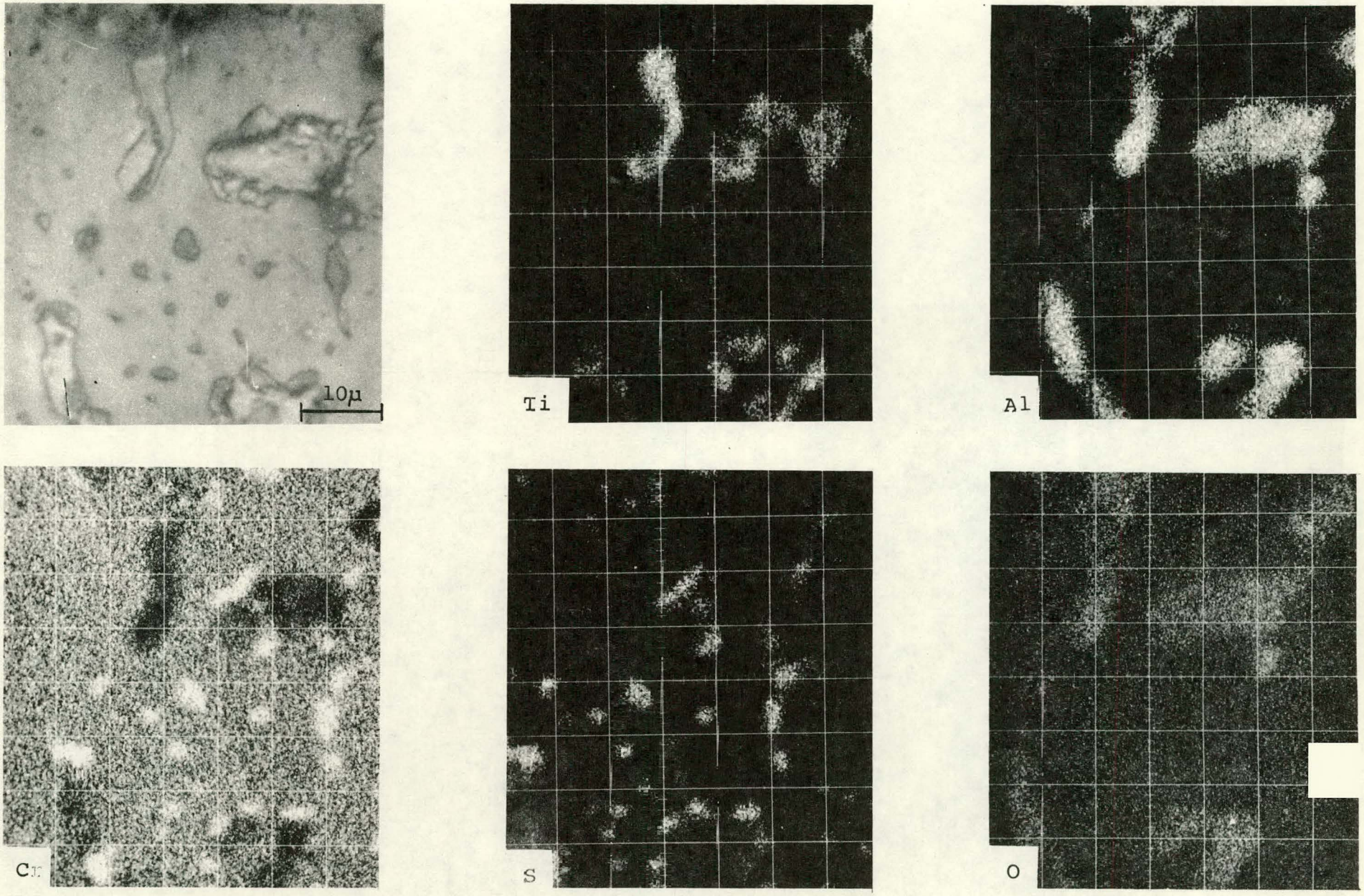

FIG. 33. ENLARGED X-RAY IMAGES OF FIG. 32.

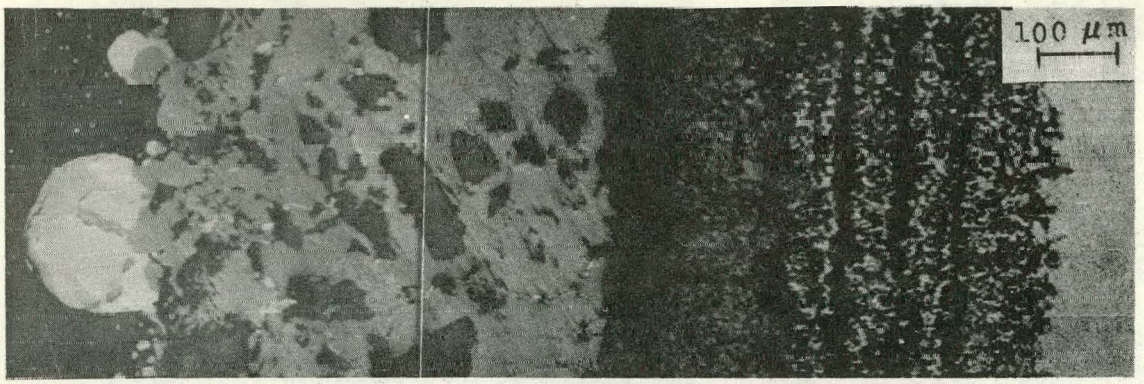

INCONEL 671

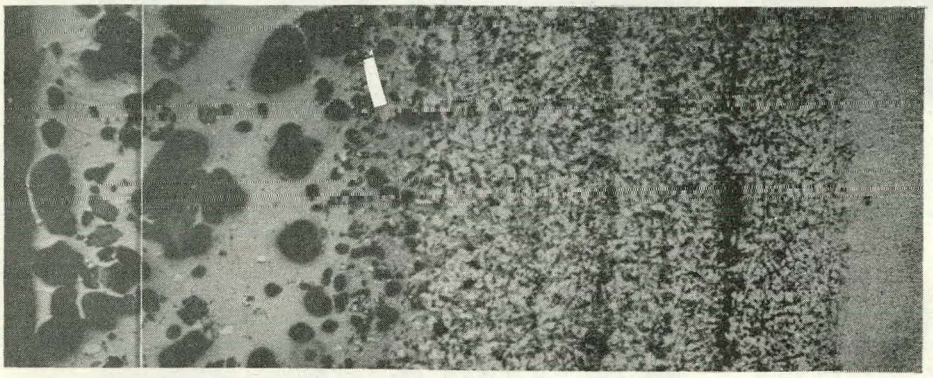

310 STAINLESS

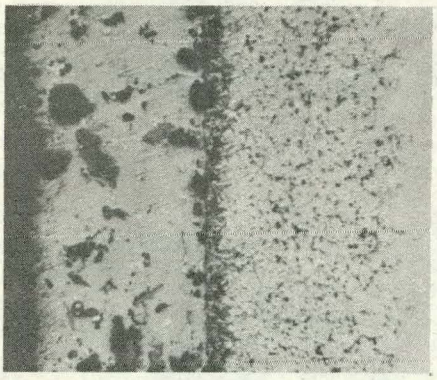

HASTELLOY X

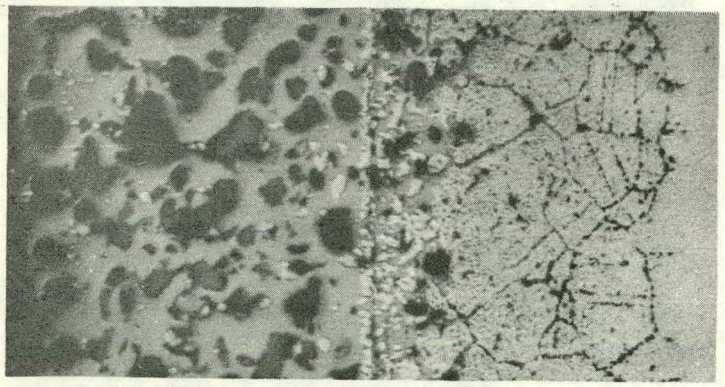

INCOLOY 800

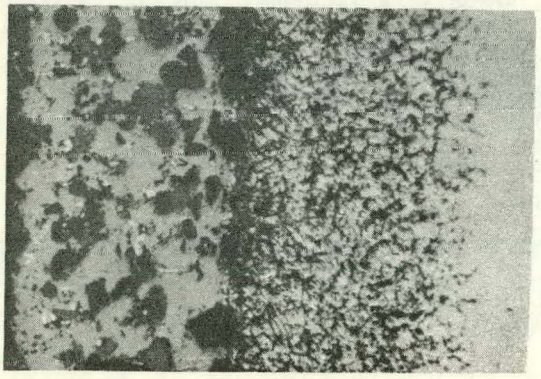

HAYNES 188

FIG. 34. MICROSTRUCTURE OF SCALES FORMED IN HUSKY CHAR AT 1800° F IN 96 HOURS.

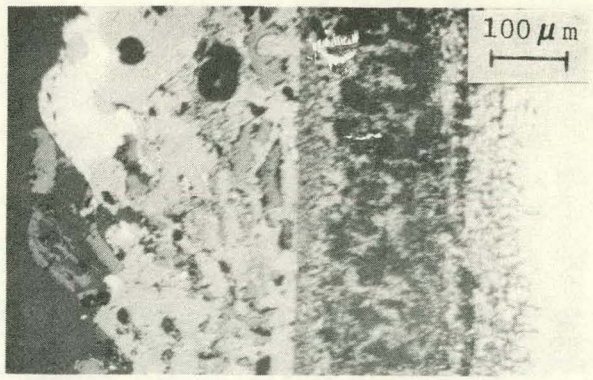

INCONEL 671

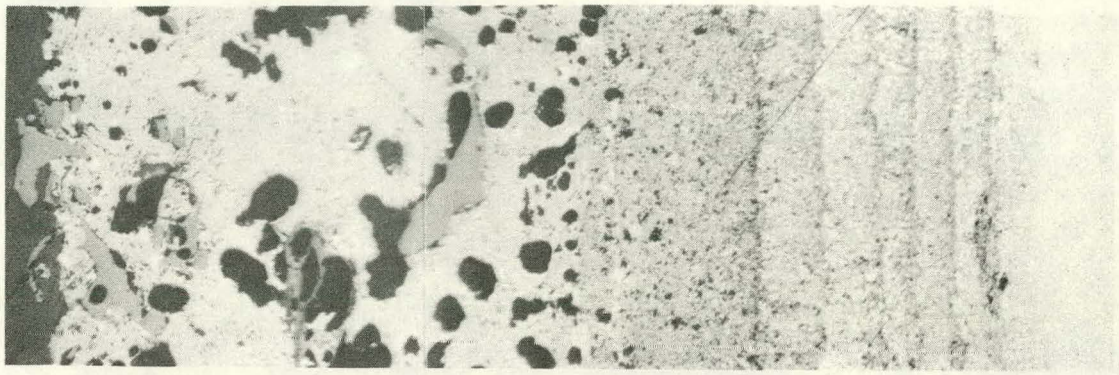

310 STAINLESS

HASTELLOY X

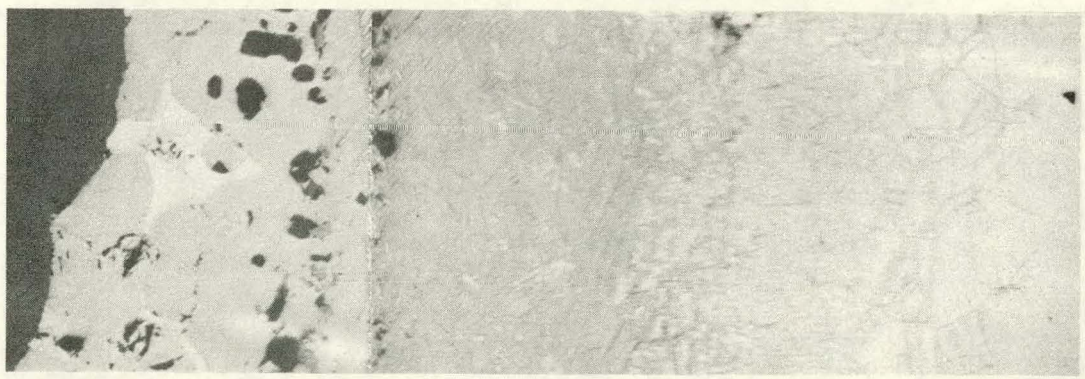

INCOLOY 800

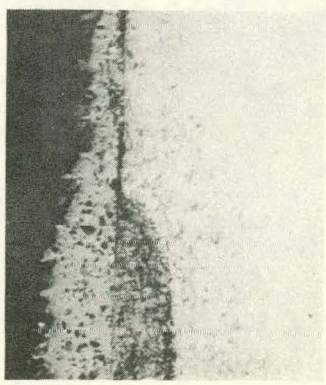

HAYNES 188

FIG. 35. MICROSTRUCTURE OF SCALES FORMED IN FMC CHAR AT 1600°F IN 96 HRS.

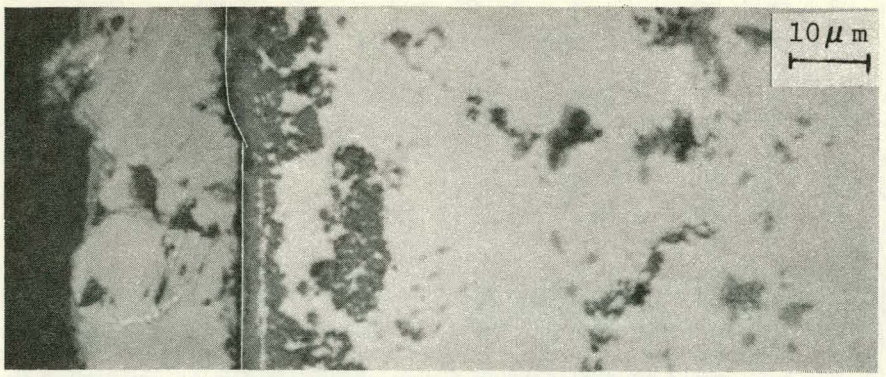

INCONEL 671

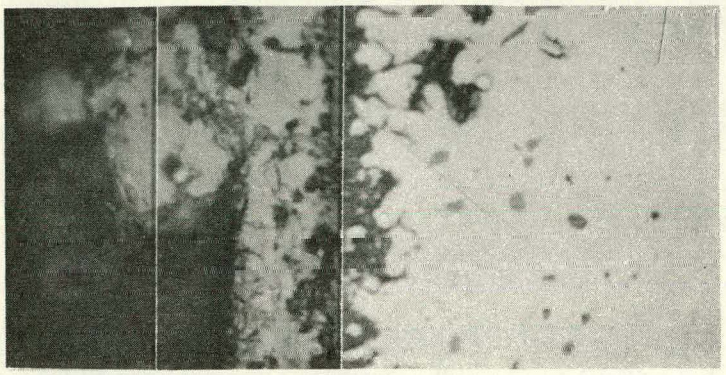

310 STAINLESS

HASTELLOY X

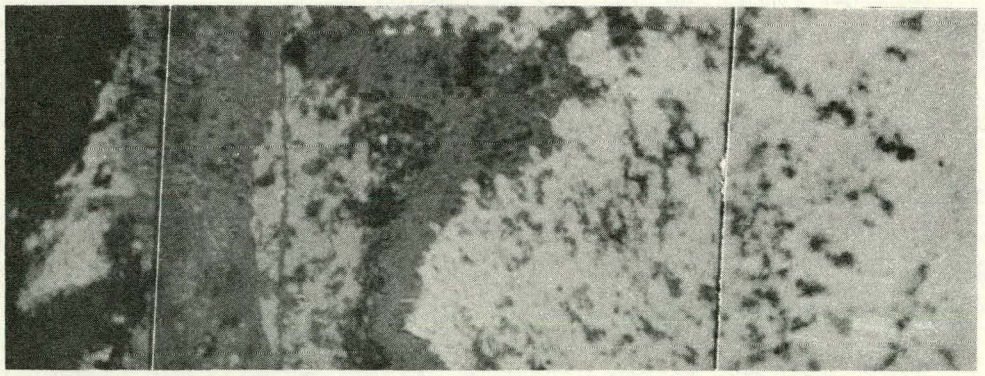

INCOLOY 800

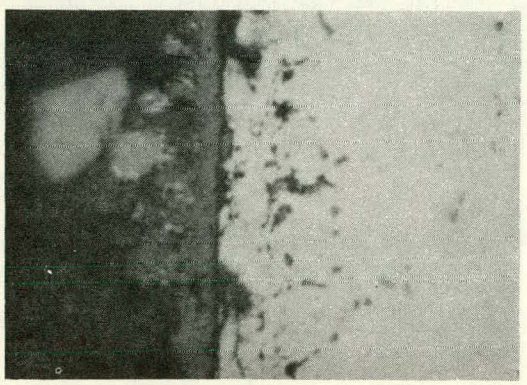

HAYNES 188

FIG. 36. MICROSTRUCTURE SCALES FORMED IN HUSKY CHAR AT 1600°F IN 96 HRS.

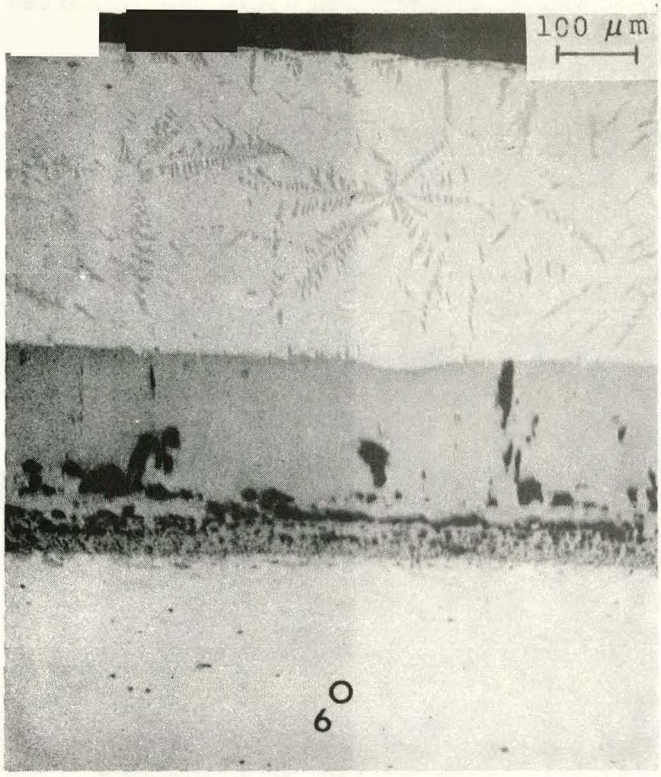

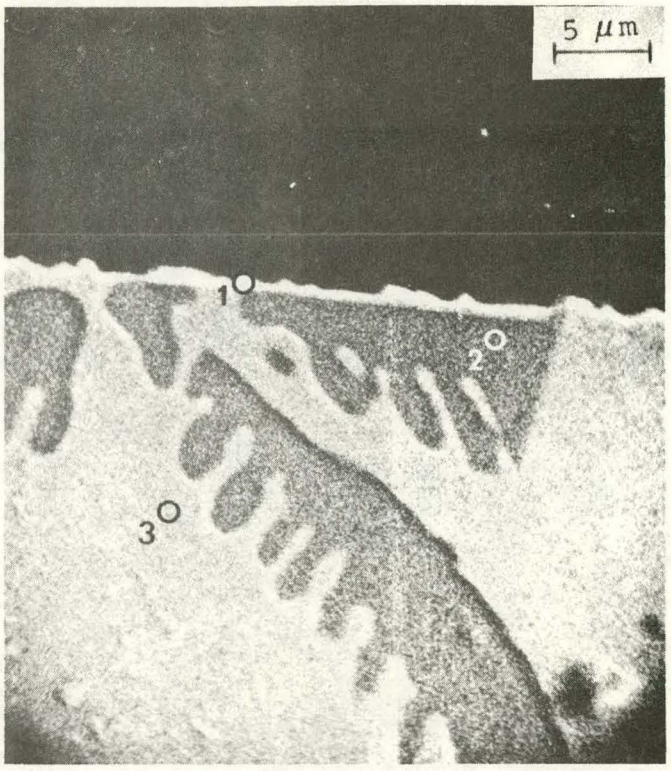

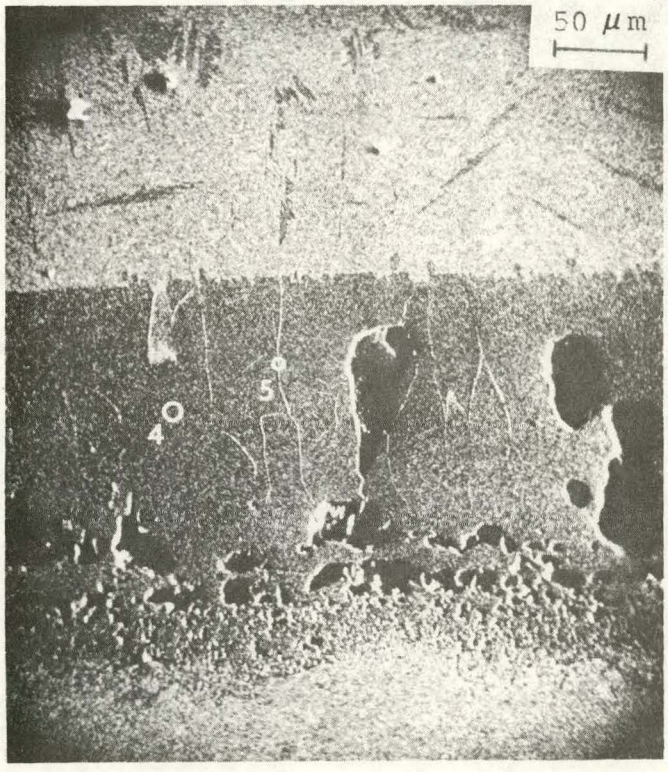

FIG. 37. MICROSTRUCTURE OF SCALE FORMED IN H_2S AT 950°C IN 50 MINS. ON INCONEL 671.

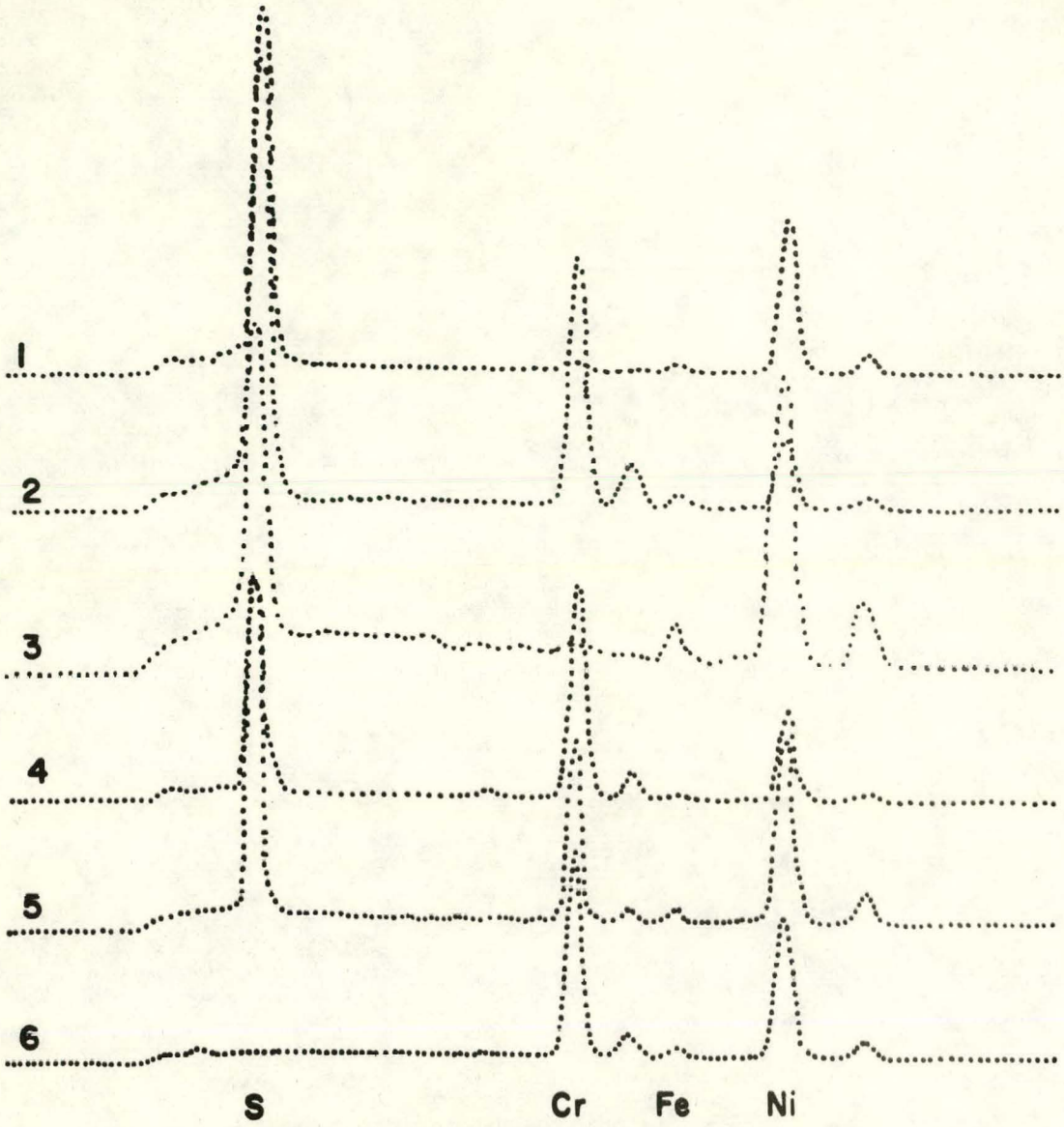

FIG. 38. EDX SPECTRA OF SCALE FORMED ON INCONEL 671 IN H_2S.
NUMBERS REFER TO AREAS IN FIG. 37.

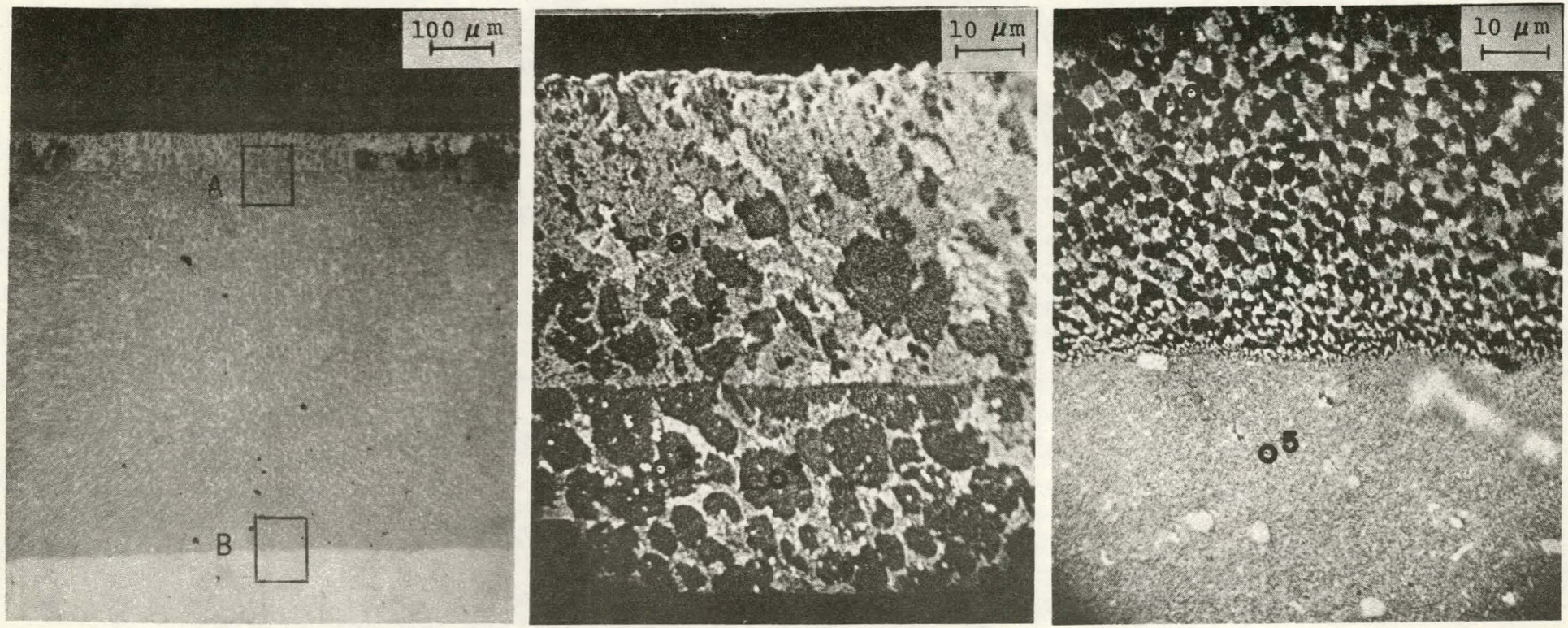

A B

FIG. 39. MICROSTRUCTURE OF SCALE FORMED IN H_2S AT 950°C IN 6 MINS. ON HASTELLOY X.

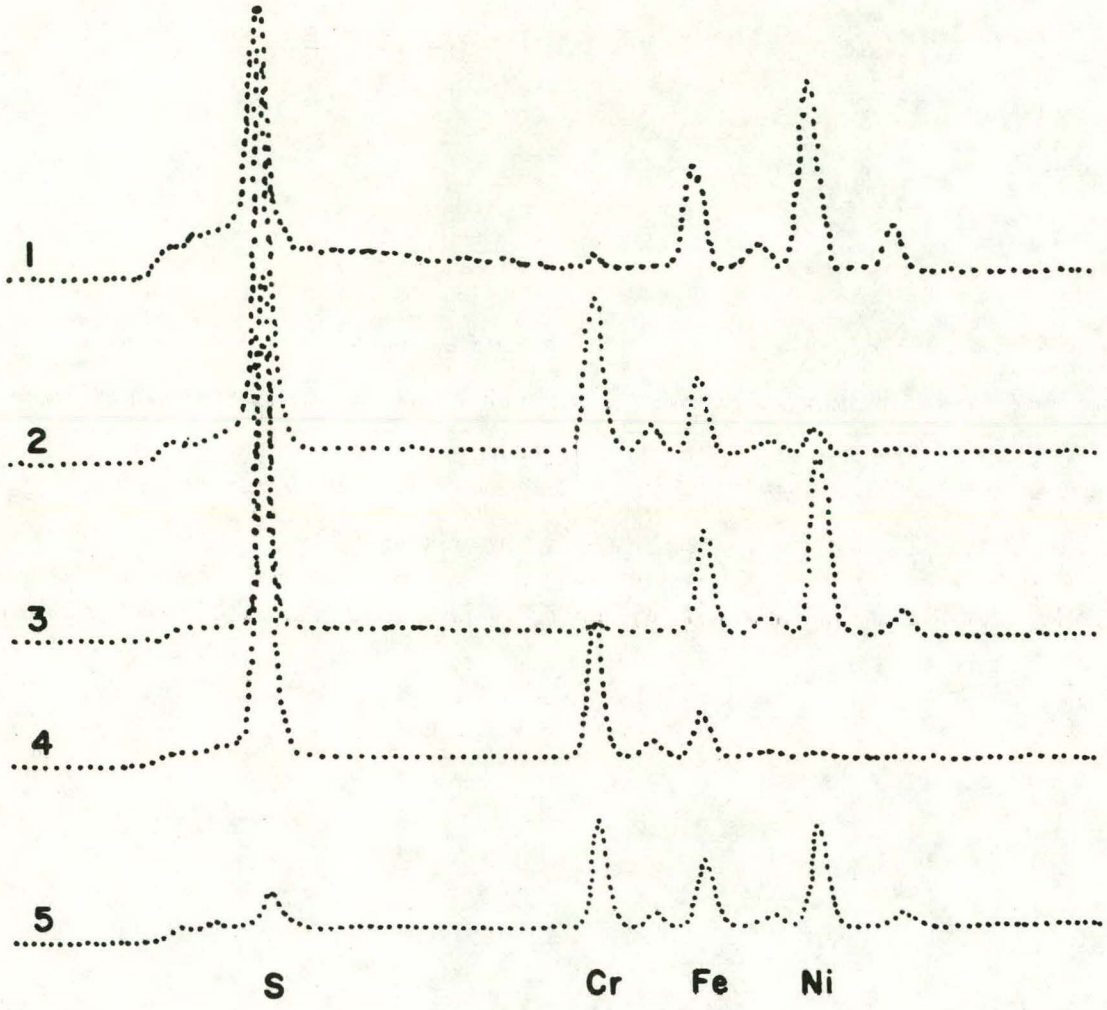

FIG. 40. EDX SPECTRA OF SCALE FORMED ON HASTELLOY X IN H_2S.
NUMBERS REFER TO AREAS IN FIG. 39.

500X

FIG. 41 CHAR PARTICLE EMBEDDED IN EXTERNAL SCALE OF OF 310 STAINLESS REACTED IN FMC CHAR FOR TWO TWELVE-HOUR INTERVALS.

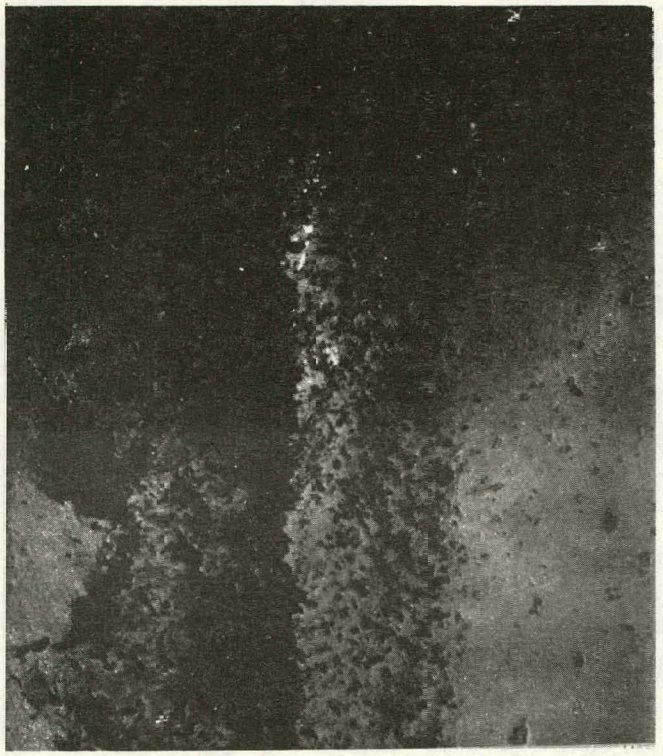

(A) ARGON AND FMC CHAR, 50 HRS. 200X

(B) CGA ONLY, 96 HRS. 1000X

FIG. 42. COMPARISON OF MICROSTRUCTURES OF SCALES FORMED ON INCONEL 671 IN (A) CHAR PLUS ARGON AND (B) CGA ONLY. 96 HRS. AT 1800°F.

125X

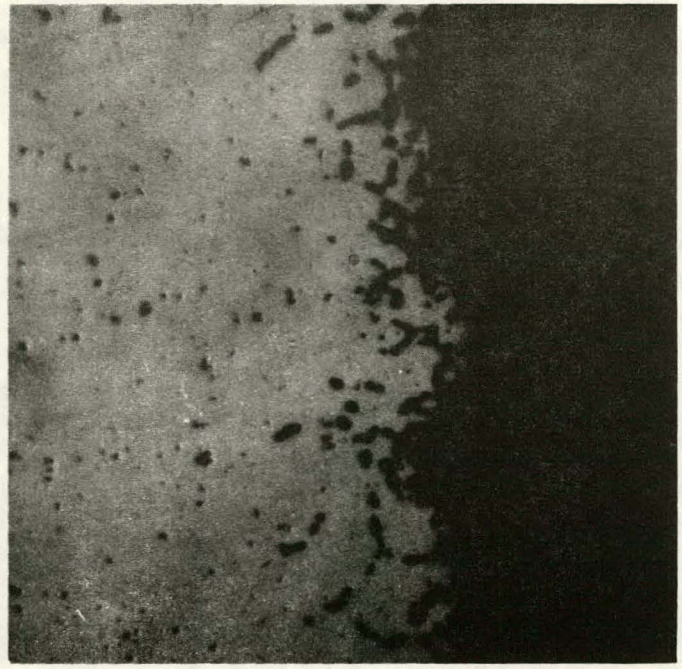

1000X

FIG. 43. COMPARISON OF MICROSTRUCTURES OF SCALES FORMED ON 310 STAINLESS STEEL IN (A) CHAR PLUS ARGON, AND (B) CGA ONLY. 96 HRS. AT 1800°F.

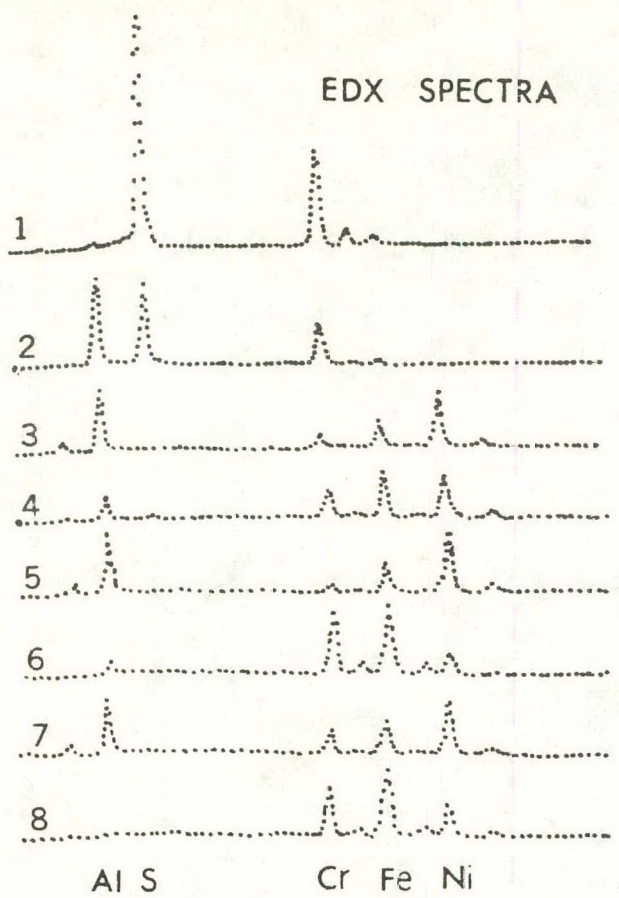

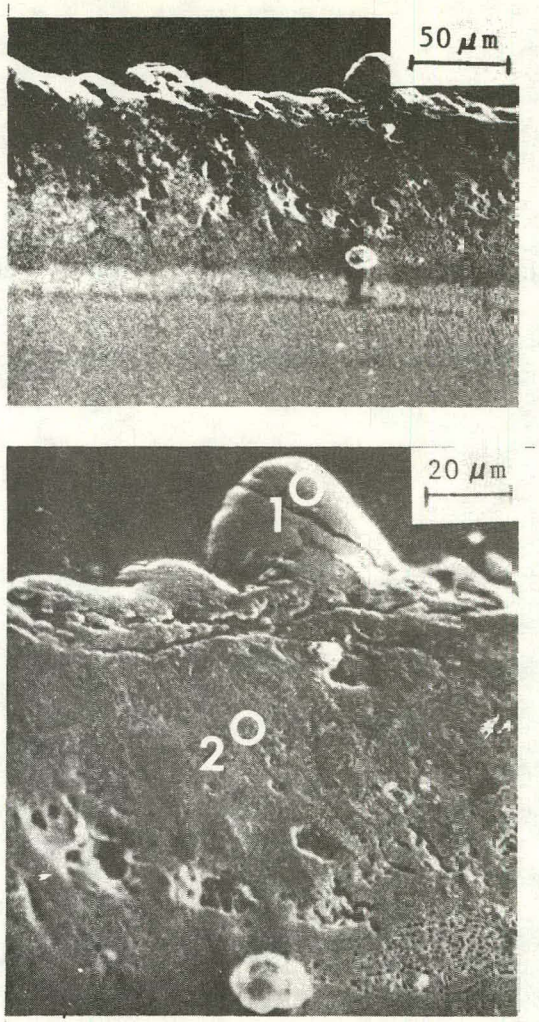

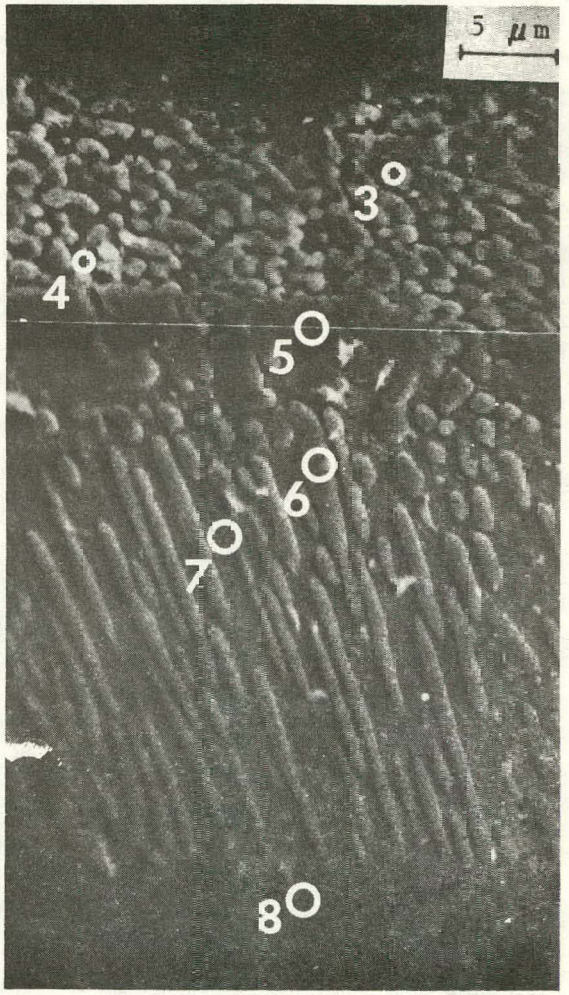

FIG. 44. MICROSTRUCTJRE OF Cr-Aℓ-Hf COATING ON INCOLCY 800 AFTER CORROSION IN FMC CHAR FOR 84 HRS. AT 1800°F.

☆U.S. GOVERNMENT PRINTING OFFICE: 1980-740-145/825